3. Climate and Atmospheric Deposition Patterns and Trends

Warren E. Heilman, John Hom, and Brian E. Potter

One of the most important factors impacting terrestrial and aquatic ecosystems is the atmospheric environment. Climatic and weather events play a significant role in governing the natural processes that occur in these ecosystems. The current characteristics of the vast number of ecosystems that cover the northeast and north central United States are, in part, the result of climate, weather, disturbance, and atmospheric pollution patterns that exist in the northeast and north central United States. For example, basic ecosystem processes (e.g., heat and moisture exchanges with the atmosphere, photosynthesis, and respiration) along with species diversity and ecosystem health throughout the region all depend, to some degree, on these patterns. Furthermore, future characteristics of ecosystems in the region will depend on future climate, weather, disturbance, and pollution patterns that may develop in response to natural or human-caused changes in our atmospheric environment.

This chapter provides an introduction to a number of climate principles and an overview of some of the current (baseline) patterns of climate, climate variability, extreme weather events, atmospheric pollution, and deposition of atmospheric pollutants that characterize the region. In particular, baseline patterns of temperature, extreme temperature events, spring freezes, midwinter thaw events, precipitation, extreme precipitation

events, flood and drought occurrences, short-term precipitation variability, extreme wind events, hurricane occurrence, and fire-weather are presented. Atmospheric pollution and deposition discussions focus on spatial and temporal trends of ozone pollution, and nitrogen, sulfur, and acidic deposition patterns in the region. The list of climate-, weather-, and pollution-related variables relevant to ecosystems in the region and covered in this chapter is not exhaustive. However, the list does include some of the more important climate and pollution variables that play a significant role in influencing basic ecosystem processes, species diversity, and ecosystem health in the region. In addition, an overview of potential climate changes that may occur in the region based on projections from current state-of-the-art climate models is also presented.

Definition of Climate

Weather at a particular location or over a particular region is usually highly variable, and the physical processes inherent in weather events are characterized by spatial and temporal scales that are much smaller than the spatial and temporal scales associated with climatic processes. McIntosh (1972) defines climate at a locality as the synthesis of the day-to-day values of the meteorological variables that affect the locality, where synthesis is more than just simple averaging. In other words, climate can be considered the synthesis of weather. The main meteorological variables used to define climate include precipitation, temperature, humidity, sunshine, wind speed, and wind direction. Associated with these meteorological variables are climate and weather events such as frost, extreme precipitation episodes, storms, hurricanes, tornadoes, drought, extreme maximum and minimum temperature episodes, and short- and long-term precipitation and temperature variability characteristics that also define the overall climate of a region. All of these climate and weather events that can impact a locality or region are influenced by surface characteristics such as land usage, vegetation coverage, land–water variations, lake and sea ice, and topography. The different patterns of climate- and weather-related variables that characterize a particular region are manifestations of both the large-scale state of the atmosphere and the small-scale, complex, atmospheric–surface interactions that occur continuously and everywhere.

Description of Climatic Forcing Factors

Nearly all the exchange of energy between the Earth and space is accomplished through radiative transfer processes (Wallace and Hobbs, 1977). When averaged over long periods of time, the amount of radiation absorbed by the Earth and its atmosphere is nearly equal to the amount of

radiation emitted. The energy source for driving the Earth's climate is the Sun (Trenberth et al., 1996), and the Earth–atmosphere system is very nearly in radiative equilibrium with the Sun (Wallace and Hobbs, 1977). The energy received from the Sun is spread mostly across the electromagnetic spectrum from infrared to ultraviolet wavelengths, with the bulk of the energy found in the visible portion of the spectrum (wavelengths between 0.39 and 0.76 μm). On average, the flux of energy at the top of the Earth's atmosphere is 342 $W m^{-2}$. About 31% of this incoming energy is reflected back to space due to back-scattering by aerosol particles and reflection by clouds (77 $W m^{-2}$), and reflection by the Earth's surface (30 $W m^{-2}$). The reflection of energy back to space leaves about 235 $W m^{-2}$ for warming the Earth–atmosphere system. A complete description of the Earth energy balance can be found in Kiehl and Trenberth (1997).

The energy available for warming the Earth–atmosphere system (about 235 $W m^{-2}$) is eventually radiated back to space in the form of infrared radiation. Of the 235 $W m^{-2}$ of energy available for warming the Earth–atmosphere system, about 40 $W m^{-2}$ of energy is re-emitted by the Earth's surface and moves relatively unimpeded through the atmosphere into space. The rest of the energy can mainly be attributed to (1) absorbed shortwave solar radiation by the atmosphere that is emitted as longwave radiation to space and (2) infrared radiation emitted from the Earth's surface that is absorbed by the atmosphere and re-emitted to space. However, the atmosphere also emits longwave radiation back to the Earth's surface, thereby acting to warm the Earth's surface and produce average surface temperatures much higher than what would be predicted from blackbody radiation principles alone. Although 99% of the Earth's atmosphere is composed of nitrogen (N) and oxygen (O), these gases do not absorb infrared radiation. However, water vapor, which makes up between 0 and 2% of the Earth's atmosphere, carbon dioxide (CO_2), and other trace gases in the atmosphere are important absorbers and emitters of infrared radiation. These atmospheric constituents are referred to as greenhouse gases because they act as a partial blanket for the thermal radiation emitted from the surface and produce substantially warmer surface conditions than if no greenhouse gases were present (Trenberth et al., 1996).

Atmospheric CO_2 concentrations have increased by more than 25% in the past century due in large part to the combustion of fossil fuels and the removal of forests (Trenberth et al., 1996). According to the Intergovernmental Panel on Climate Change (IPCC), projections point to a future rate of increase of CO_2 concentrations in the atmosphere such that concentrations will double from preindustrial levels within the next 50 to 100 years (Houghton et al., 1994). It has been estimated that an increase of this magnitude could lead to an average global warming of the Earth's surface on the order of 2.5°C (Houghton et al., 1990), although the estimates of future warming are still under debate by the scientific

community. Furthermore, other greenhouse gas concentrations in the atmosphere besides CO_2 are also observed to be increasing. Human activities such as biomass burning, landfill development, rice-paddy development, agricultural practices, animal husbandry, and industry contribute to enhanced atmospheric concentrations of methane (CH_4), nitrous oxide (N_2O), and tropospheric ozone (O_3). These gases tend to reinforce the changes in radiative forcing from increased CO_2 concentrations. Schimel et al. (1996) provide a summary of the known concentration trends and radiative forcing impacts of these gases.

Human activities have also affected aerosol concentrations in the atmosphere. Aerosol particles are responsible for the scattering of solar radiation back to space, which tends to cool the Earth's surface. Some aerosol particles can also absorb solar radiation, and thus increase local temperatures. Finally, many aerosol particles can act as nuclei for the formation of cloud droplets, thereby influencing cloud formation on a regional basis and the reflection and absorption of solar and infrared radiation. Each year, human activities lead to more than 350 Tg of aerosols in the atmosphere (Schimel et al., 1996). These activities include industrial emissions of dust, soot emissions from fossil fuel burning, soot emissions from biomass combustion, sulfur dioxide (SO_2) emissions (gaseous precursor of sulfate aerosols) from power stations and biomass combustion, and nitrogen oxide (NO_x) emissions (gaseous precursor of nitrate aerosols) from fossil fuel combustion. Because the residence time of aerosols in the atmosphere is short compared with many greenhouse gases, their impact is generally regional in scale (Trenberth et al., 1996; Schimel et al., 1996). The overall cooling effect of aerosols in the atmosphere can mask the warming effect of increased atmospheric CO_2 concentrations, especially on regional scales. However, their presence does not cancel the global-scale warming effects of greenhouse gases that reside in the atmosphere for long periods of time (Trenberth et al., 1996).

The presence of greenhouse gases and aerosols in the atmosphere produce large-scale changes in the radiative forcing over the entire Earth–atmosphere system. These large-scale changes in radiative forcing have the potential for altering atmospheric and oceanic dynamics. On an annual mean basis, the tropics receive more incoming solar radiation than what is emitted as longwave radiation, while the midlatitudes and high latitudes emit more longwave radiation than the shortwave solar radiation received. The net temperature gradients from the equator to the poles that exist because of this global radiation pattern produce large-scale atmospheric and oceanic circulation patterns that redistribute heat from the equator to the poles. The band of atmospheric westerlies that exists over the midlatitudes results from these temperature gradients and the Earth's Coriolis force. Within the band of westerlies, flow instabilities can develop (i.e., baroclinic instability [Holton, 1979]) that ultimately evolve into cyclones and anticyclones and migrate within the band of westerlies. We

observe migrating cyclones and anticyclones as part of our day-to-day weather experience. In addition to the large-scale radiative forcing changes and associated temperature changes that occur from enhanced greenhouse gas concentrations in the atmosphere, there exists the potential for induced changes in the patterns of cyclone and anticyclone development from enhanced greenhouse gas concentrations. Potential climate change on regional scales, such as over the northeast and north central United States, will depend to a large extent on the development and behavior of weather systems in response to the large-scale radiative forcing changes caused by elevated greenhouse gas concentrations.

Regional Climate vs. Global Climate

Climatic conditions over any region, including the northeast and north central United States, are a manifestation of both large-scale climate processes (e.g., global atmospheric circulation patterns, oceanic circulation patterns, global radiative forcing in the presence of greenhouse gases) and smaller, regional-scale climate processes that depend more on specific Earth–atmosphere interactions (e.g., topographic impacts on temperature, precipitation, and wind; land–water variations; land usage; urbanization; vegetation variations). The high degree of uncertainty in determining potential climate changes over specific regions of the Earth is due, in part, to the extreme complexity of Earth–atmosphere interactions and an inability to account for critical small-scale surface–atmospheric interactions in climate models due to computational limitations. For this reason, climate model projections such as the typical 2- to 3-°C increase in global mean surface temperatures due to elevated greenhouse gas concentrations should not be interpreted to mean that average surface temperatures over the region will also increase by 2 to 3°C. The specific surface characteristics within the region and the associated complexities of surface–atmosphere interactions and weather system development and evolution in the region affect the region's climate, and will continue to do so in the future.

Spatial and Temporal Temperature Patterns

Species composition and ecosystem structure in the northeast and north central United States and elsewhere are influenced by the atmospheric environment. This environment limits the types of species or organisms that can thrive and the amounts of plant tissues that can be sustained (Melillo et al., 1996). Descriptions of spatial and temporal patterns of near-surface maximum and minimum temperatures are critical in any assessment of the atmospheric environment and its impact on species composition and structure. The spatial and temporal patterns of temperature

in the north central and northeastern United States presented in this section are based on kriged National Climate Data Center (NCDC) daily maximum and minimum temperature data from observation sites within the Cooperative Observer Network over the period 1950 to 1993 (EarthInfo, 1995). The spatial interpolation scheme of kriging does not explicitly account for small-scale elevation variations that may exist between observation sites, which can have a major impact on diurnal temperature trends. For this reason, only the broad patterns of temperature variations are considered and discussed in this section. Any analyses and discussions of local temperature variations require the use of interpolation or modeling schemes that account for the small-scale topographic variations that exist between observation sites.

Average Daily Maximum Temperature Patterns

Average daily maximum temperature patterns over the northeast and north central United States reflect not only latitudinal variations over the region, but variations in land–water coverage, elevation, and longitude as well. Fig. 3.1 (color insert) shows the average January, April, July, and October daily maximum temperatures over the region. During the late fall and winter months, the lowest average daily maximum temperatures in the region can typically be found over the northwestern sections of the region (Minnesota and northern Wisconsin) where cold Canadian air masses moving southward have a strong influence on temperatures (Fig. 3.1a). The Great Lakes tend to moderate the southward- and eastward-moving Canadian air masses (Weisberg, 1981) so that daily maximum winter temperatures over the central and eastern Great Lakes states are somewhat higher than over the western Great Lakes states. The highest maximum temperatures during the winter months can be found over the southern tier of states in the region, with the eastern half of Virginia typically having the warmest conditions in the region. The consistently low maximum temperatures indicated over northern New Hampshire during the winter months as well as throughout the year are due to the cold conditions on Mt. Washington, where a temperature reporting station is located. The use of temperature data from this station in the kriging interpolation scheme tends to reduce interpolated maximum and minimum (discussed in the next section) temperature values in the area immediately surrounding Mt. Washington. However, the spatial influence of Mt. Washington's low maximum and minimum temperatures on the interpolated maximum and minimum temperature values in the areas surrounding Mt. Washington is minimized because the number of other reporting stations in Maine, New Hampshire, Vermont, and Massachusetts that were used to develop the kriged pattern of temperatures in the 4-state area was relatively large (50). Furthermore, only broad regional patterns are being considered in this discussion.

During the spring months, temperatures increase over the northern sections of the region, but the predominant north–south temperature gradient over the region persists (Fig. 3.1b). Unlike the winter months, when eastern Virginia typically has the warmest conditions over the entire region, the spring months usher in a more uniform longitudinal maximum temperature distribution over the southern tier of states in the region. Topographic influences on the regional-scale temperature patterns are evident in the spring months, particularly over the Appalachian Mountains in West Virginia. During the spring months, when gradually warmer conditions begin to characterize the northern sections of the region, the relatively cold Great Lakes water temperatures tend to reduce average daily maximum temperatures in the vicinity of the Great Lakes. In Michigan, for example, average daily maximum temperatures over some of the interior sections of the lower peninsula are about 2°C higher than over some areas close to the shore of Lake Michigan. The cold water in Lake Michigan and Lake Superior also reduces the maximum temperatures observed in northeastern Minnesota and the upper peninsula of Michigan.

By July, the highest maximum temperatures in the region are found in Missouri, with parts of Missouri experiencing average daily maximum temperatures near 32°C (Fig. 3.1c). Average maximum temperatures decrease from west to east over the southern tier of states, with a relative minimum in maximum temperatures persisting over eastern West Virginia and western Virginia during the summer months. Average maximum temperatures increase again from the Appalachian Mountains in these states to the Atlantic coast. The coolest sections of the region during the summer months are northeastern Minnesota, northern Wisconsin, northern Michigan, north central Pennsylvania, northeastern New York, northern New Hampshire, and northern and eastern Maine. These areas of relatively low maximum temperatures are the result of Great Lakes cooling effects, high elevations in the Appalachian Plateau and Adirondack Mountains, and normal latitudinal variations.

The fall months are characterized by a return of relatively cold conditions over the northwestern and northeastern sections of the region (Minnesota, Wisconsin, and Maine) and a maximum in temperatures over eastern Virginia (Fig. 3.1d). As air temperatures over the northern sections of the region fall below water temperatures in the Great Lakes, the modifying effects of the Great Lakes on maximum daily temperatures become more pronounced, especially over Michigan and near Lake Erie and Lake Ontario.

Average Daily Minimum Temperature Patterns

Average daily minimum temperature patterns over the northeast and north central United States are very similar to the average daily

maximum patterns. Fig. 3.2 (color insert) shows the average daily minimum temperature patterns over the region for the months of January, April, July, and October. As with the maximum temperatures during the late fall and winter months, minimum temperatures are lowest over northern Minnesota and Wisconsin (Fig. 3.2a). Northern Maine also has average daily minimum temperatures comparable to those observed in Minnesota and Wisconsin. The relatively warm water in Lake Michigan, Lake Huron, and Lake Erie during the winter months keeps the observed average minimum temperatures over much of Michigan (especially near the Lake shores) higher than at similar latitudes in the states of Minnesota and Wisconsin. Over the southern half of the region, there is a general increase in average daily minimum temperatures with decreasing latitude. However, the presence of the Appalachian Mountains in West Virginia and western Virginia leads to slightly lower average minimum temperatures in these areas compared with similar latitudes in Kentucky and eastern Virginia.

The spring and summer months of April to September are characterized by smaller overall minimum temperature variations over the entire region. For example, average daily minimum temperatures in April range from −9°C in northern New Hampshire to about 10°C in southeastern Missouri (Fig. 3.2b), compared with January average daily minimum temperatures ranging from about −24°C in northwestern Minnesota to about 0°C in eastern Virginia (Fig. 3.2a). In July, average minimum temperatures range from about 21°C in southeastern Missouri and eastern Virginia to about 6°C in northern New Hampshire (Fig. 3.2c). The spring and summer seasons are also characterized by an increase in topographic impacts on minimum temperature gradients near the southern Appalachian Mountains. A significant west-to-east minimum temperature change is clearly evident from central Kentucky through southern and western Virginia into eastern Virginia (Fig. 3.2b,c).

During the fall months of October to December, the average minimum temperature variations over the region increase over what is observed during the late spring and summer months. In October (Fig. 3.2d), average daily minimum temperatures range from about 11°C in eastern Virginia to about −3°C in northern New Hampshire. By December, average minimum temperatures range from about 0.5°C to about −20°C over the same area. From October to December, the impact of the Great Lakes on average minimum temperatures is pronounced. Across the northern half of the northeast and north central United States, average minimum temperatures are lowest over the northwestern and northeastern sections of the region. The north central portion of the region (including the state of Michigan, northern Ohio, and western New York) typically experiences minimum temperatures that are higher than at similar latitudes in the northwestern and northeastern sections of the region. The relatively warm water in Lake Michigan, Lake Huron, and Lake Erie during the fall months tends to keep nighttime temperatures higher in the

north central portion of the region than in the northwestern and northeastern sections. The warm water also tends to modify the temperatures of cold air masses that move southward into the region from Canada during the fall months. The highest minimum temperatures in the region during the fall months are typically found in southeastern Missouri, Kentucky, eastern Virginia, eastern Maryland, and Delaware.

Surface Temperature Trends

The IPCC has reported that annual, globally averaged, surface air temperature anomalies relative to average temperatures measured between 1961 and 1990 generally increased from about −0.5°C in 1890 to about 0.3°C in 1990 (Houghton et al., 1966; based on analyses of Jones, 1994). On regional scales, however, annual and seasonal temperature trends are quite variable across the globe. Over North America, the most significant observed temperature changes over the last 40 years have occurred from the north central U.S. (including the western Great Lakes area) through the northwestern sections of Canada into Alaska. Annual average surface temperatures from the period 1955 to 1974, to the period 1975 to 1994 have increased from 0.25 to 1.5°C over this region (Jones, 1994). Over the far northeastern sections of the northeast and north central United States, annual average surface temperatures have increased by about 0.25°C over the same two periods. Other sections of the region have experienced annual average surface temperature increases of less than 0.25°C.

On a seasonal basis, annual average surface temperature differences between the 1955 to 1974 and 1975 to 1994 periods over the region were largest during the winter (December to February) and spring (March to May) seasons (Jones, 1994). During the winter and spring months, the northwestern sections of the region experienced seasonally averaged temperature increases on the order of 0.25 to 0.75°C over the two periods. The far northeastern sections of the region also experienced increases on the order of 0.25 to 0.5°C. The only section of the region that experienced an overall decrease in seasonally averaged surface temperatures during the winter and spring months was the southern portion of the region extending from Illinois and Indiana southward. Over this section of the region, average wintertime surface temperatures decreased on the order of 0 to 0.25°C. During the summer and fall months, average temperature differences from the 1955 to 1974 period to the 1975 to 1994 period were generally smaller both globally and regionally. Surface temperatures averaged about 0.25 to 0.5°C warmer during the summer months (June to August) for the period 1975 to 1994 compared with the 1955 to 1974 period for most of the region. The fall season (September to November) was the only season characterized by lower average surface temperatures

during the 1975 to 1994 period compared with the 1955 to 1974 period over the region; average fall temperatures were about 0.25 to 0.5°C lower during the latter period.

Diurnal Temperature Range Trends

Several recent studies indicate that worldwide diurnal temperature ranges have decreased since 1950 (Horton, 1995; Karl et al., 1993b; Houghton et al., 1992). The decrease in diurnal temperature range can be attributed to a worldwide increase in minimum land–surface air temperatures. Karl et al. (1993b) found that minimum land–surface air temperature increases have been about twice the magnitude of maximum temperature increases. Over most of the continental U.S. and most of the northeast and north central United States, overall diurnal temperature ranges from 1981 to 1990 relative to the 1951 to 1980 values have decreased on the order of 0 to 0.5°C (Houghton et al., 1996). The observed decreases in diurnal temperature ranges over this period have been attributed to increases in cloud cover (Plantico et al., 1990; Henderson-Sellers, 1992; Dessens and Bücher, 1995; Jones, 1995). The diurnal temperature range decreases have been observed in both rural and urban areas, and thus, cannot be attributed to urban heat island effects.

Extreme Maximum Temperature Occurrences

Occurrences of extreme maximum temperatures vary considerably over the northeast and north central United States. The far western sections of the region are often influenced by continental air masses that can be very cold or warm, and minimally affected by bodies of water that tend to moderate their temperatures. Sections of the region further east are more often influenced by northward moving maritime air masses from the Gulf of Mexico that are usually warm and moist but produce fewer temperature extremes than continental air masses. The variations in extreme maximum temperature occurrences over the region based on 1950 to 1993 daily maximum temperature observations are shown in Fig. 3.3 (color insert). In this discussion, "extreme" is defined as a daily maximum temperature for a particular month greater than or equal to 11.1°C (20°F) above or below the average daily maximum temperature for that month. Although other definitions of "extreme" are possible and even statistically significant or biologically relevant, the application of the 11.1°C difference threshold across the entire region yields a general characterization of the broad baseline patterns of very high and low daily maximum temperature occurrences in the region. It is one of many ways to assess baseline maximum temperature variability in the region. Portions of northwestern and southwestern Minnesota, central and western Iowa, and eastern Missouri experienced more than 500 occurrences from 1950 to 1993 of

daily maximum temperatures greater than or equal to 11.1°C above the average daily maximum temperature for a particular month (Fig. 3.3a). This corresponds to an average of more than 11 extreme-warm events each year. The southern and Atlantic coastal sections of the region along with areas near Lake Superior and Lake Michigan experienced the fewest extreme-warm events over the 44-year period, averaging about 3 to 4 events each year. The remaining areas in the region averaged between 7 and 10 extreme-warm events per year over the 1950 to 1993 period.

It is during the period from October through May that most extremely high daily maximum temperature events occur in the region; such events are infrequent during the summer months. Beginning in October, the likelihood of extremely high maximum temperatures typically increases over western Minnesota and northern Wisconsin, and the upper peninsula of Michigan. About one event each October can be expected in these areas. Less than one event every two years during the month of October can be expected over the southern half of the region. During the months of November and December, more extremely high maximum temperature events begin to occur over portions of Iowa, eastern Missouri, and the northern Ohio River Valley. Each year, these areas typically experience 1 to 2 days during each of these months when the 11.1°C difference threshold is exceeded for daily maximum temperatures. Areas in the vicinity of Lake Superior, Lake Michigan, and the Atlantic coast tend to have fewer episodes of extremely high maximum temperatures during the winter months due to the moderating influence of these bodies of water on warm air masses that move into these regions. In January, most extremely high maximum temperature episodes tend to occur over the extreme northwestern portion of Minnesota, eastern Missouri, and the Ohio River Valley (~2 to 3 events each January). In February and March, the area of relatively frequent extreme-warm events (~2 to 3 events each month) shifts northward somewhat to encompass the region from southern Iowa and northern Missouri eastward to western Pennsylvania. By April, high maximum temperature episodes are rare in the southern-tier states of the region. Western Minnesota, northern Wisconsin, northern Michigan, central Pennsylvania, and western New York tend to experience more extreme events (~2 events) than any other portion of the region during this month. The overall impact of the month-to-month variations in high maximum temperature occurrences over the region over the 44-year period from 1950 to 1993 leads to the total extreme-event pattern shown in Fig. 3.3a.

Fig. 3.3b shows the total number of occurrences of extremely low daily maximum temperatures (≥11.1°C below the average daily maximum temperature for a particular month) over the region from 1950 to 1993. As with the extremely high maximum temperature event, this type of extreme temperature event is more likely to occur over the far western sections of

the region where continental air masses play a significant role in daily temperature trends. Between 11 and 15 episodes of extremely low maximum temperatures can be expected each year over western Minnesota, western Iowa, and western Missouri. This contrasts with most of Michigan and the Atlantic coastal region where fewer than 5 episodes typically occur each year. Extremely low maximum daily temperatures are more likely to occur during the fall, winter, and spring seasons than during the summer, although these types of episodes during the summer are more common than extremely high summertime maximum temperature episodes over the region.

Extreme Minimum Temperature Occurrences

The influence of continental air masses on extreme minimum temperature occurrences is similar to their influence on extreme maximum temperature occurrences. Fig. 3.4 (color insert) shows the distribution of extreme minimum temperature occurrences across the northeast and north central United States based on 1950 to 1993 minimum temperature observations and using a similar definition of extreme for minimum temperatures as that used for maximum temperatures (daily minimum temperatures $\geq 11.1°C$ above or below the average daily minimum temperature for a particular month). Most anomalously high and low minimum temperature episodes tend to occur in the northern sections of Minnesota and Wisconsin ($\sim$12 to 16 events each year). Parts of northern New York, Vermont, and New Hampshire also tend to experience more extreme minimum temperatures than other parts of the region. Fig. 3.4a suggests that anomalously high minimum temperatures are relatively infrequent in the Atlantic coastal states from Virginia to southern Maine, and in Michigan ($\sim$1 to 5 events each year). The typical number of yearly high minimum temperature events decreases from northern Minnesota to southern Iowa, northern Missouri, and central Illinois, but increases again over the southwestern and south central sections of the region. Analyses of the monthly patterns of anomalously high minimum temperature occurrences indicate that the maxima in yearly extreme-event occurrences over northern Minnesota, Wisconsin, New York, Vermont, and New Hampshire, as shown in Fig. 3.4a, are wintertime (December to March) events. During the month of April, anomalously high daily minimum temperatures become much less frequent over northern Minnesota; most extreme events of this type during the month of April occur in Michigan ($\sim$1 event each April). Following the summertime period when anomalously high minimum temperature events are rare over the entire region, extreme events tend to become more frequent over the western sections of the region in October ($\sim$1 event each October) and over the southern sections of the region in November ($\sim$1 to 2 events each November).

The pattern of anomalously low minimum daily temperature occurrences over the region is shown in Fig. 3.4b. The spatial variations in occurrences of this type of extreme temperature event are very similar to the variations in the anomalously high minimum temperature events shown in Fig. 3.4a. Northern Minnesota and Wisconsin, and parts of northern Vermont and New Hampshire experienced between 600 and 800 extremely low minimum temperature events over the period 1950 to 1993 (~13 to 18 events each year). Large bodies of water such as Lake Michigan, Lake Huron, Lake Erie, and the Atlantic Ocean reduce the probabilities of extremely cold conditions in western and eastern Michigan, western New York, and along the East Coast from Massachusetts to Virginia. The vast majority of extreme events of this type occur during the months of November to March over the region. For example, in the month of January, parts of northern Minnesota, northern Wisconsin, and northern New York typically experience 3 to 4 days when minimum temperatures exceed 11.1°C below normal. Other sections of the region, excluding the Atlantic coastal states from Virginia northward to Massachusetts, typically experience about two days each January when minimum daily temperatures exceed the defined extreme threshold. The Atlantic coastal section of the region typically experiences one extreme minimum January temperature event each year or every two years.

Late Spring Freeze Occurrences

The annual timing of temperature extremes is as important as the magnitude of the extremes. Freezes that occur late in the spring, after trees have begun to flush, can damage established trees, destroy seed crops, and kill regeneration. Fig. 3.5 shows an example of the effect of such freezes on shoot lengths for oak (*Quercus* spp.) and ash (*Fraxinus* spp.) seedlings in northern Wisconsin. A freeze was observed on calendar day 146 in research plots at the Willow Springs Oak Regeneration Study (Zasada et al., 1994) on the Chequamegon National Forest near Rhinelander, Wisconsin, in 1994 that killed the new growth on ash seedlings but not on oak, while a freeze on day 152 killed oak shoots. In both freezes, temperatures dropped to about −5°C at a height of 0.25 m above the ground. These observations demonstrate the impact of late spring freezes, and the variations in impact between tree species.

Fig. 3.6a is a map depicting average temperatures for late spring freezes following 250 growing degree days (GDDs), base 5°C. Fig. 3.6b is a similar map, for freezes following 300 GDDs (see color insert). Both maps show kriged data derived from NCDC records of daily maximum and minimum temperatures from Cooperative Observer Network stations for the period 1961 through 1990 (EarthInfo, 1995). The effects of proximity to large bodies of water are apparent from the maps. Regions close to

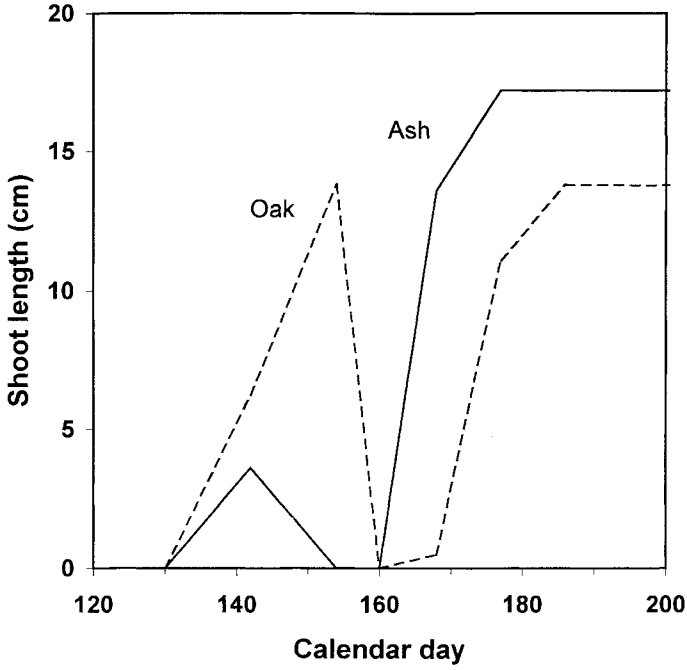

Figure 3.5. Measured oak and ash shoot lengths at the Willow Springs Oak Regeneration Study site on the Chequamegon National Forest near Rhinelander, WI from 30 April 1994 (calendar day 120) to 19 July 1994 (calendar day 200).

water are inclined to have milder freezes. Some coastal regions of New England, and the area around Sheboygan, Wisconsin, have no freezes after reaching 250 GDDs.

This lack of freezes following 250 or 300 GDDs along coastal regions (white areas in Figs. 3.6a and 3.6b) is somewhat deceptive. It does not mean that these areas are especially warm, or that they experience abrupt transitions from below- to above-freezing temperatures. Rather, they are areas that tend to warm slowly in the spring. Inland locations may reach 250 GDDs by large steps on a few days, while coastal locations do so in small steps over many days. This can be seen by comparing Fond du Lac and Sheboygan, Wisconsin. Both stations are at roughly the same latitude, yet Fond Du Lac reaches 250 GDDs on calendar day 125, while Sheboygan doesn't reach it until day 130; this 5-day difference widens to 7 days if one considers the 300-GDDs dates.

Andresen and Harman (1994) examined trends in springtime freezes in the western lower peninsula of Michigan. They found that stations in this area are reaching GDD thresholds earlier in the year than they have in the past, and that there is a trend toward more freezes occurring after a given

threshold as a result. Such a trend could lead to decreased regeneration of freeze-sensitive tree and plant species, as they are subjected to more freeze events over the years.

Midwinter Thaw Occurrences

At the opposite end of the spectrum from freezes during warm seasons are warm spells during cold seasons, that is, periods of thawing that occur in the middle of winter. Previous studies have indicated that midwinter thaws play a significant role in red spruce injury in the northeast and north central United States (DeHayes et al., 1990; DeHayes, 1992; Friedland et al., 1984). For the present discussion, a midwinter thaw is a period between December and March when the temperature rises above 0°C for at least one day, followed by the temperature dropping below −16°C at some time during the next three days. The use of these temperature thresholds is based on observed episodes associated with tree dehardening and subsequent tissue damage in the northern Great Lakes region. Fig. 3.7 (color insert) shows the distribution of the number of such thaw–freeze events occurring from December 1961 through March 1990, a total of 29 complete winters, based on NCDC records of daily maximum and minimum temperature observations from Cooperative Observer Network stations (EarthInfo, 1995). Thaw–freeze episodes of this nature are most frequent in high-elevation regions of New England, where they average two or three per year. Areas of Iowa, Minnesota, Missouri, and Wisconsin experience about one event each year, while the remainder of the region experiences less than one event per year.

Spatial and Temporal Precipitation Patterns

As with the spatial and temporal patterns of temperature in the northeast and north central United States, any assessment of the atmospheric environment and its impact on species composition and structure must include descriptions of precipitation patterns. Moisture influences a variety of fundamental ecosystem processes, including C gain through photosynthesis and C loss through respiration (Melillo et al., 1996). Species distributions across the region are, in part, the result of characteristic precipitation patterns that occur. Extreme precipitation events or drought episodes can have significant impacts on ecosystem health and modify landscapes in the region. There are also social and economic implications of the typical and anomalous precipitation patterns that occur in the region (e.g., human responses to severe flooding or drought).

The spatial and temporal precipitation patterns discussed in the following sections are based on kriged daily precipitation data from the NCDC for the years 1950 to 1993 (EarthInfo, 1995). Because local

elevation changes can influence precipitation amounts (Daly et al., 1994; Groisman and Easterling, 1994), only the broad precipitation patterns over the region are assessed; local topographic influences on local precipitation amounts at locations between reporting stations are not explicitly accounted for in the kriging interpolation scheme. As shown in the figures in the following sections, the spatial influence of precipitation observations at individual reporting stations (e.g., Mt. Washington in New Hampshire) on the kriged precipitation patterns in the vicinity of the stations is minimized because of the relatively large number of reporting stations in each state. Again, only the broad patterns of precipitation are assessed in this discussion; sporadic and isolated precipitation maxima and minima that appear across the region are not the focus of the discussions in the following sections.

Average Monthly Precipitation Patterns

Precipitation patterns over the northeast and north central United States are highly variable. Fig. 3.8 (color insert) shows the average monthly precipitation amounts over the region for the months of January, April, July, and October. During the winter months, monthly precipitation amounts generally increase from northwest to southeast over the western half of the region (Fig. 3.8a). Average monthly precipitation amounts are generally less than 38 mm over Minnesota, Wisconsin, Iowa, and the northern sections of Illinois and Missouri during January and February, while maximum winter precipitation between 76 to 127 mm occurs over Kentucky, West Virginia, the southern portions of Illinois, Indiana, and Ohio, and along the Atlantic coast. The Great Lakes exert a strong influence on wintertime precipitation over the states of Michigan, northeastern Ohio, western Pennsylvania, and western New York. Relatively warm water during the winter tends to increase atmospheric instability over the Great Lakes, thereby increasing the probability of lake-effect snow events to the south of Lake Superior, east of Lake Michigan, and east of Lake Erie and Lake Ontario (Paulson et al., 1991). The Appalachian Mountains also exert an influence on wintertime precipitation. Precipitation amounts are larger along the western slopes of the Appalachian Mountains in winter, especially in West Virginia and western Pennsylvania. Drier conditions prevail near the eastern slopes of the mountains, especially in central Virginia, Maryland, Pennsylvania, and New York. Average monthly winter precipitation amounts increase from the eastern slopes of the Appalachian Mountains to the Atlantic coast.

During the spring months, precipitation amounts increase over the northwestern sections of the region (Fig. 3.8b), with an accompanying westward and northward shift of the wintertime precipitation maximum over Kentucky to the western sections of Missouri, and the states of Iowa,

eastern Minnesota, western Wisconsin, and northern Illinois by June. Precipitation maxima and minima persist over the western and eastern slopes of the Appalachian Mountains, respectively, during the spring months. The increased heating of the Earth's surface during the spring months increases the probability of atmospheric convective activity and thunderstorm development over the western sections of the region. Warmer air masses during the spring months are able to hold more moisture so that precipitation events associated with the passage of frontal boundaries in the region can be more significant than winter precipitation events. The Great Lakes exert an opposite influence on precipitation amounts than that which occurs during the winter months. Great Lakes water temperatures tend to be lower than adjacent land temperatures during the spring and summer months. This inhibits atmospheric convective activity over the Great Lakes and leads to diminished precipitation amounts in Michigan and western New York by late spring. The precipitation maxima along the Atlantic coast also disappear by late spring. By June, the driest conditions in the region typically occur over the northeastern sections of Michigan and most of Virginia.

In July, central Michigan is typically the driest section in the region due to the influence of Lake Michigan (Fig. 3.8c). Relatively dry conditions also tend to prevail over western New York and the eastern slopes of the Appalachian Mountains. The region of maximum precipitation covers a broad area from the western slopes of the Appalachian Mountains (West Virginia, western Pennsylvania, and eastern Kentucky) through the Ohio River Valley to Illinois, northern Missouri, Iowa, Wisconsin, and eastern Minnesota. Maxima also occur in eastern Pennsylvania, New Jersey, eastern Maryland, Delaware, and northern New Hampshire. During the midsummer to late summer months, the driest conditions in the region occur over the northern Ohio River Valley, western Minnesota, and the eastern slopes of the Appalachian Mountains. By September, the largest precipitation amounts occur in northern Wisconsin, western Missouri, northeastern New York, eastern Pennsylvania, and northern New Hampshire.

During the fall months, precipitation maxima return to the southern and Atlantic coast states in the region (Fig. 3.8d). Relatively dry conditions reappear over the northwestern sections of the region (Minnesota, Wisconsin, and Iowa). The fall months also bring a return to enhanced precipitation over western Michigan and parts of western New York in response to the relatively warm water temperatures in Lake Michigan and Lake Erie. The accumulated effect of the average monthly precipitation patterns over the region is shown in Fig. 3.9 (color insert), which depicts the average yearly precipitation amounts over the region. The largest yearly precipitation amounts extend in a band from western Pennsylvania through West Virginia and Kentucky into southeastern Missouri. The year-around influence of the Appalachian Mountains

produces a "precipitation shadow" effect along the eastern slopes of the mountains. Yearly precipitation amounts increase as you move eastward from this relatively dry region to the Atlantic coast. On a yearly basis, Minnesota, northwestern Iowa, and eastern Michigan are the driest sections in the region.

Recent Precipitation Trends

There have been numerous studies performed recently that have examined various precipitation trends over large geographical regions. Diaz and Quayle (1980) performed time series analyses of U.S. precipitation data weighted by area and found relatively large and statistically significant increases in contemporary (1955 to 1977) mean autumn precipitation over the 1895 to 1920 mean autumn precipitation for the states of New York, Pennsylvania, West Virginia, Maryland, and Virginia. More recently, Groisman and Easterling (1994) analyzed precipitation data from Canada and the United States over the past 100 years and found that annual precipitation has increased in southern Canada to the south of 55°N by 13% and increased by 4% in the contiguous United States. They determined that these precipitation increases can be attributed mainly to precipitation increases that have occurred in eastern Canada and the adjacent northern regions of the United States, which includes states within the region.

Karl et al. (1993a) found a 2 to 3% per decade increase in annual precipitation over the contiguous United States in the past four decades. They also found that the interannual variability of the ratio of solid to total precipitation increased substantially during the 1980s. In analyzing snow-cover trends over North America, they identified several temperature-sensitive snow-cover regions where area-averaged maximum temperature, snow cover, and snowfall are highly correlated with each other. The western sections of the region, including the states of Indiana, Illinois, Wisconsin, Minnesota, and Iowa fall within a December to March temperature-sensitive snow-cover region, while the New England states fall within the boundaries of an April to May temperature-sensitive snow-cover region. Karl et al. (1993a) found after analyzing 19 years of North American snow-cover climatology that decreases in snow-cover extent occur simultaneously with increases in North American temperatures, and that a global warming of 0.5°C could result in roughly a 10% decrease in the mean annual North American snow-cover extent. The previously noted states within the region would likely experience this potential snow-cover retreat.

Vining and Griffiths (1985) examined the precipitation variability from decade to decade at 10 stations located across the U.S. for the period 1890 to 1979. Three stations in their analysis were within the region: Minneapolis, Ann Arbor, and New York City. Regression lines of decadal precipitation variances indicate a slight increase in precipitation

variability over the period of record for most of the United States. The observed changes in variances for the three stations in the region as measured by regression coefficient magnitudes were larger than the U.S. average, although none of the trends was statistically significant.

Nicholls et al. (1996) reported global trends in precipitation over the last half of this century as well as changes over the entire century using two data sets: "Hulme" (Hulme, 1991; Hulme et al., 1994) and the "Global Historical Climate Network" (Vose et al., 1992; Eischeid et al., 1995). Increases in precipitation from the period 1955 to 1974 to the period 1975 to 1994 have occurred over most continents with the notable exceptions of central Africa and west central South America, where decreases as high as 50% have been observed. Precipitation increases at the higher latitudes are clearly evident. Average precipitation increases on the order of 10% have occurred over the north central and northeastern United States during this period. Over the period 1900 to 1994, the north central and northeastern United States experienced an average increase in precipitation on the order of 2 to 5% per decade.

Karl and Knight (1998) examined 20th century trends of precipitation amount, frequency, and intensity across the United States. Their analyses indicate that precipitation has increased by about 10% across the contiguous United States and that the increase can be attributed mainly to increases in heavy and extreme daily precipitation events (upper 10% of all daily precipitation amounts). Within the region, this upward trend is most evident over states in the northwestern part of the region (Minnesota, Wisconsin, Michigan, and Iowa) and over the New England states in the spring, summer, and autumn seasons.

Extreme Precipitation Occurrences

The occurrence of heavy or extreme precipitation events is also an important climatic factor that impacts the natural, social, and economic resources of the northeast and north central United States. Heavy or extreme precipitation events are generally associated with thunderstorm activity or hurricane movement into the northeastern region of the United States. However, prolonged or frequent periods of lesser amounts of precipitation can also adversely impact resources in the region. The extreme flooding in the eastern Dakotas and western Minnesota during the spring of 1997 was the result of an unusually large number of snowstorms and blizzards that cumulatively produced record or near-record snowfall amounts for the winter season. As one indicator of the spatial variability of extreme precipitation over the region, Fig. 3.10 (color insert) shows the number of extreme precipitation occurrences during the months of January, April, July, and October over the period 1950 to 1993, where extreme is defined as daily events that result in at least 5.08 cm of liquid precipitation. Data for Fig. 3.10 were obtained from NCDC daily

precipitation observations from stations in the Cooperative Observer Network within the region (EarthInfo, 1995). Although this definition of extreme is one of many that could be utilized and it biases the analysis toward liquid precipitation events, the analysis does provide a regional assessment of one form of extreme precipitation occurrence that influences basic ecosystem processes, particularly during growing seasons.

As expected in this type of analysis, extreme daily precipitation events are generally confined to the southern and Atlantic coastal sections of the region during the winter months (Fig. 3.10a). Over the 44-year period, about 10 to 15 extreme events have occurred during January, February, and March individually over parts of Kentucky and the southern sections of Illinois, Missouri, and Indiana. Connecticut, Massachusetts, and the Mt. Washington region of New Hampshire also experienced relatively large numbers of extreme wintertime precipitation events over the 44-year period. Extreme events in most of the other sections of the region were fairly rare.

During the months of April, May, and June, more extreme precipitation events tend to occur in the western and northwestern sections of the region. In early spring (Fig. 3.10b), the area of increased probability of extreme precipitation expands northward from Kentucky and southern Missouri to encompass much of Illinois and Iowa. By June, more extreme precipitation events tend to occur in northern Missouri, Iowa, and Minnesota, as opposed to the wintertime pattern in which most of the extreme events occurred in Kentucky and southeastern Missouri. The northward and westward propagation of this extreme precipitation maximum is the result of springtime thunderstorm development over the central United States. Much of the northern sections of the northern-tier states (Minnesota, Michigan, New York, Vermont, and Maine) in the region are characterized by infrequent extreme precipitation events during the spring. West Virginia has also experienced relatively few springtime extreme precipitation events over the 44-year period. During the month of June, there is a general decrease in frequency of extreme events as you move eastward from the states of Minnesota, Iowa, and Missouri, to the Ohio River Valley, and then a general increase in the frequency of extreme events as the Atlantic coast is approached. However, the nature of the extreme events in the eastern sections of the region in June is quite spotty in comparison with the large area of maximum extreme events in the western sections of the region.

The summer months of July, August, and September typically bring on more frequent extreme precipitation events along the Atlantic coast from Virginia to Massachusetts. Hurricane occurrence and the potential for hurricane landfall along the eastern U.S. coast are greatest during the late summer and early autumn months (NOAA National Hurricane Center, 1999). Numerous extreme precipitation and flooding events associated with hurricanes tracking along the eastern U.S. coast or making landfall

have been recorded during the 20th century (Paulson et al., 1991) and contribute to this overall pattern of extreme precipitation occurrence in the region. It is noteworthy that in the state of Virginia, average summertime precipitation is relatively low in comparison with adjacent states (see Fig. 3.8c) and yet a relative maximum in extreme precipitation events exists over a significant portion of the state. The springtime maximum in extreme events over the western sections of the region is also prevalent in the summer months (Fig. 3.10c), although by September, less frequent extreme events characterize Minnesota and northwestern Iowa. In July, Michigan, New York, northern Vermont, and Maine are characterized by few extreme events in comparison with other states in the region. In August and September, Ohio shows a decline in the number of extreme events over the number occurring in July.

The spatial patterns of extreme precipitation occurrence for the fall months of October, November, and December reveal a transition from the summertime to wintertime patterns. With the onset of colder temperatures in the northern sections of the region, extreme precipitation events become much less frequent. By October (Fig. 3.10d), extreme precipitation maxima in the western sections of the region are confined to western Missouri, while in the eastern part of the region, maxima cover the Atlantic coastal states of Virginia, Delaware, New Jersey, Connecticut, Rhode Island, Massachusetts, and southern Maine. Between these sections of extreme precipitation maxima, few extreme events have occurred, particularly in West Virginia, Ohio, Michigan, Wisconsin, Iowa, and Minnesota. In November and December, there is a return to the wintertime pattern discussed previously, in which most prevalent extreme precipitation occurrences are in Kentucky and the New England coastal sections.

Floods

Floods are the result of weather phenomena that deliver more precipitation to a drainage basin than can be stored or absorbed by the basin (Hirschboeck, 1991). Included in these weather phenomena are convective thunderstorms, hurricanes, and frontal passages. The sources of atmospheric moisture for these weather phenomena are mainly oceans and lakes. Hirschboeck (1991) presented an overview of the primary large-scale moisture delivery pathways over the United States. For atmospheric moisture moving over the conterminous United States, the primary air-mass source regions are the Pacific Ocean, the Atlantic Ocean, the Gulf of Mexico, and the Arctic Ocean. The Great Lakes are also a source of moisture for air masses moving over the north central and northeastern United States. There is a seasonal dependence of atmospheric moisture transport from the source regions to the different sections of the United States, which in turn affects the average precipitation, streamflow, and

flooding characteristics across the United States. During the winter months, most moisture delivery pathways over the region originate from air masses situated over the north central and northeastern United States. The southeastern portions of the region are also typically influenced by moisture originating from the Gulf of Mexico. During the spring months, the northward transport of Gulf moisture intensifies, leading to much of the southern and eastern sections of the region being influenced by weather phenomena containing moisture from the Gulf of Mexico. The northern-tier states in the region are typically influenced by the southward transport of moisture from the Arctic Ocean region in early spring, although the cold air masses originating over the Arctic Ocean region have much lower moisture contents than the Gulf air masses. During the summer, the entire eastern half of the United States is dominated by precipitation events in which the moisture has been transported northward from the Gulf of Mexico. The average precipitable water associated with these summertime air masses originating over the Gulf of Mexico is significant. The fall months in the region are also dominated by Gulf-influenced precipitation events. However, moisture originating from the Pacific Ocean may be a factor in some precipitation events over the region, particularly over the western Great Lakes section.

The occurrence of significant precipitation and associated floods depends on appropriate atmospheric uplifting mechanisms that lead to condensation and cloud formation. Convective processes such as thunderstorms, mesoscale convective systems, and convection due to orographic lifting can lead to precipitation events that cause local or widespread flooding. Thunderstorms are primarily responsible for flash flooding in small drainage basins (Hirschboeck, 1991) and their occurrence over the region is seasonally dependent. The average number of days during which thunderstorms develop ranges from less than one over the northern-tier states in the region during the winter months to between 10 and 25 days over the entire region during the summer months (Hirschboeck, 1991).

Unlike typical short-duration thunderstorms that have an areal extent less than 100 km^2 and the potential for mainly localized flooding, longer-lasting mesoscale convective complexes (MCCs) typically have areal extents up to 200,000 km^2 and can cause severe flash flooding (Bosart and Sanders, 1981; Maddox, 1983). Mesoscale convective complexes are defined as large, highly organized, multiple-celled, and convectively induced thunderstorm systems lasting longer than 6 hours with cloud shields having an area greater than or equal 100,000 km^2, infrared cloud-shield temperatures less than or equal to −32°C, and interior cloud region temperatures less than or equal to −52°C. Almost 1 of every 4 MCCs results in injuries or fatalities, and they can produce other weather phenomena, such as tornadoes, hail, high winds, and intense electrical storms. Numerous MCCs have been documented over the midwestern

United States, mainly during the spring and summer months. During the spring months, most complexes tend to occur over the south central United States and the southwestern sections of the region. During the summer months, MCCs are prevalent over the Great Plains and the western sections of the region. The summertime pattern of MCCs is consistent with spatial patterns of summertime extreme precipitation occurrences as shown in Fig. 3.10c. The fall months are characterized by many fewer MCCs, although the fall MCCs that have been previously documented tend to occur mainly over the western Great Lakes section of the region.

Another type of convective system that can produce massive amounts of precipitation and significant flooding is the mesoscale convective system (MCS). Chappell (1986) defines an MCS as a multicell storm or group of interacting storms that have organized features, such as a squall line or a cluster of thunderstorms. Slow-moving MCSs have been responsible for some of the most severe localized flooding on record (Hirschboeck, 1991). For example, the July 1977 floods in western Pennsylvania were the result of a quasi-stationary MCS.

The movement of extratropical cyclones through the region also has the potential for causing major flooding in large drainage basins. Unlike many convective thunderstorms that develop within a single air mass, precipitation associated with extratropical cyclones is dependent on increased atmospheric instability due to the convergence of different air masses at frontal boundaries. There are seasonally dependent preferred tracks of extratropical cyclone movement over the conterminous United States, and many of these tracks directly impact the region. In the northeastern United States, significant winter precipitation can result from extratropical cyclones originating over the eastern Rocky Mountain region and western Canada, as well as cyclones that originate along the Atlantic coast and track northeastward along the coast, sometimes creating coastal storm surges. In the spring months, extratropical cyclone paths tend to shift slightly northward. The increased heating during the spring months compared with wintertime heating leads to greater density variations in converging air masses associated with extratropical cyclones. This fact in addition to more precipitable water being available in warmer air masses is the reason springtime extratropical cyclones usually result in much larger precipitation amounts than wintertime extratropical cyclones. Saturated soils, frozen ground surfaces, and concurrent snowmelt during the passage of extratropical cyclones over the region in the spring can increase the flooding potential. During the summer, cyclone paths are mainly confined to the northern states and Canada. Precipitable water contents are large during the summer months, enhancing the potential for flooding in the region. Extratropical cyclone paths in the fall shift slightly southward from the preferred summertime paths, and flooding is somewhat less common because of typically lower precipitable water contents in the cooler fall months.

Precipitation associated with orographic lifting is an important atmospheric process in certain sections of the region. Air masses originating over the Gulf of Mexico or the Atlantic Ocean that are forced up the slopes of the mountainous terrain in the eastern United States can produce significant precipitation and local flash floods. Frequent orographic lifting of air masses during winter in the Appalachian Mountain section of the region can lead to significant accumulations of snow. Widespread flooding during spring snowmelt is possible in this region.

Because many of the states within the region experience significant snowfall during the winter and spring months, flooding can be a direct consequence of the melting of accumulated snow. Flooding can be made more adverse when the ground is frozen or when rain falls on snow, thereby enhancing snowmelt. Over most of the region, winter and spring flooding is most often the result of rain from extratropical cyclones falling on frozen ground covered with snow in conjunction with ongoing snowmelting. Most of Minnesota, northwestern Wisconsin, the western part of the upper peninsula of Michigan, and the northern half of Maine average more than four months of frozen ground per year, while average snow depths in these regions and over much of Michigan, Pennsylvania, part of West Virginia, New York, and the rest of the New England states exceed 101 cm per year (Hirschboeck, 1991).

The northeast and north central U.S. region has experienced numerous floods this century. A compiled listing of some of the major floods that have occurred in each state within the region can be found in Paulson et al. (1991).

Droughts

Many definitions of drought have been proposed, although most definitions refer to abnormal dryness (McNab and Karl, 1991). Mather (1974) defined drought as a phenomenon that occurs when the supply of moisture from precipitation or that stored in the soil is insufficient to fulfill the optimum water needs of plants. Changnon (1987) points out that the definitions of drought are dependent on specific components of the hydrologic cycle, including precipitation, surface runoff, soil-moisture storage, streamflow conditions, and groundwater availability. Precipitation deficits are usually the first indicators of drought occurrence, while streamflow and groundwater levels often respond to these precipitation deficits much later and are usually the last indicators of drought occurrence.

Precipitation deficits and associated droughts that periodically occur in different regions of the country are manifestations of the atmosphere's large-scale general circulation (Namias, 1983). There are specific circulation patterns that can lead to prolonged periods of below-normal precipitation over certain regions of the United States. The atmospheric mechanism responsible for most drought episodes is persistent subsidence

of air. This air warms during subsidence, and the relative humidity of the air is low. Over the Great Plains, including the western states in the region (Minnesota, Iowa, and Missouri), summer drought is most often associated with a deep warm anticyclone situated over the central United States. Westerlies along the northern U.S. border often bring additional dry subsiding air into the anticyclone system (Namias, 1983). This atmospheric circulation pattern results in high surface temperatures over the Great Plains and low relative humidity throughout the lower troposphere.

Droughts over the eastern sections of the region are typically caused by different types of atmospheric circulation patterns. Namias (1983) noted that drought in the northeastern United States can occur during a persistent northward displacement of the jet stream, which can lead to sinking motion south of the jet stream over the northeastern United States. Another drought-producing mechanism identified by Namias (1983) in the northeastern United States. is increased cyclonic activity off the northeastern U.S. coast. Temperatures are typically cooler than normal during drought periods associated with this circulation pattern. A third type of circulation pattern that often leads to reduced precipitation over the eastern half of the region is characterized by the westward propagation of the Bermuda high pressure system into the southeastern United States. This westward shift can result in dry conditions over the southeastern and northeastern U.S. because the northward transport of moisture from the Gulf of Mexico by southerly winds to the west of the high pressure system is too far to the west for precipitation to occur in these regions. This particular pattern has also been identified by Heilman (1995) as being conducive to severe wildfire occurrence in the southeastern and northeastern United States.

One particularly useful measure of drought severity is the Palmer Drought Severity Index (PDSI) developed by Palmer (1965). This index takes into account the different degrees of dryness required for drought to occur in regions having different average precipitation amounts, where the criterion for drought is a "deviation from normal experience" (Mather, 1974). Drought severity as measured by the PDSI is based on the numerical values of the index. Positive values of the PDSI indicate an excess of soil moisture, values of 0 to −0.5 are considered near normal, −0.5 to −1 indicate an incipient drought, −1 to −2 indicate a mild drought, −2 to −3 indicate a moderate drought, −3 to −4 indicate a severe drought, and −4 or below indicate an extreme drought. The National Drought Mitigation Center (1997) has provided decade-long analyses of severe or extreme drought occurrence (PDSI ≤ -3) in each climate division across the U.S. for much of the 20th century. In the 1940s, drought occurrence in the northeast and north central United States was relatively rare, with severe or extreme drought only affecting the western and far northeastern sections of the region less than 20% of the time. Western Montana, southern Arizona, and southwestern Kentucky were the driest parts of the

country during this decade. The western sections of the region experienced more drought conditions in the 1950s. Climate divisions in southern Iowa and western Missouri experienced severe or extreme drought conditions between 30 and 50% of the time in the 1950s. This drought pattern was part of a larger drought pattern that characterized most of the southern Great Plains and parts of the Rocky Mountain states. In the 1960s, more climate divisions in the northern and northeastern sections of the region experienced drought conditions. Climate divisions in southern Wisconsin, northeastern Illinois, southern Michigan, northwestern Ohio, and most of the New England states experienced drought conditions between 20 and 30% of the time. Drought conditions during the 1970s were not common throughout the region. Only a few climate divisions in the northwestern sections of the region experienced drought conditions more than 10% of the time. The 1980s were also characterized by infrequent drought conditions in the region. Even though 1988 was a year of extreme drought in the Great Plains, the entire decade of the 1980s was marked by only the western sections of the region experiencing drought conditions between 10 and 20% of the time, with two climate divisions in Minnesota and one in Illinois experiencing drought more than 20% of the time. Between 1990 and 1995, severe or extreme drought was rare in the region.

Great Lakes Water Levels

Water levels in the Great Lakes are a useful indicator of the long-term precipitation and evaporation trends for a large portion of the region. Since the late 1960s, water levels in Lake Michigan, Lake Huron, and Lake Erie have been above the long-term averages (Nicholls et al., 1996). Since 1988, water levels in Lake Superior have been slightly below normal. Changnon (1987) examined climate fluctuations and changes in Lake Michigan water levels, and found that the record high water levels observed during 1985 and 1986 were due mainly to above-normal precipitation since 1981. A decrease in evapotranspiration across the Lake Michigan basin resulting from increased cloudiness and a decrease in observed temperatures since about 1940 was also found to have contributed to higher water levels in Lake Michigan. Changes in Great Lakes water levels can have both positive and negative impacts. For example, impacts on shipping, hydropower, and recreational boating can be positive when water levels increase. In contrast, high water levels can have an adverse effect on shorelines and numerous environmental conditions (Changnon, 1987).

Short-Term Precipitation Variability Patterns

Weather patterns responsible for local and regional precipitation events have relatively short time scales. Convective thunderstorms, cyclones,

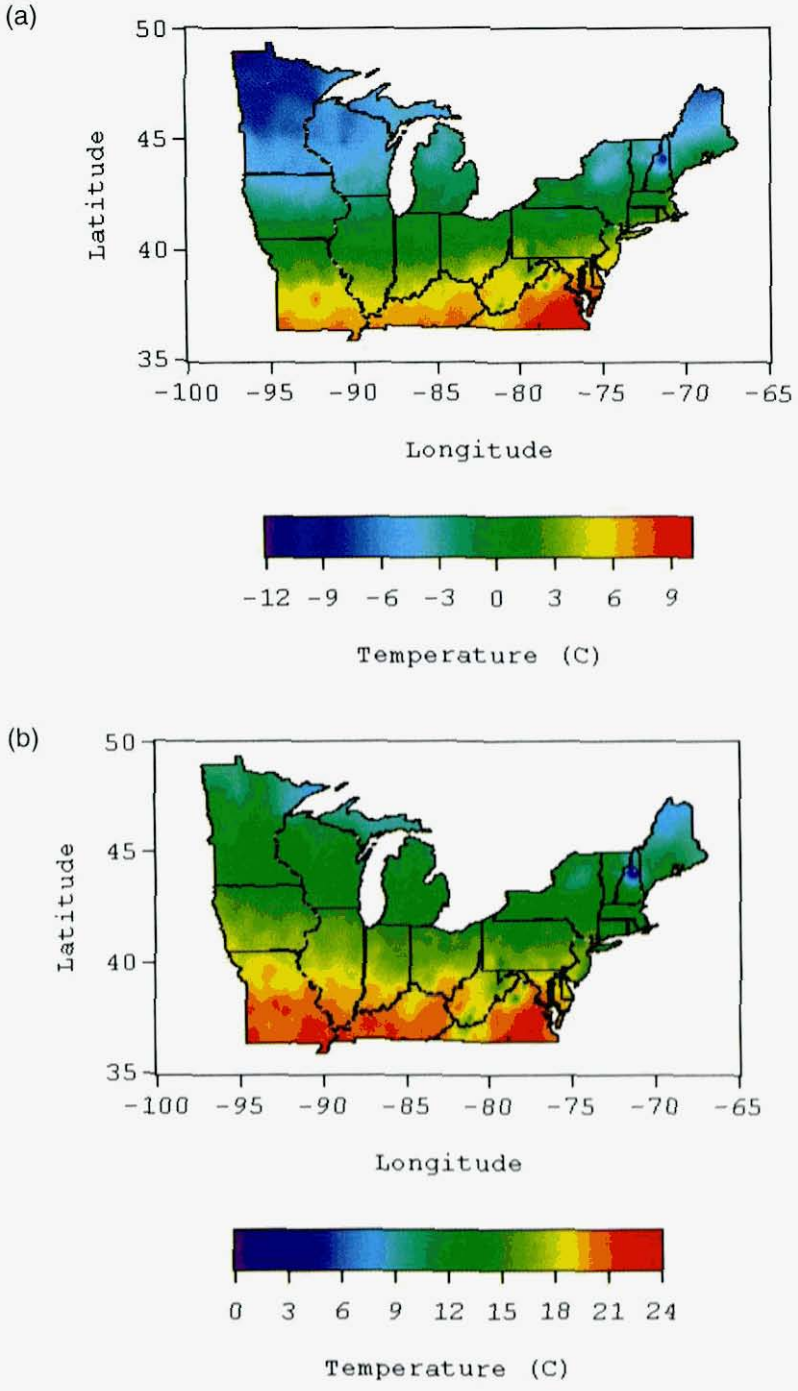

Figure 3.1. Average daily maximum temperatures (°C) in the region during the months of (a) January, (b) April, (c) July, and (d) October based on maximum temperature observations from 1950–1993. *(Continued)*

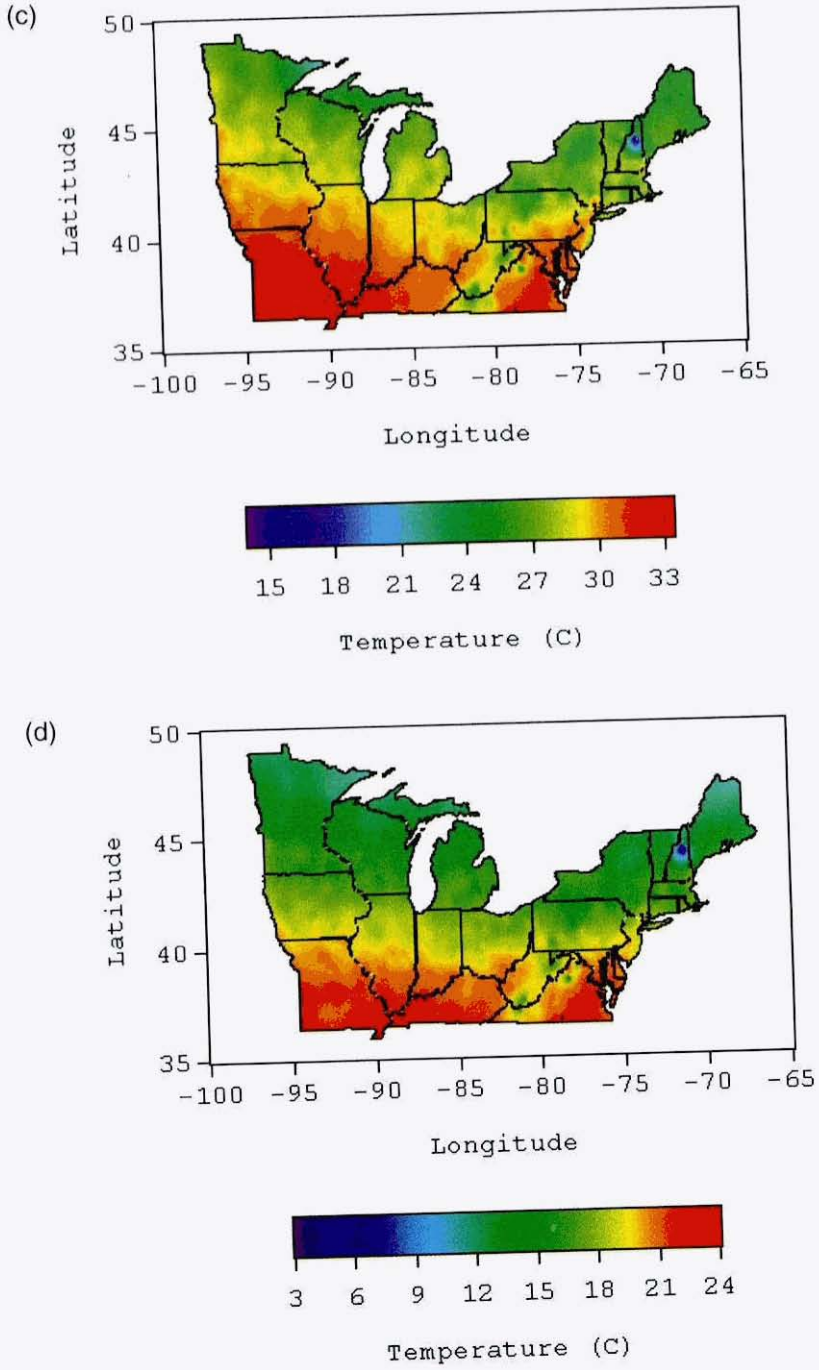

Figure 3.1c,d (*Continued*).

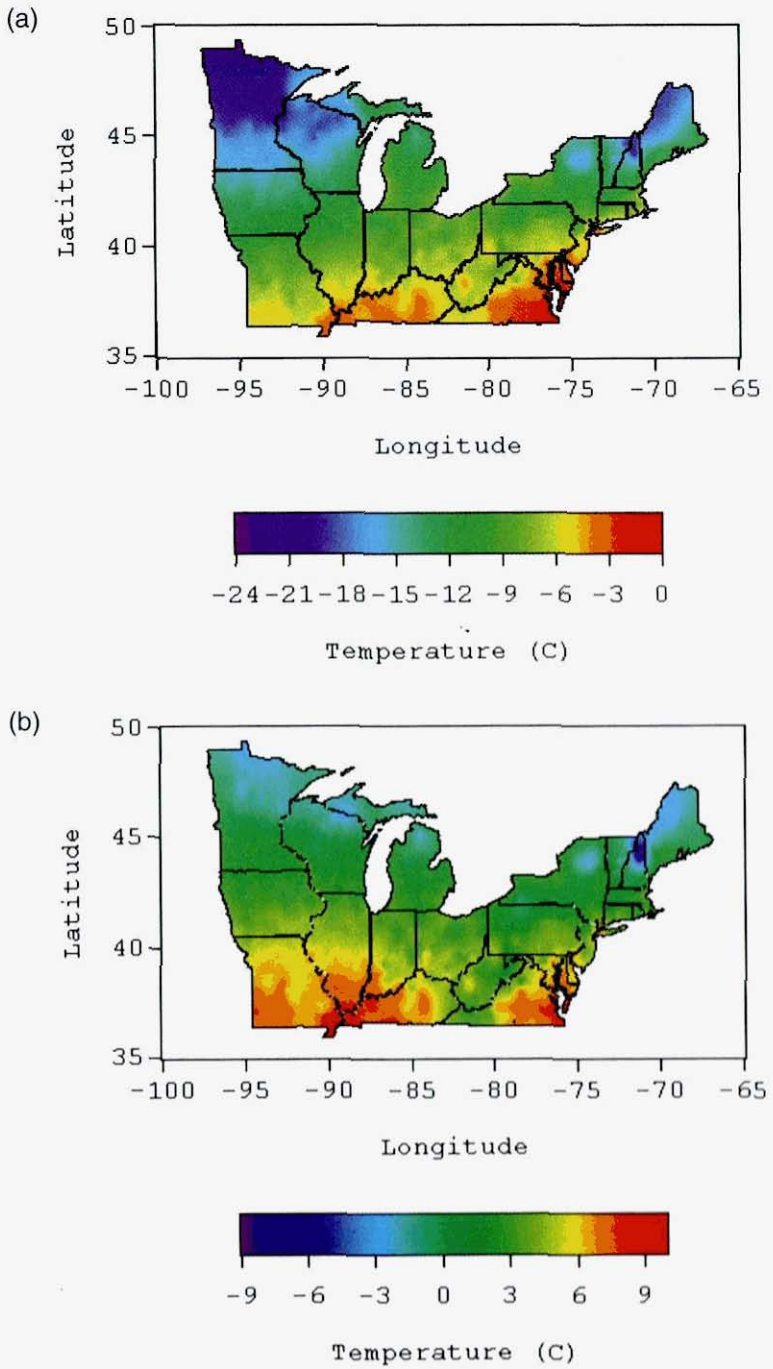

Figure 3.2. Average daily minimum temperatures (°C) in the region during the months of (a) January, (b) April, (c) July, and (d) October based on minimum temperature observations from 1950–1993. *(Continued)*

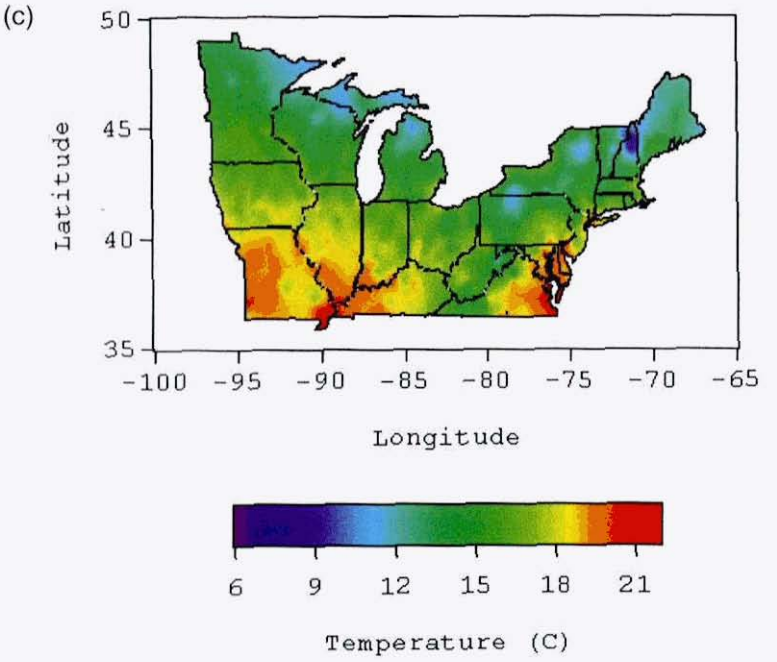

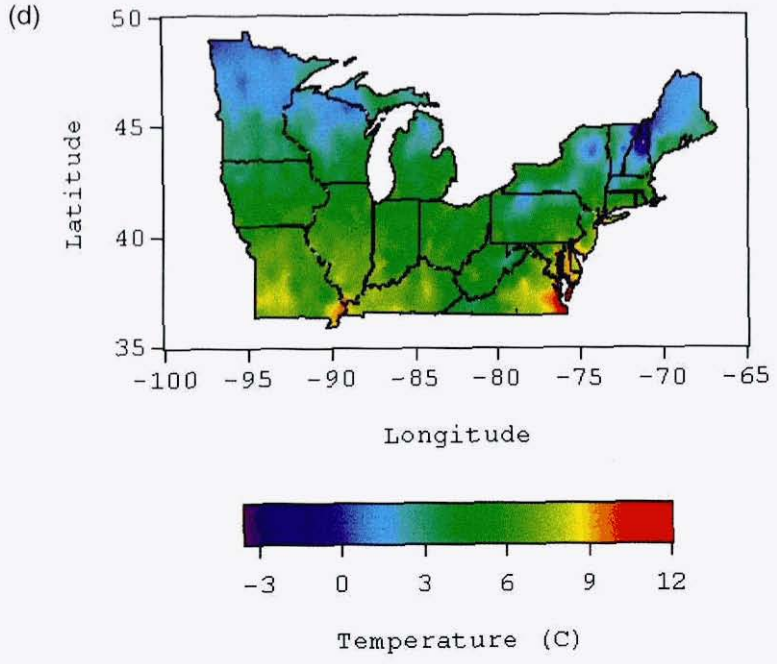

Figure 3.2c,d (*Continued*).

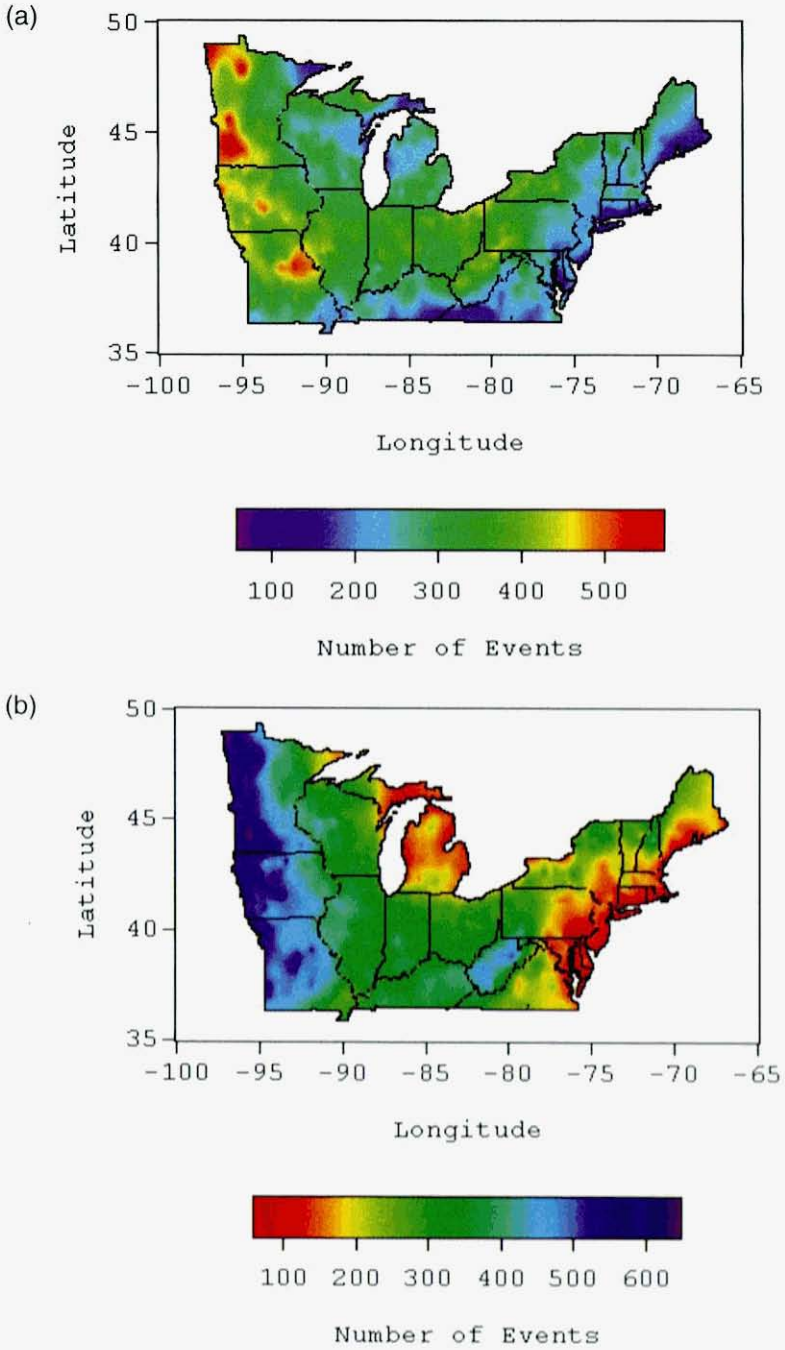

Figure 3.3. Total number of days when daily maximum temperatures exceeded 11.1°C (a) above normal and (b) below normal in the region for the period 1950–1993.

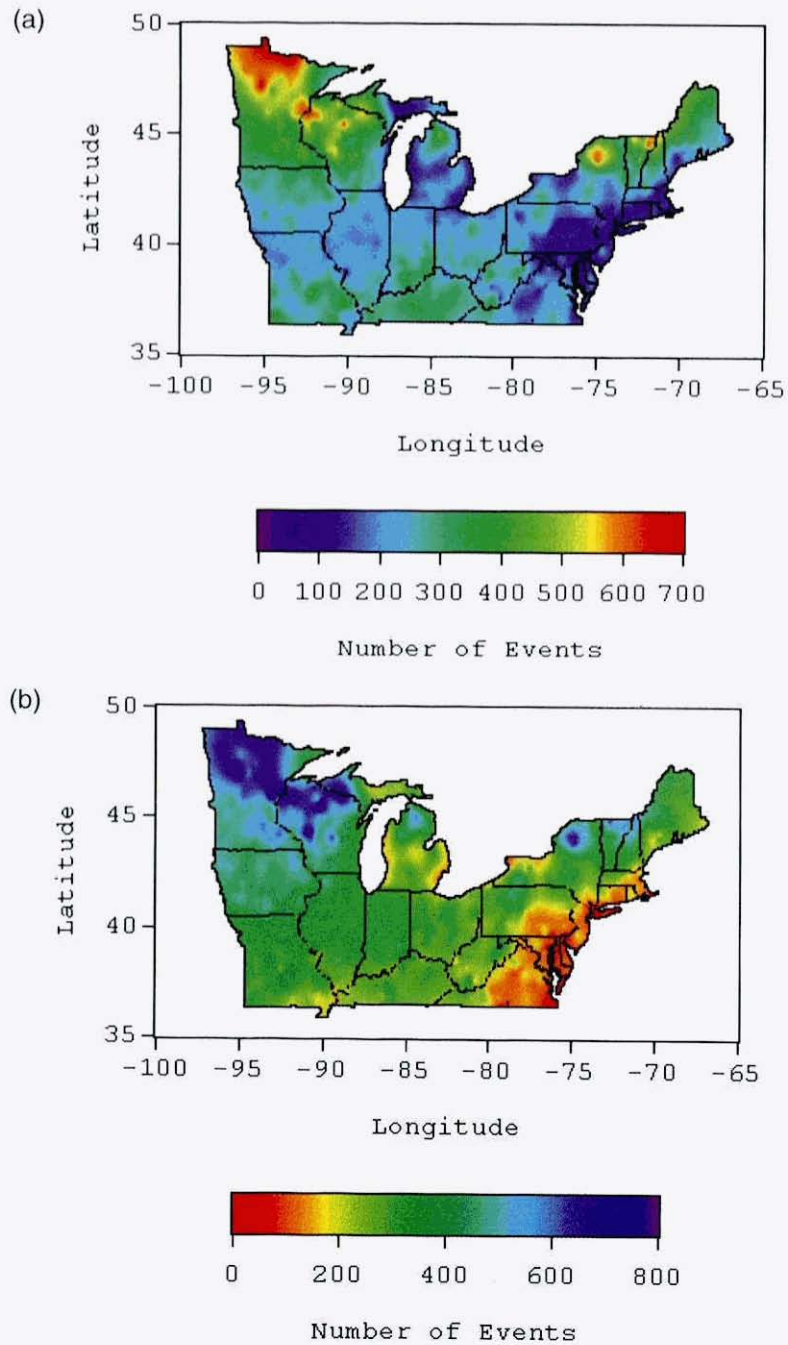

Figure 3.4. Total number of days when daily minimum temperatures exceeded 11.1°C (a) above normal and (b) below normal in the region for the period 1950–1993.

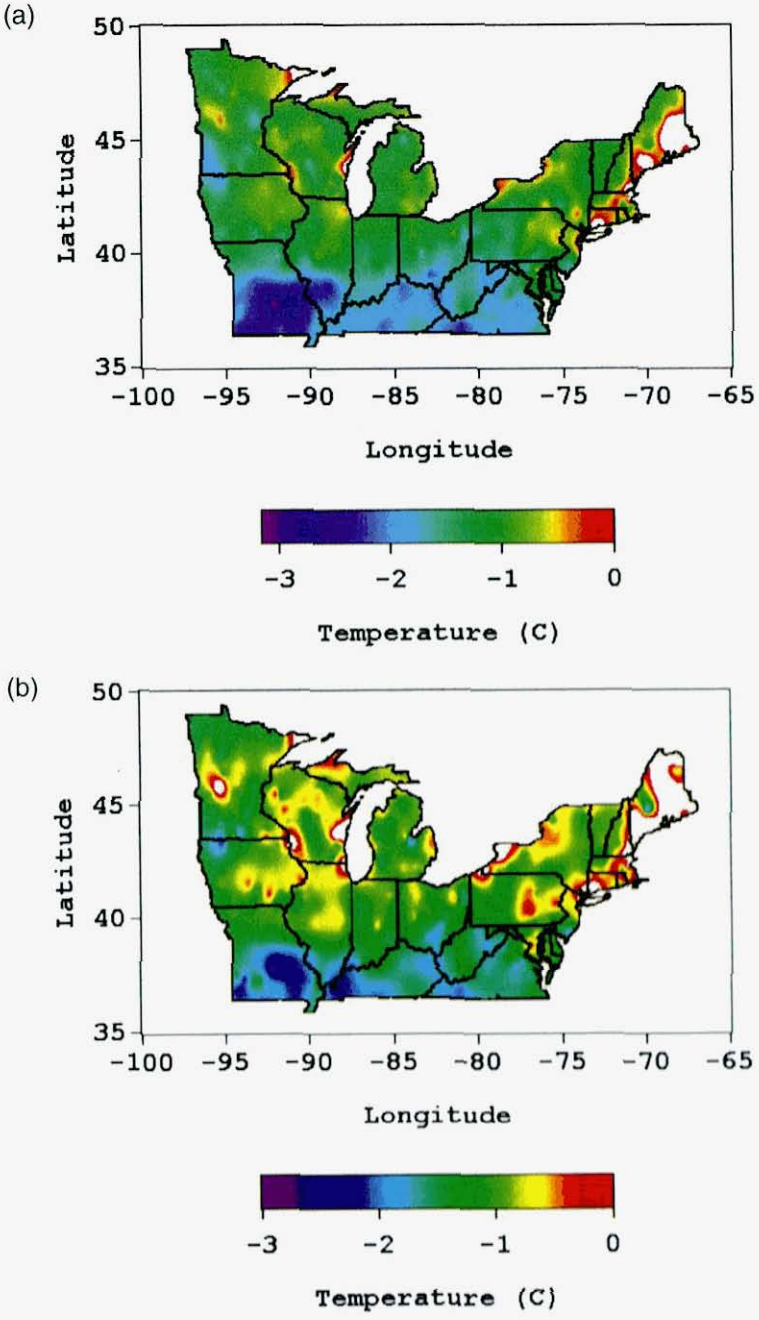

Figure 3.6. Average late-spring freeze temperatures (°C) over the region following (a) 250 growing-degree days and (b) 300 growing-degree days (base 5°C). Areas where no late-spring freezes occurred following 250 or 300 growing-degree days over the period 1961–1990 appear as white areas in the figure.

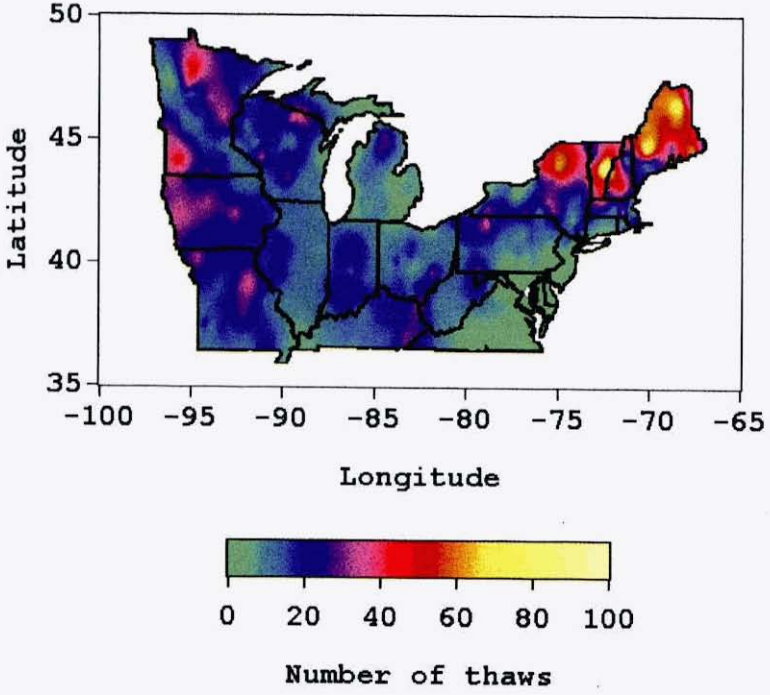

Figure 3.7. Total number of thaw-freeze episodes over the region from December 1961 to March 1990.

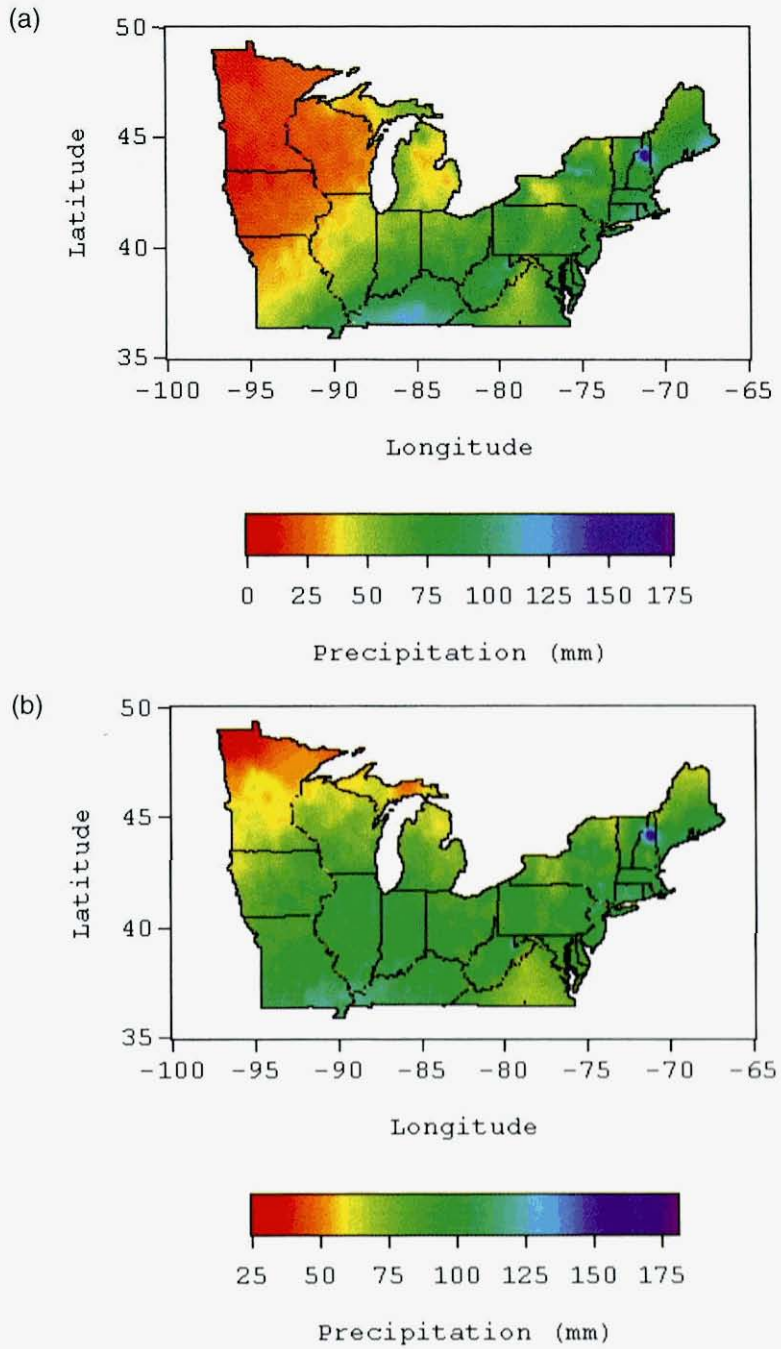

Figure 3.8. Average total precipitation amounts (mm) over the region during the months of (a) January, (b) April, (c) July, and (d) October based on daily precipitation observations from 1950–1993. *(Continued)*

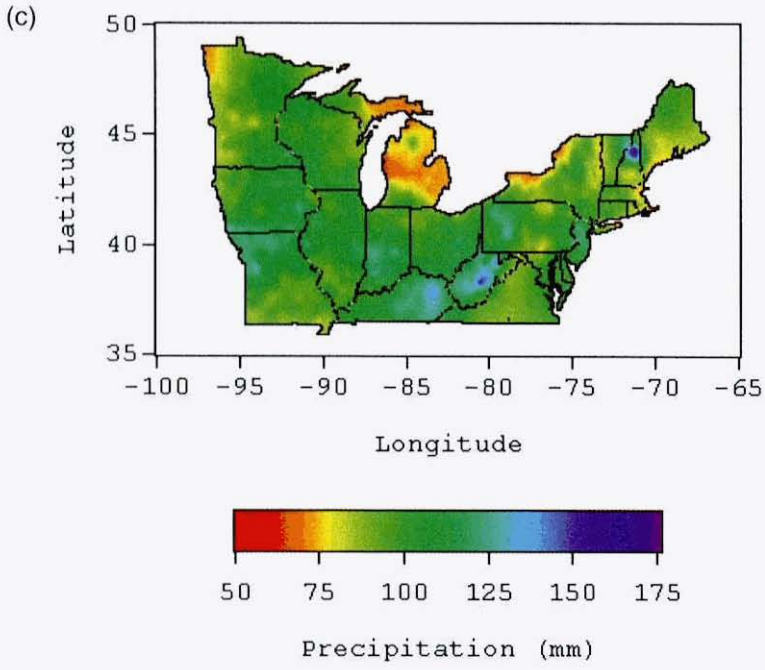

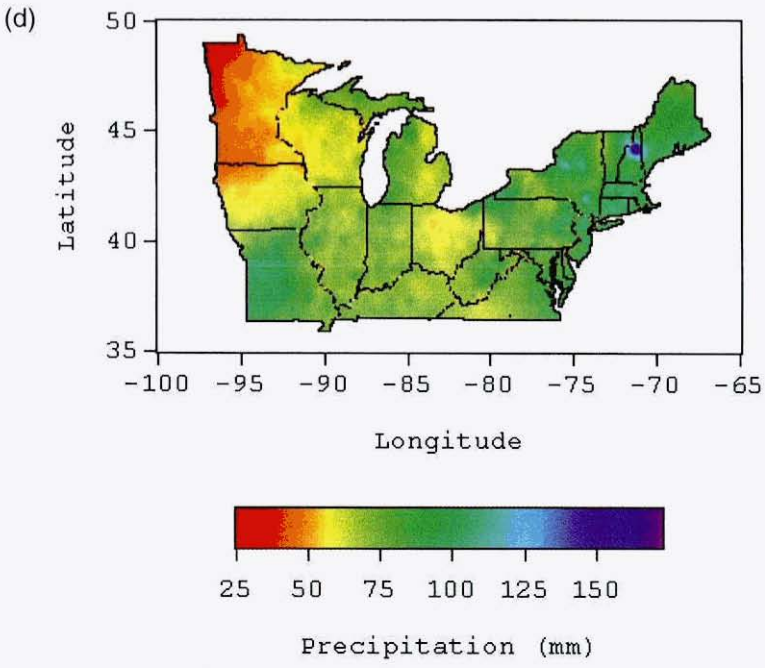

Figure 3.8c,d (*Continued*).

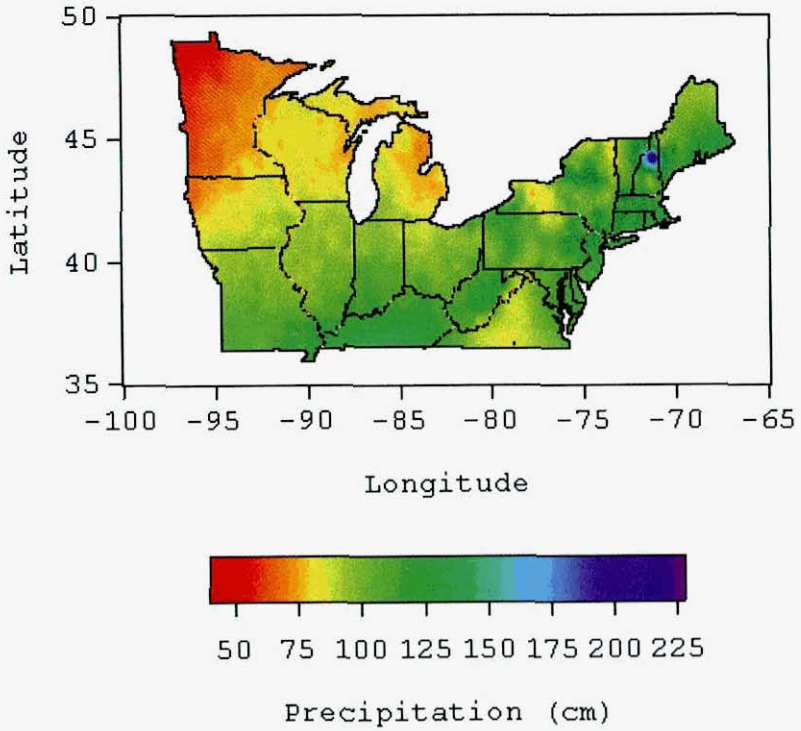

***Figure* 3.9.** Average annual precipitation amounts (cm) over the region based on daily precipitation observations from 1950–1993.

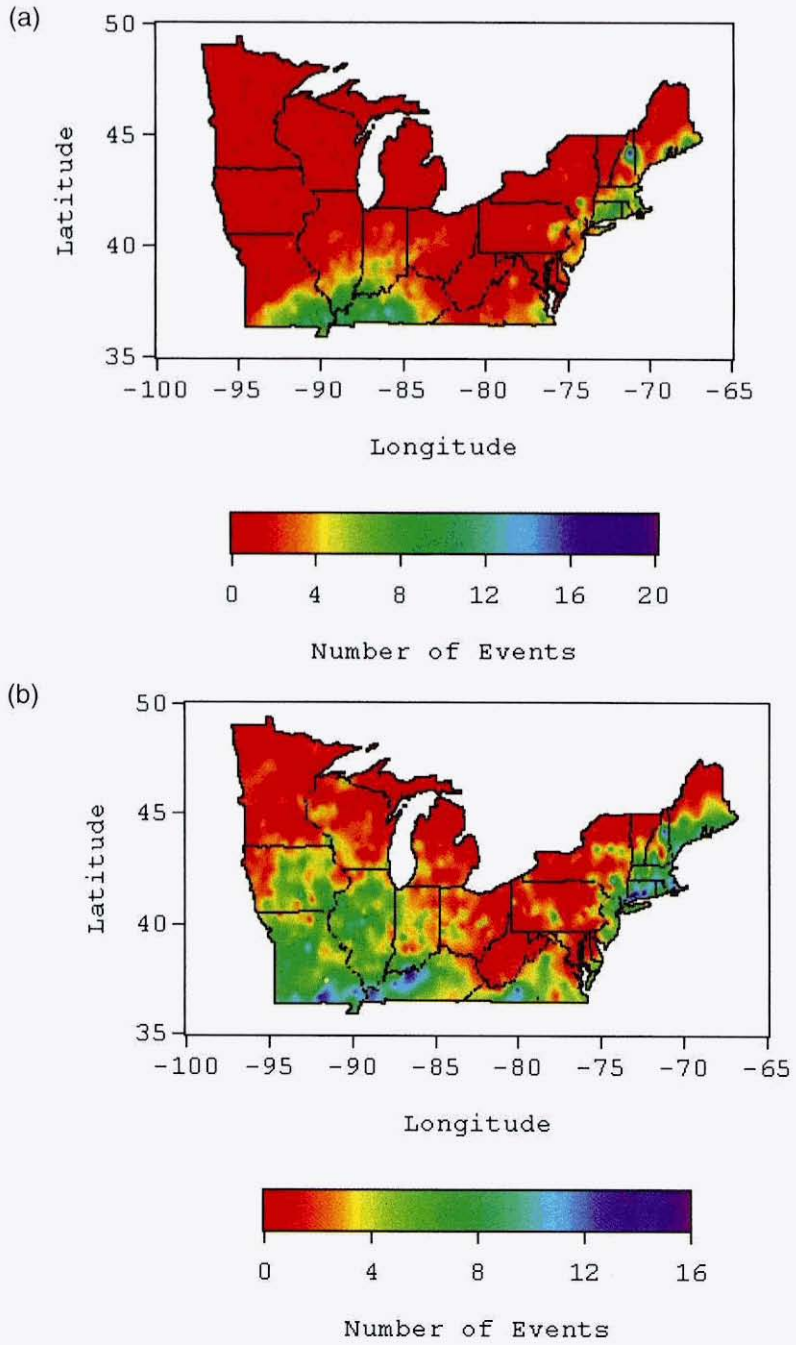

Figure 3.10. Total number of occurrences of daily precipitation exceeding 5.08 cm over the region during the months of (a) January, (b) April, (c) July, and (d) October for the period 1950–1993. *(Continued)*

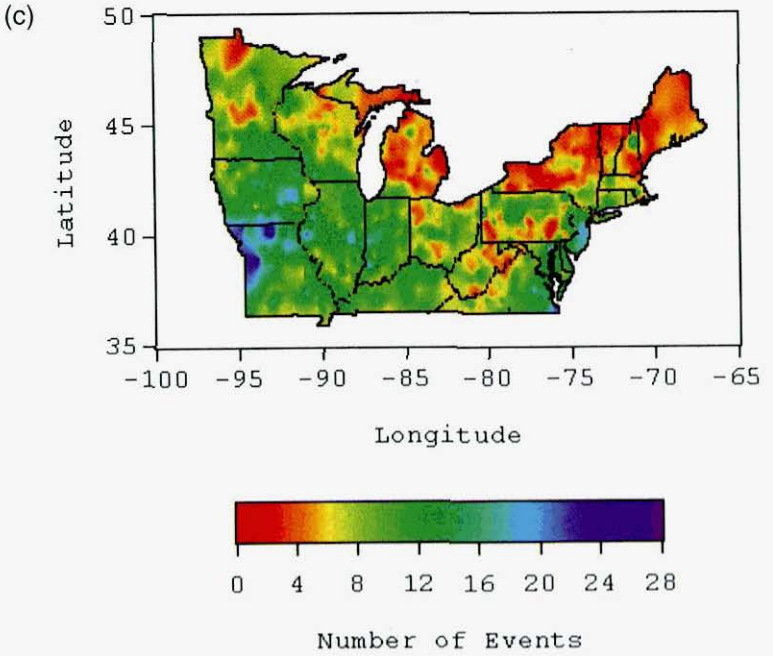

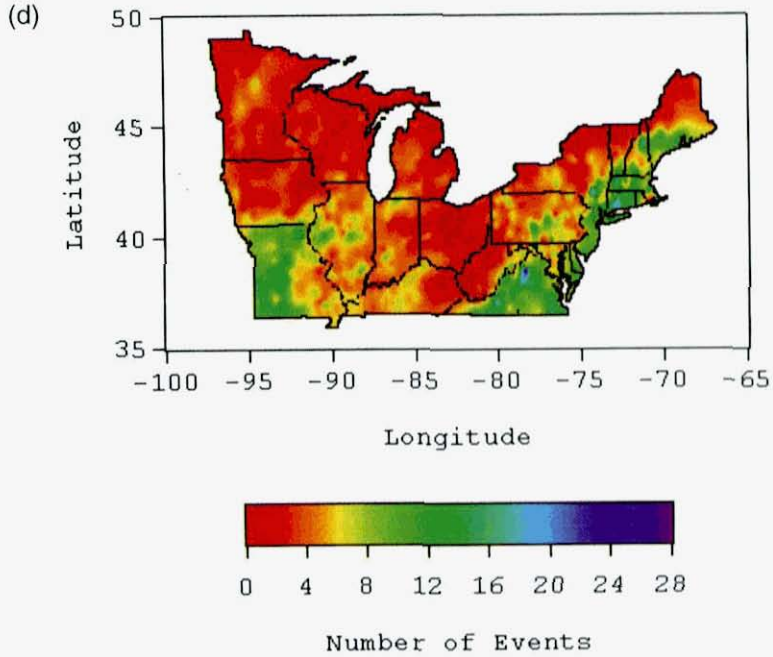

Figure 3.10c,d (*Continued*).

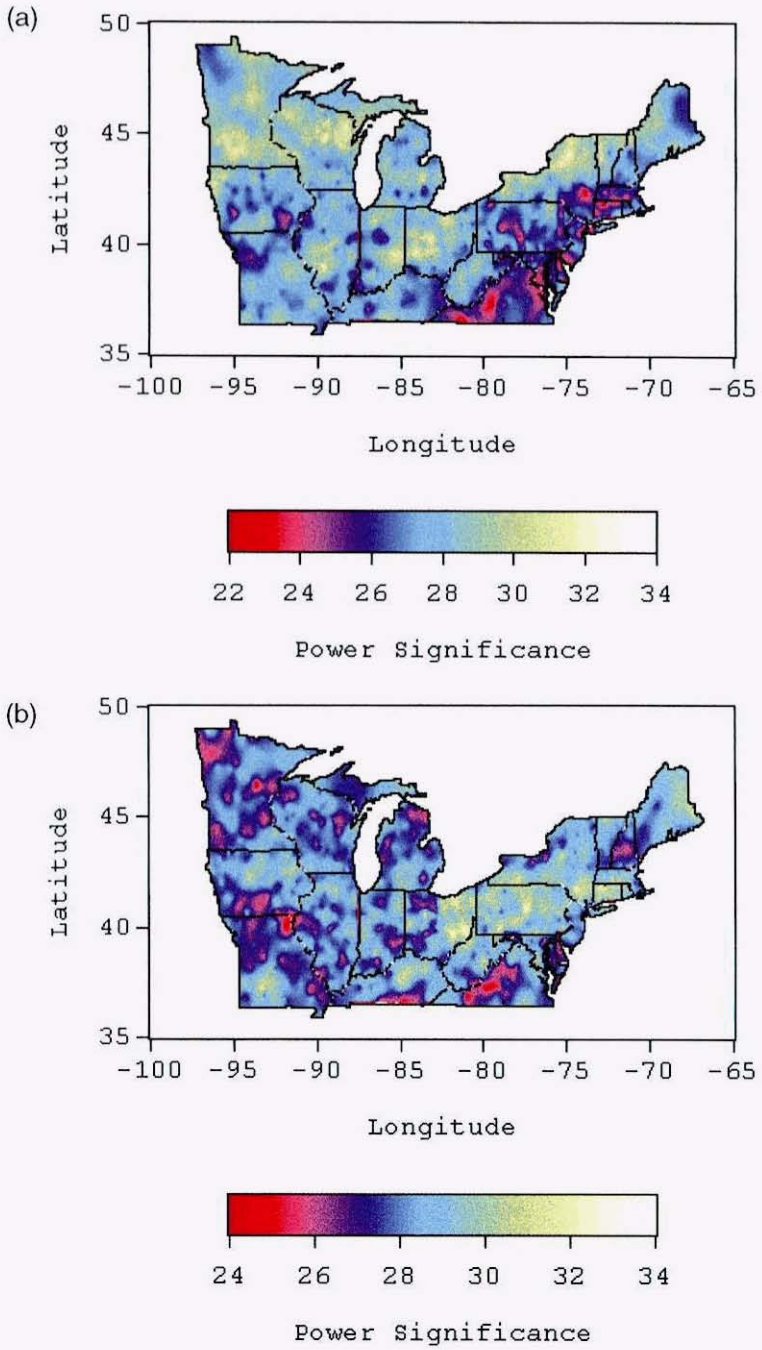

Figure 3.11. Normalized power spectrum values that show the relative significance across the region of summer (July–September) precipitation events that occur every (a) 2–4 days, (b) 4–8 days, (c) 8–16 days, and (d) 16–32 days.

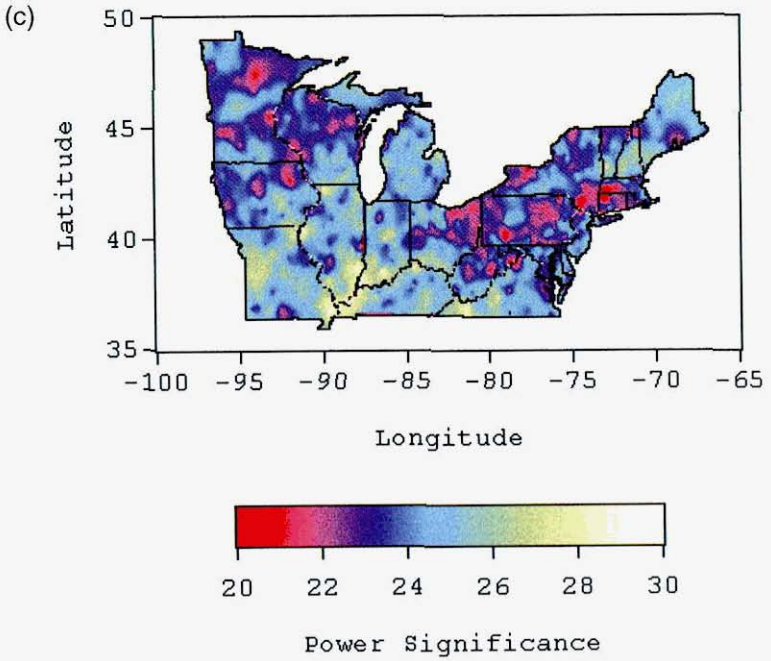

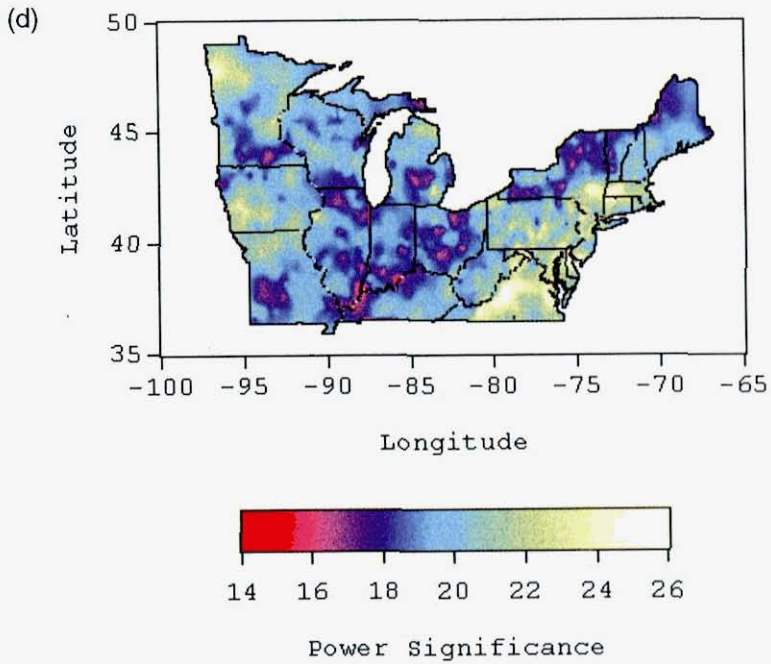

Figure 3.11c,d (*Continued*).

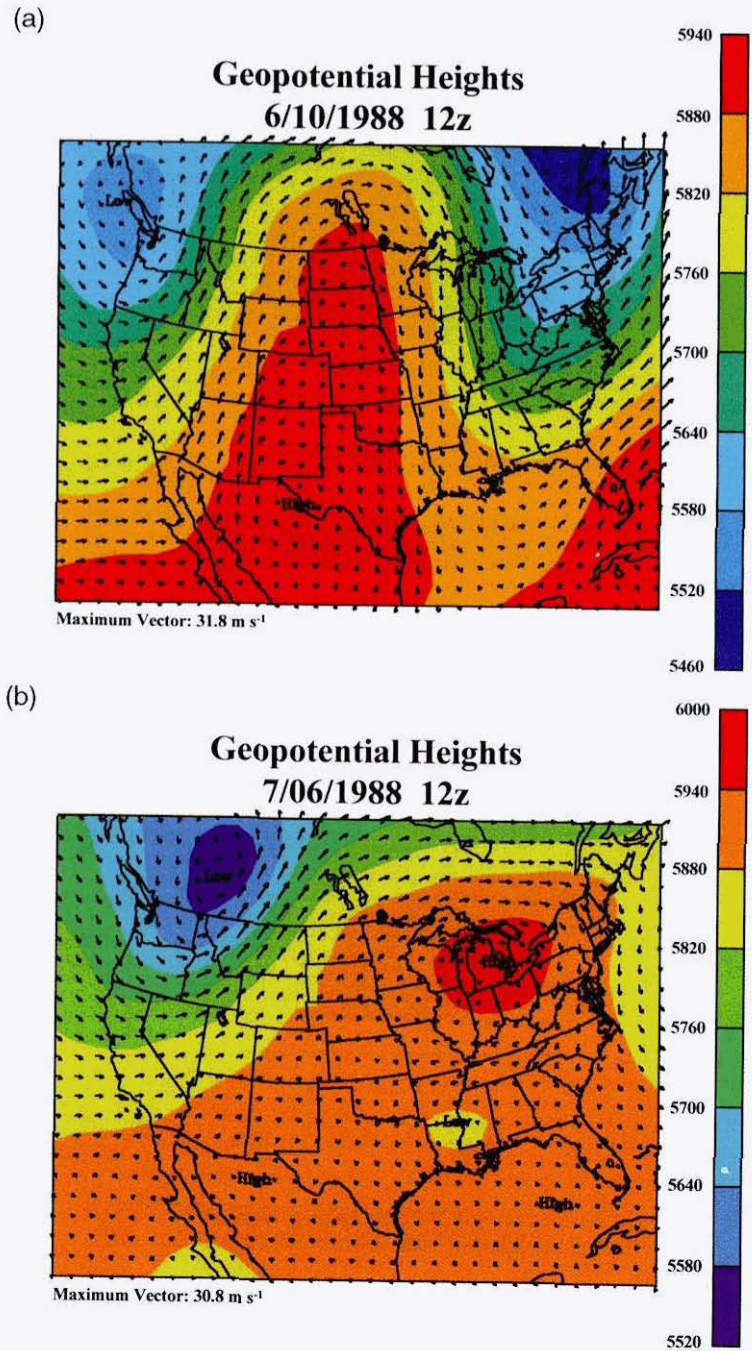

Figure 3.13. Recent examples of three 500 mb geopotential height (contours in meters) and circulation (vectors in m s^{-1}) patterns associated with severe wildfires in the north-central U.S. that occurred on (a) 10 June 1988, (b) 6 July 1988, and (c) 19 April 1989. *(Continued)*

(c)

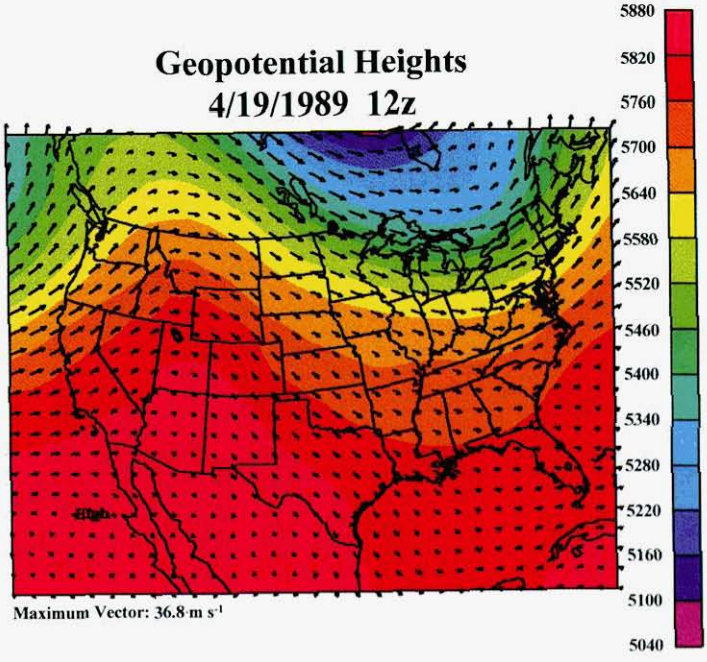

Figure 3.13c (*Continued*).

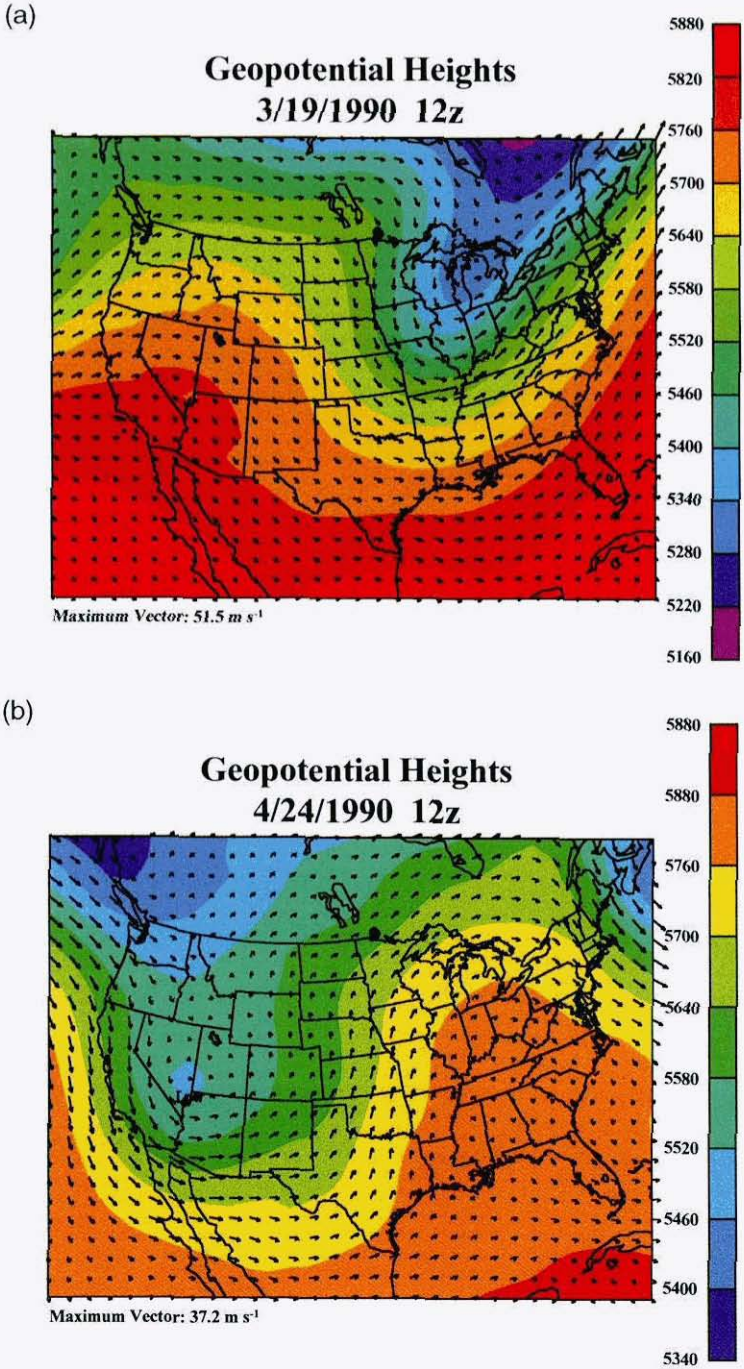

Figure 3.14. Recent examples of two 500 mb geopotential height (contours in meters) and circulation (vectors in m s^{-1}) patterns associated with severe wildfires in the northeastern U.S. that occurred on (a) 19 March 1990 and (b) 24 April 1990.

(a)

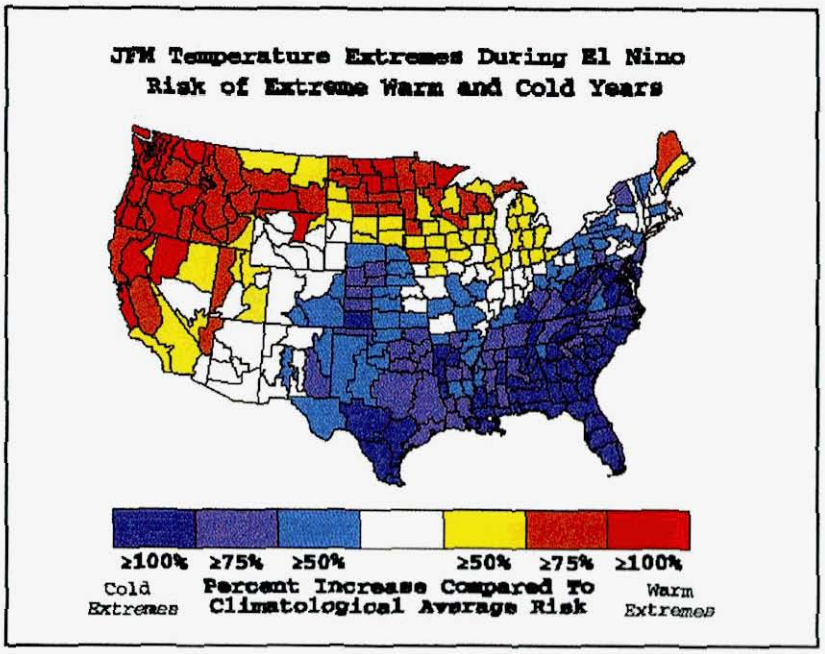

(b)

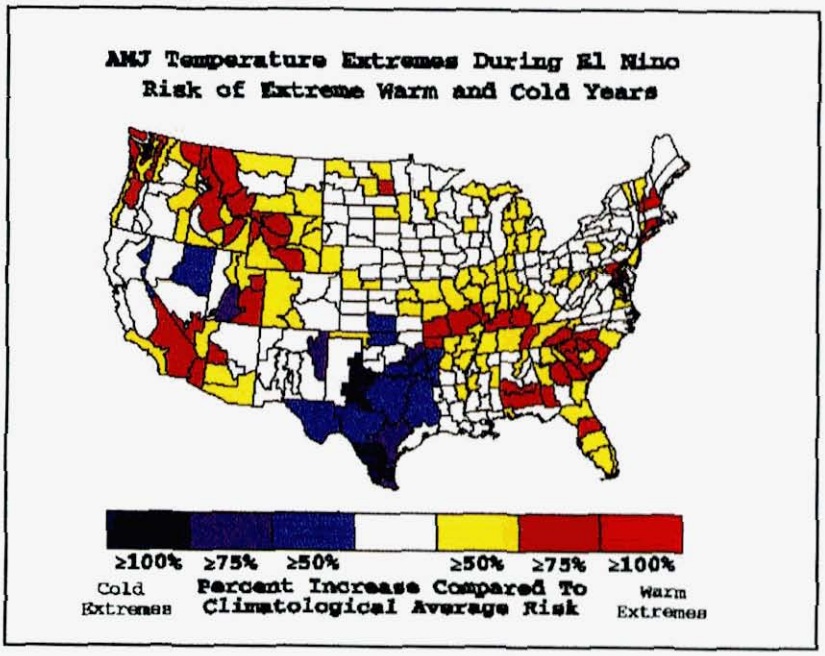

Figure 3.15. Risk of seasonal extreme temperature occurrences in each climate division across the U.S. during ENSO episodes for the periods (a) January–March, (b) April–June, (c) July–September, and (d) October–December (from NOAA-CIRES Climate Diagnostics Center, 1997). *(Continued)*

(c)

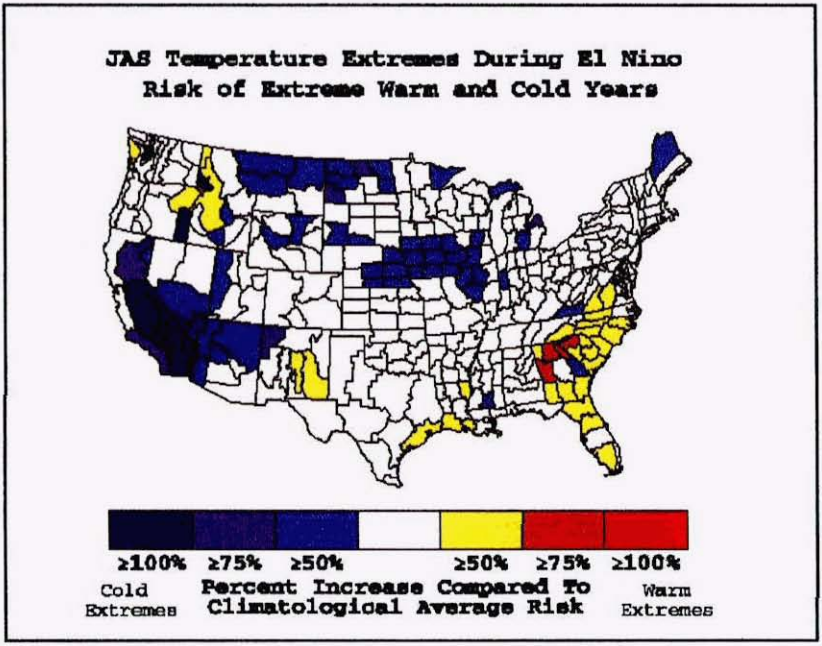

(d)

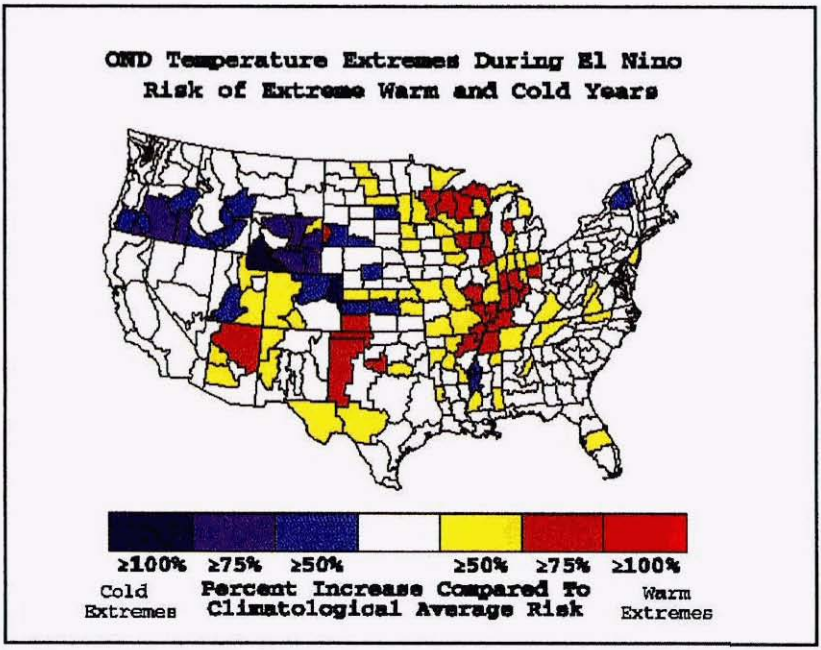

Figure 3.15c,d (*Continued*).

(a)

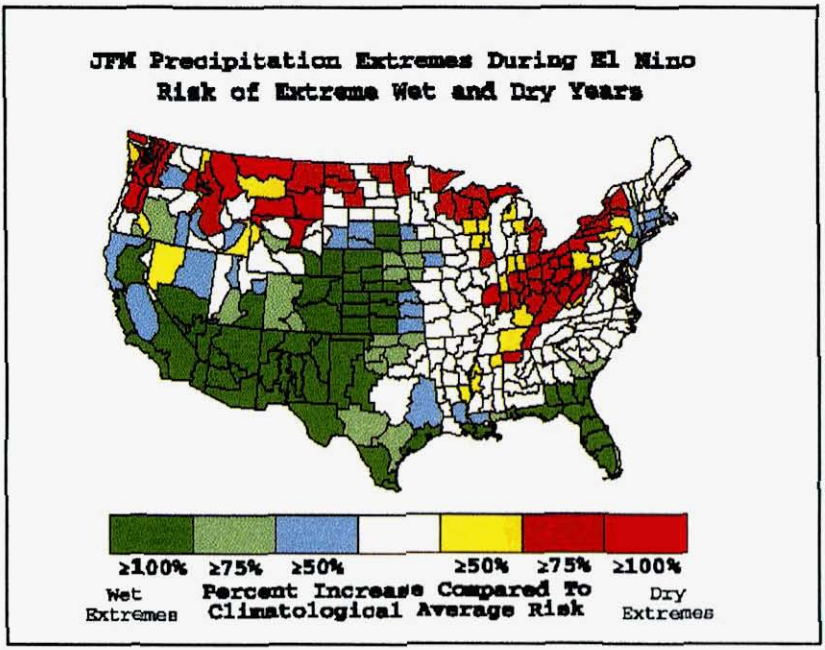

(b)

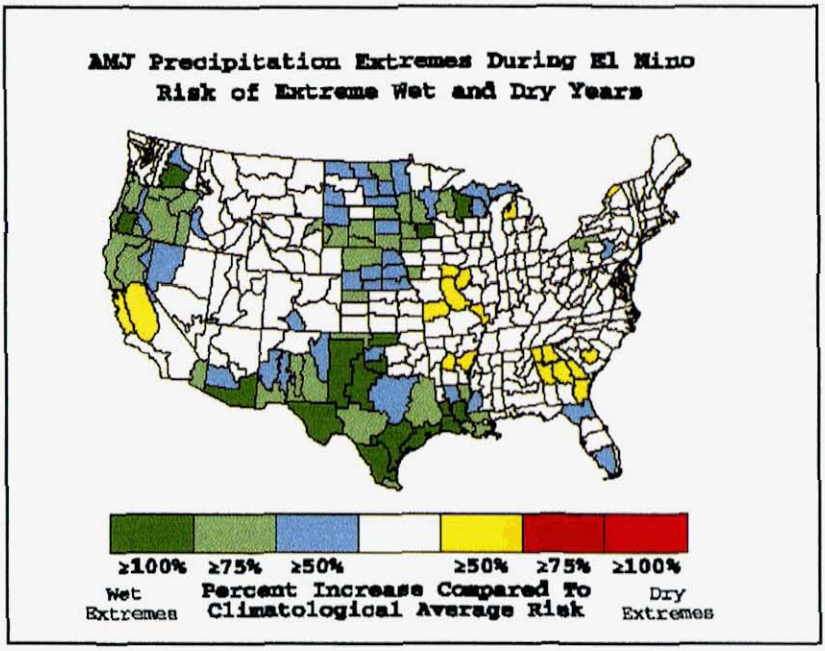

Figure 3.16. Risk of seasonal extreme precipitation occurrences in each climate division across the U.S. during ENSO episodes for the periods (a) January–March, (b) April–June, (c) July–September, and (d) October–December (from NOAA-CIRES Climate Diagnostics Center, 1997). (*Continued*)

(c)

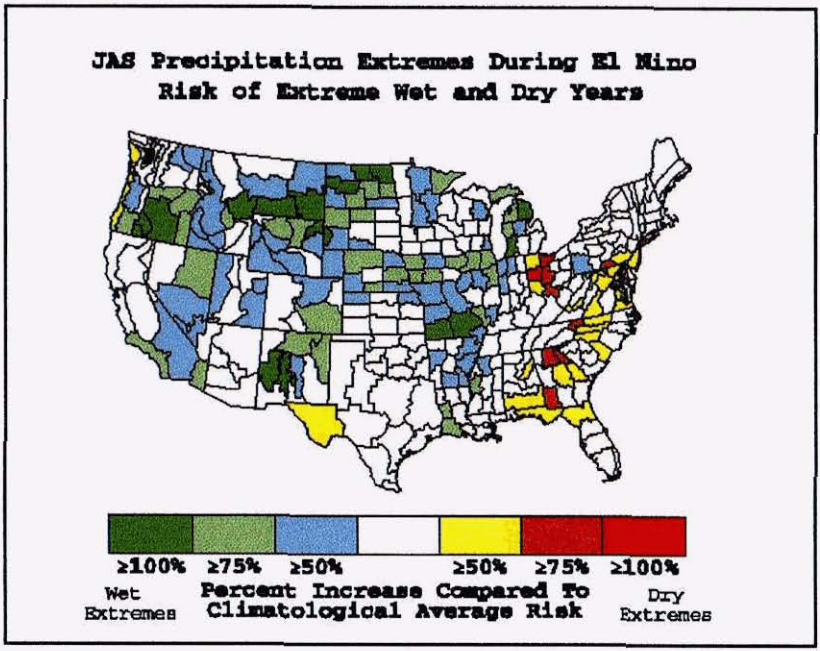

(d)

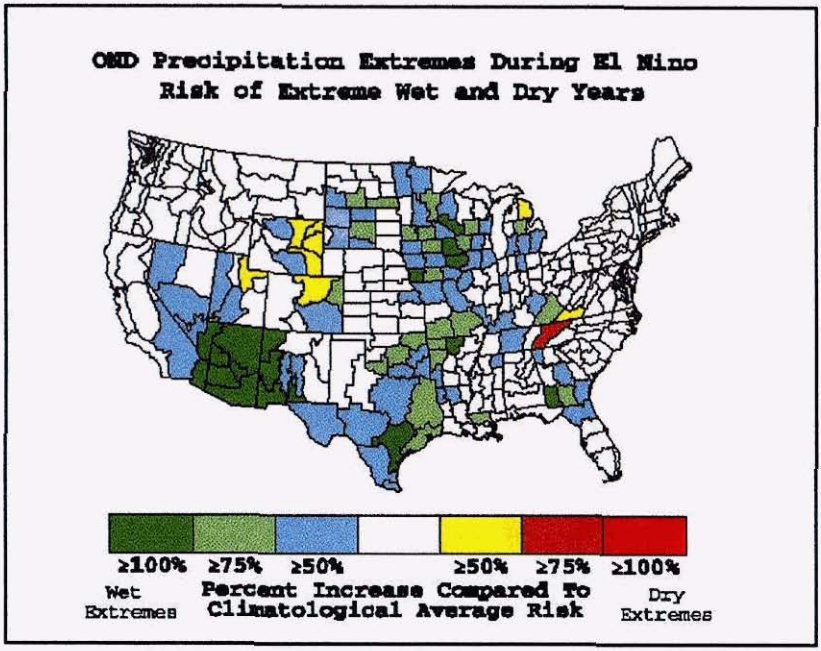

Figure 3.16c,d (*Continued*).

(a)

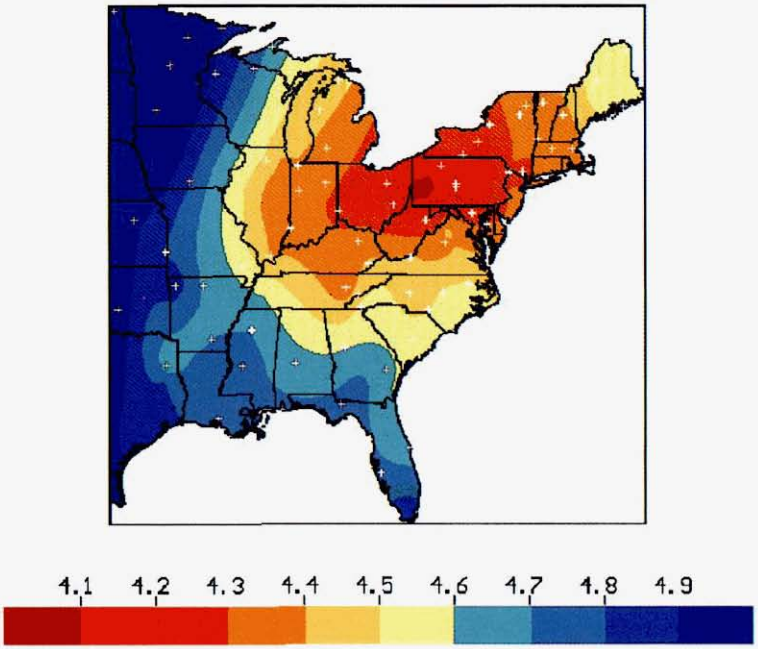

(b)

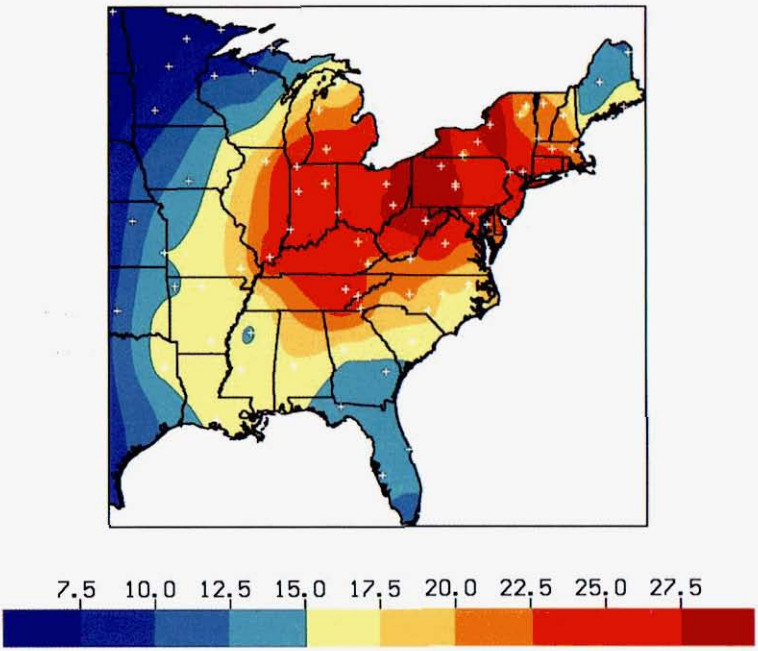

Figure 3.17. (a) Annual trend of pH at NADP/NTN sites (+) in the eastern U.S. from 1983 to 1994. (b) Annual trend of sulfate deposition (kg/ha SO_4^+) at NADP/NTN sites (+) in the eastern U.S. from 1983–1994. *(Continued)*

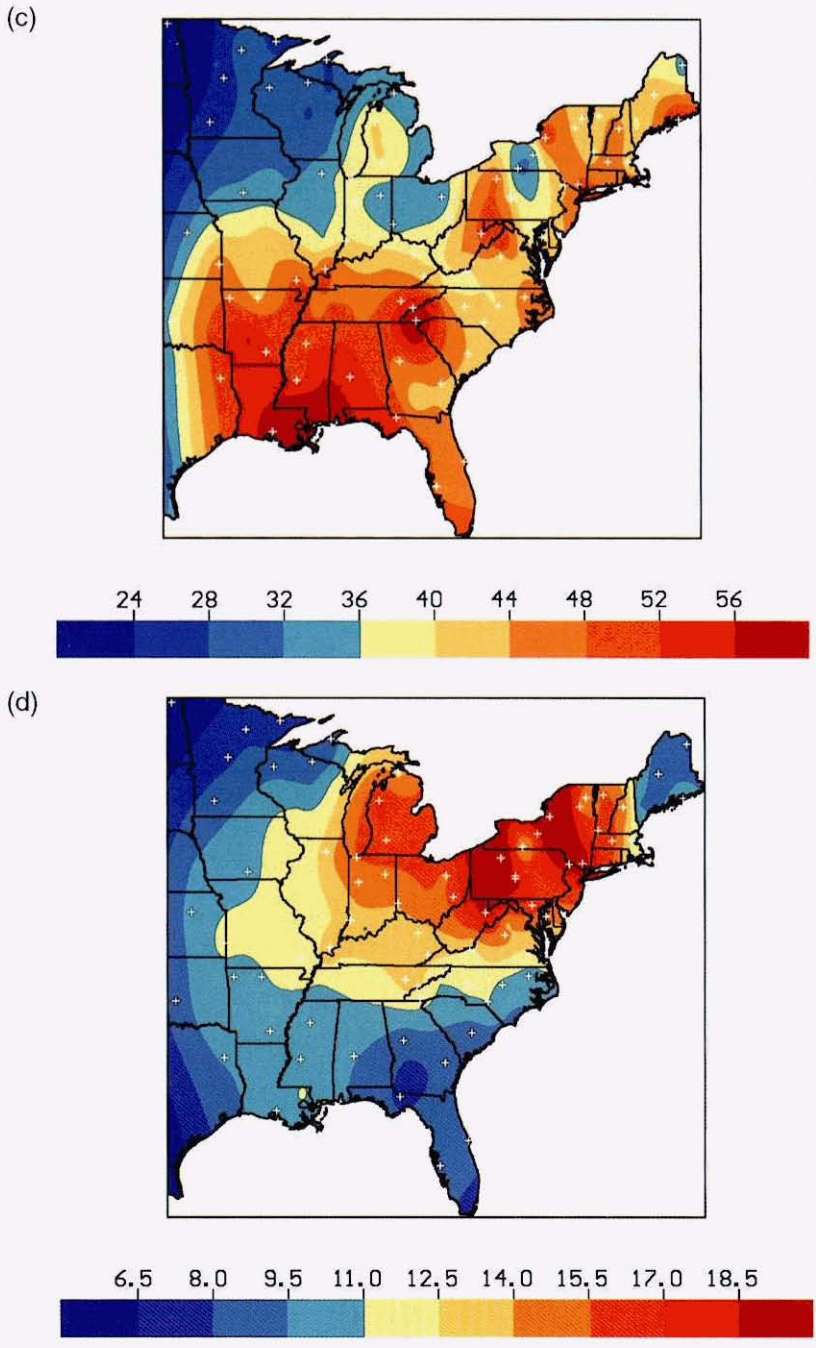

Figure 3.17. (*Continued*) (c) Annual trend of precipitation (inches) at NADP/NTN sites (+) in the eastern U.S. from 1983–1994. (d) Annual trend of nitrate deposition (kg/ha NO_3^-) at NADP/NTN sites (+) in the eastern U.S. from 1983–1994.

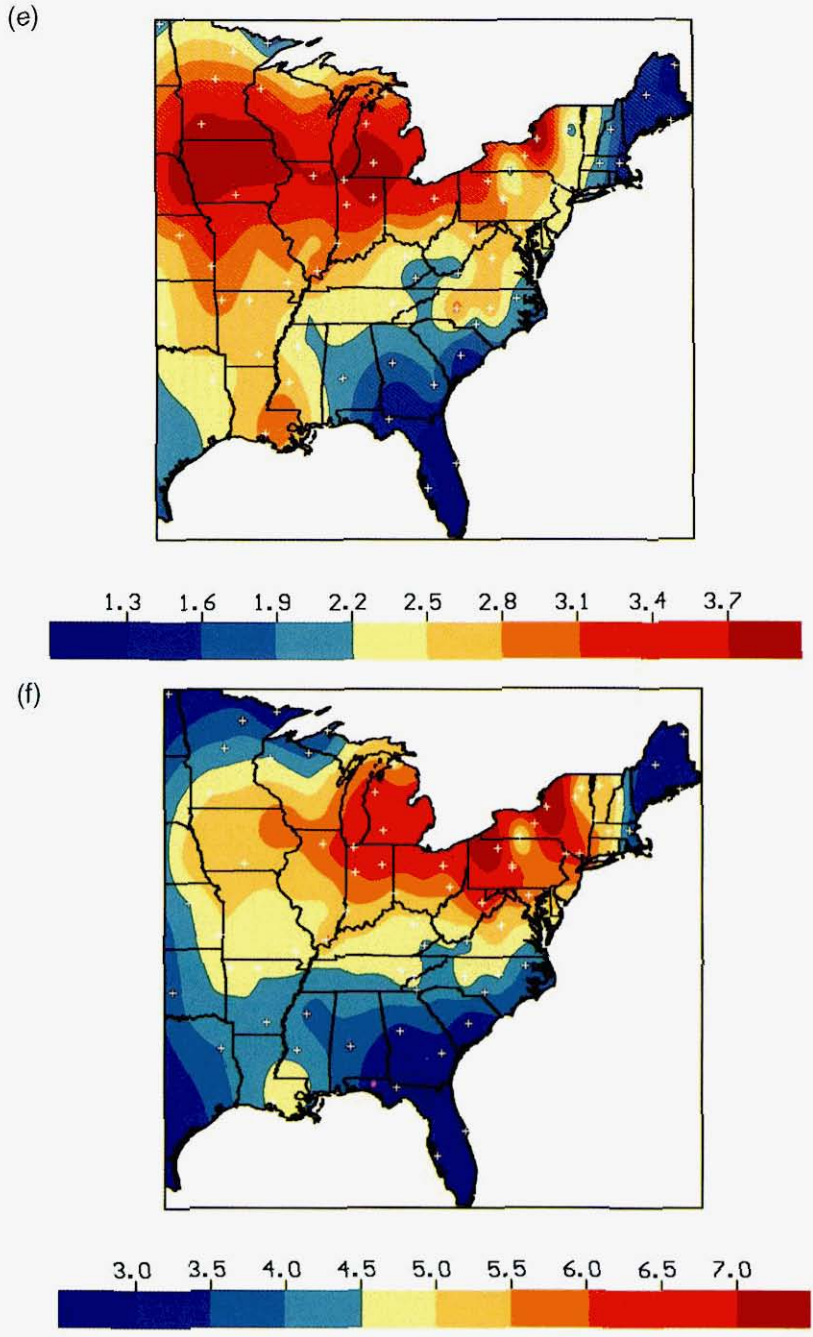

Figure 3.17. (*Continued*) (e) Annual trend of ammonium deposition at NADP/NTN sites (+) in the eastern U.S. from 1983–1994. (f) Annual trend in total N wet deposition ($NO_3^- + NH_4^+$) at NADP/NTN sites (+) in the eastern U.S. from 1983–1994.

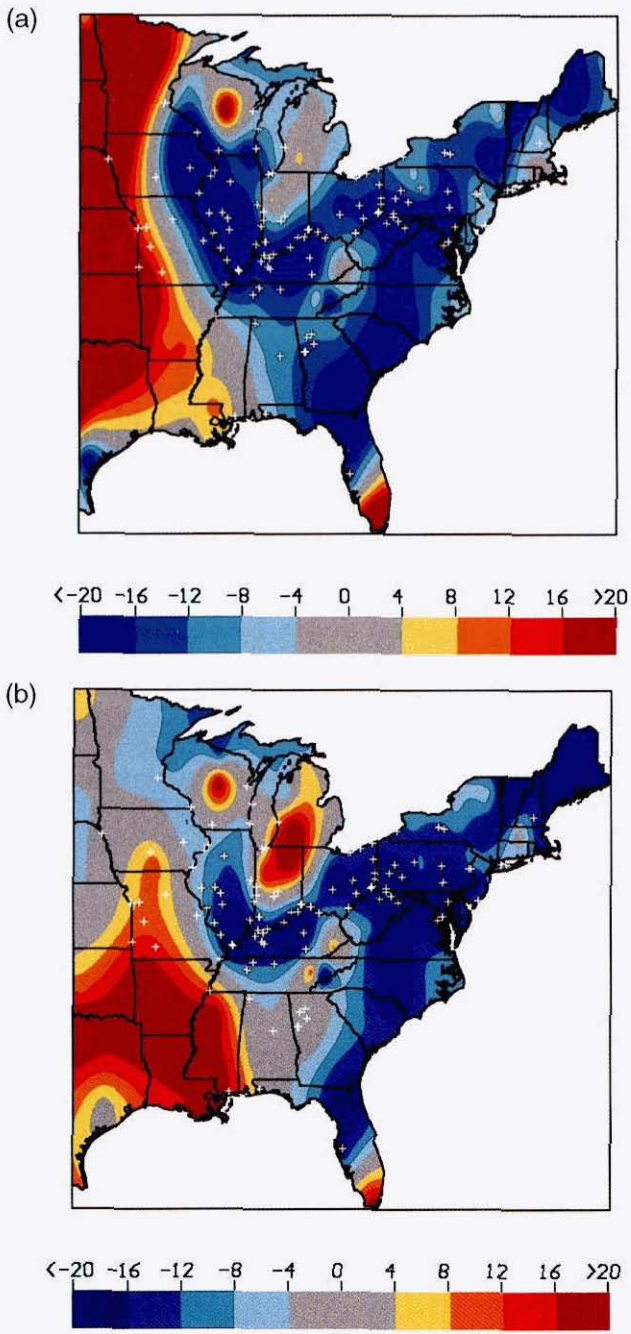

Figure 3.18. Percent departure of 1995 annual (a) H^+, (b) sulfate, (c) nitrate, and (d) precipitation data from 1983–1994 trends modeling. Electric power plants affected by Phase I of the CAAA-90, Title IV, are indicated by plus (+) signs. *(Continued)*

(c)

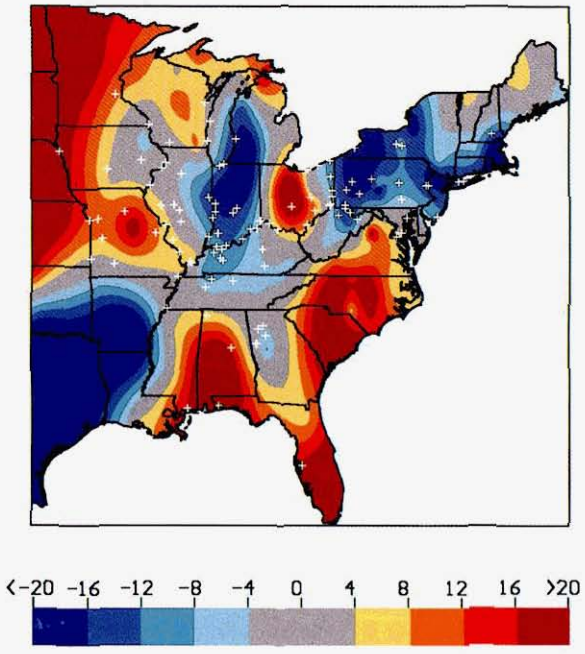

(d)

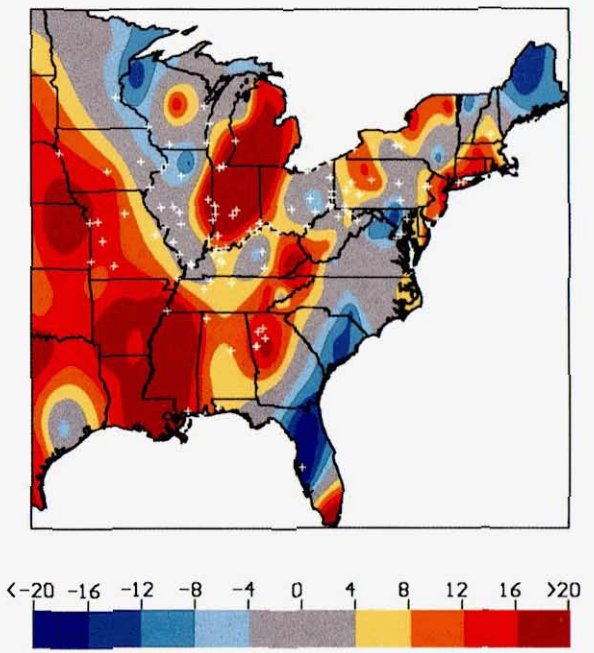

Figure 3.18c,d (*Continued*).

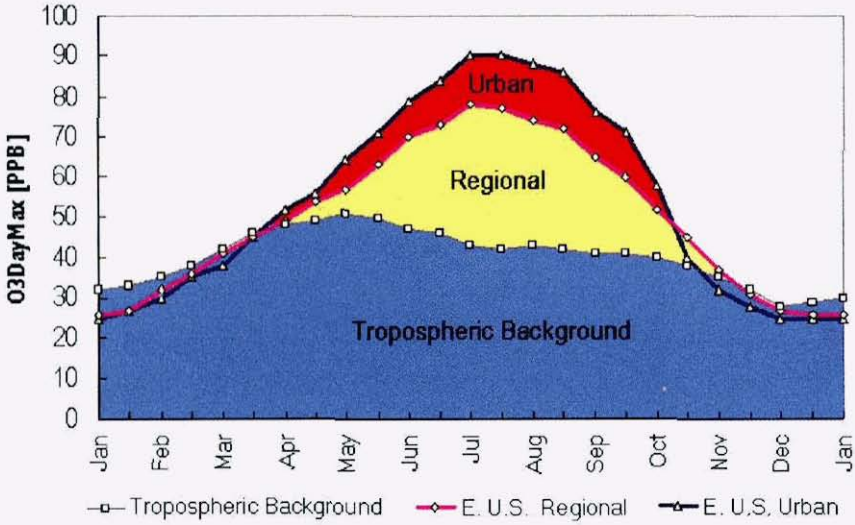

Figure 3.19. Typical monthly average of daily maximum ozone for background, regional, and urban areas.

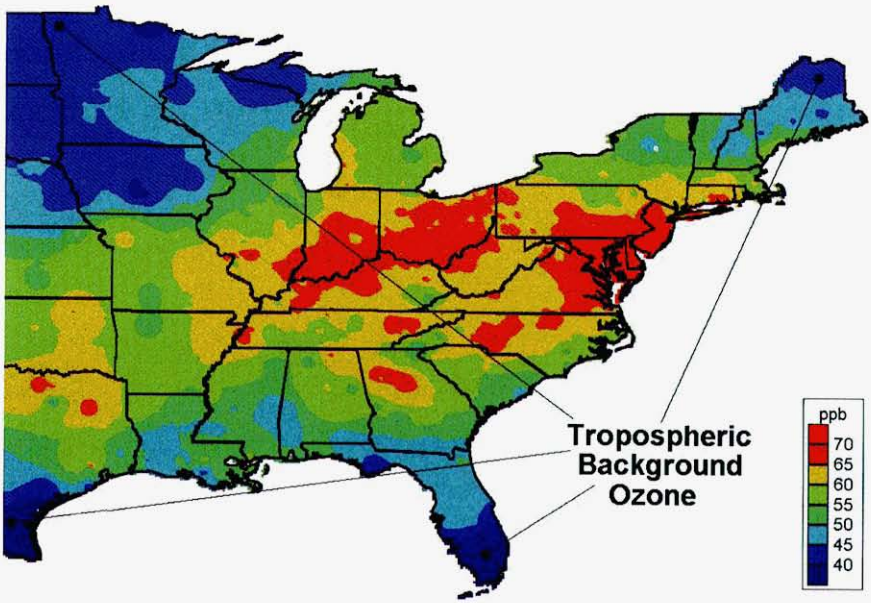

Figure 3.20. Average daily maximum ozone for the eastern (OTAG) region, 1991–1995.

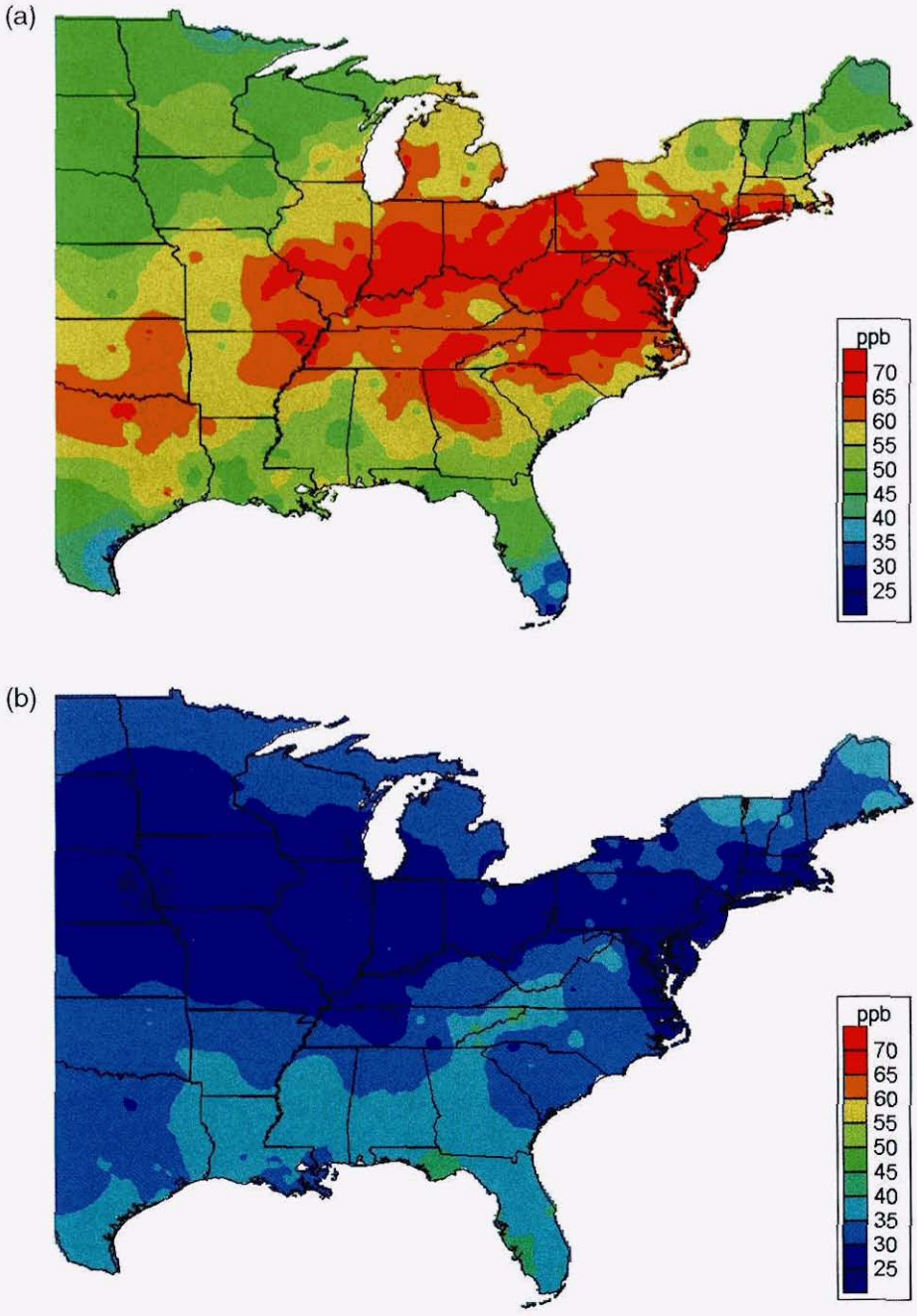

Figure 3.21. Seasonal ozone: maximum daily ozone for (a) summer (June–August), (b) winter (December–February), and (c) seasonal difference (summer–winter) for the eastern U.S. 1991–1995. *(Continued)*

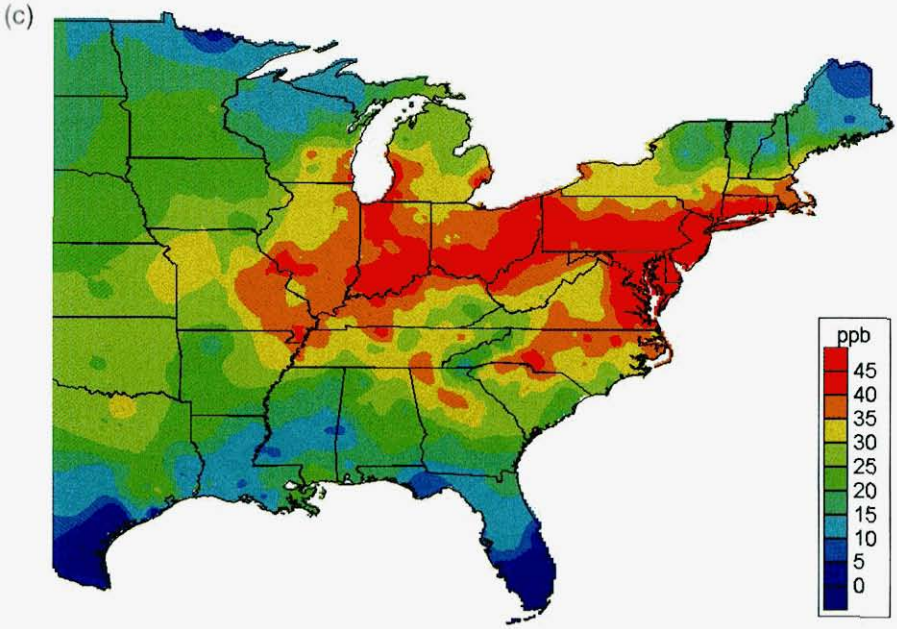

Figure 3.21c (*Continued*).

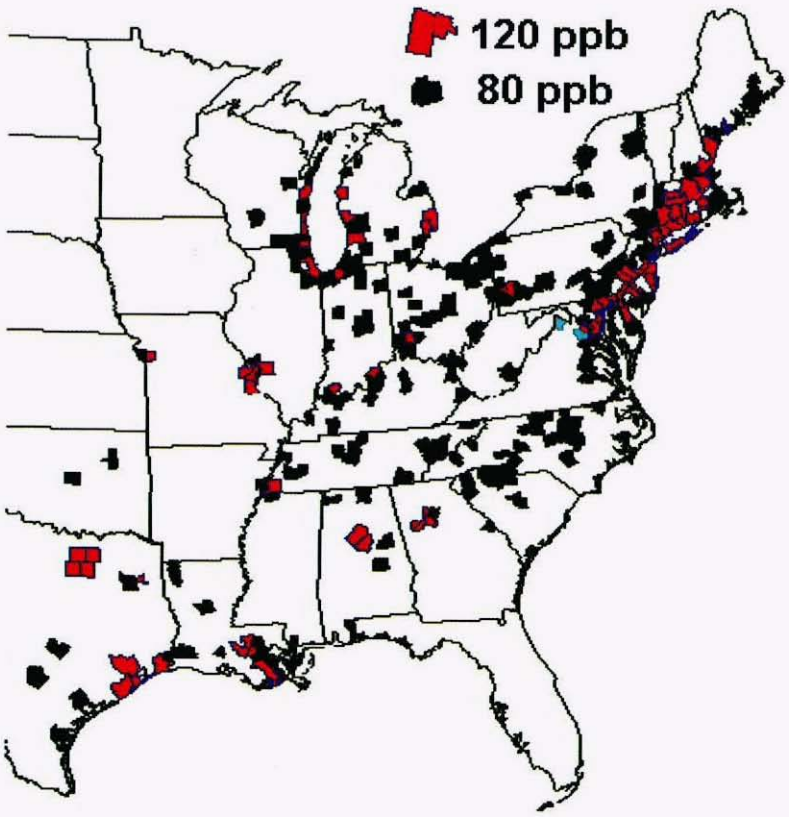

Figure 3.23. Ozone nonattainment counties at 120 and 80 ppb.

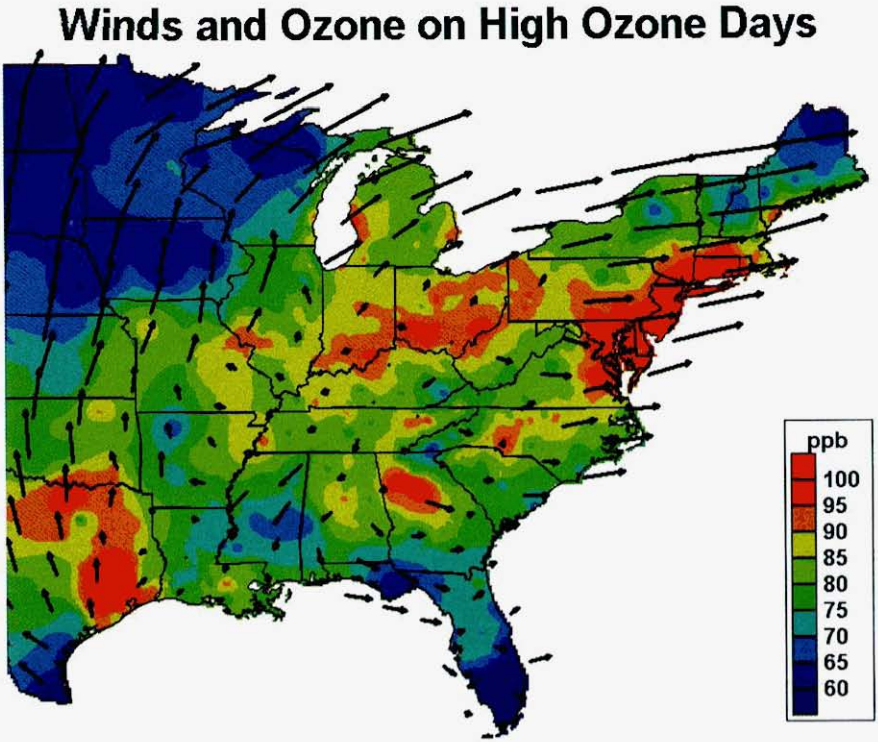

Figure 3.24. Regional transport patterns with high local ozone for the eastern U.S. 1991–1995.

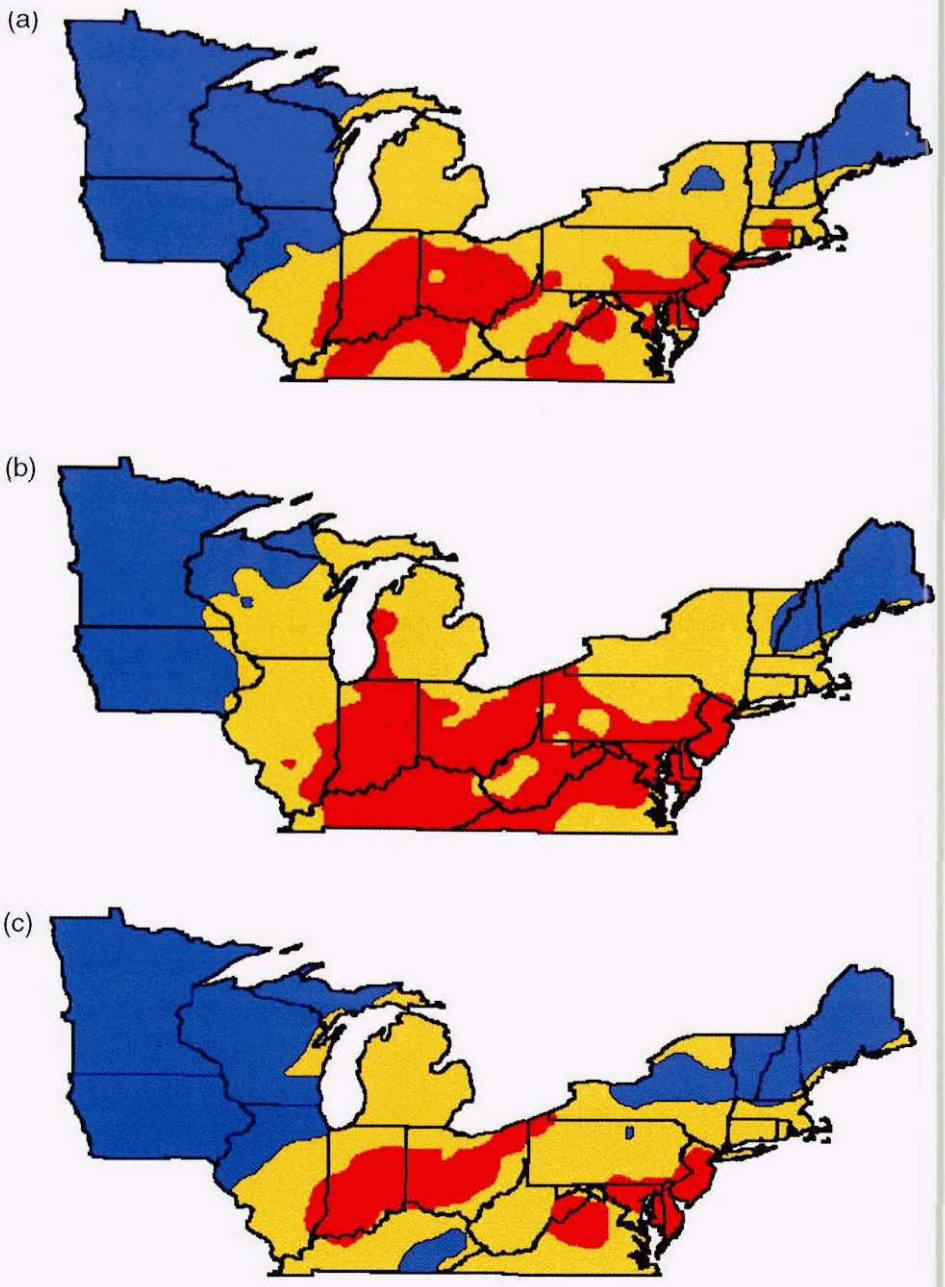

Figure 3.25. Seasonal ozone exposure W126 index for the Northern Region for (a) 1994, (b) 1995, and (c) 1996.

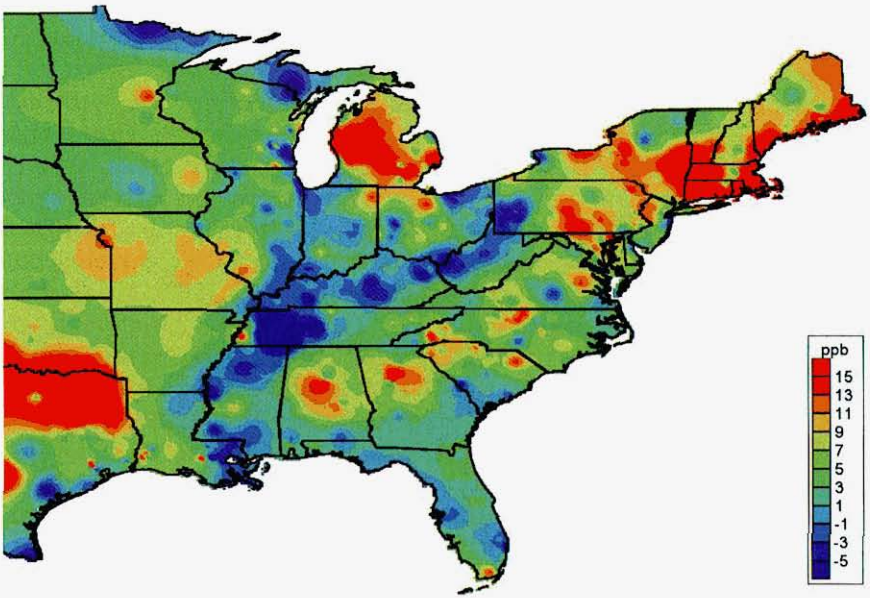

Figure 3.26. Weekly cycle in ozone: difference at the end of the workweek versus the weekend (Friday–Sunday).

anticyclones, air-mass movements, and frontal passages, which all play a role in precipitation occurrences, have time scales on the order of hours to a few weeks. While spatial patterns of monthly averages of precipitation and extreme precipitation events describe one particular facet of precipitation variability across the region, another important variability characteristic is the pattern of precipitation frequency in different seasons across the region on time scales ranging from a couple of days to a month. In order to examine the prevalent short-term precipitation variability modes during each season across the region, power spectrum analyses (Press et al., 1992) were performed on 1950 to 1993 daily precipitation records from the NCDC from 1204 stations across the region (EarthInfo, 1995). Power significance values within specific frequency/period "windows" (i.e., 2 to 4 days, 4 to 8 days, 8 to 16 days, and 16 to 32 days) were determined for each station during the spring, summer, fall, and winter seasons. These power significance values provide an indication of the prevalence or significance of precipitation events at each station within a particular frequency/period "window" compared with precipitation events occurring within the other 3 frequency/period "windows," regardless of how precipitation amounts are distributed across the region in each season.

Power spectrum analyses performed on precipitation data from the winter season, defined as the months of January, February, and March, suggest that precipitation events occurring every 2 to 4 days in the region are generally most prevalent in central Wisconsin, eastern Iowa, and along the Atlantic coast, with the most power significance occurring in eastern Maine. The 2 to 4 days variability mode is least significant in Minnesota, central Missouri, and along the Ohio River Valley. The eastern half of the region is characterized by the prevalence of winter precipitation events occurring on slightly longer time scales of 4 to 8 days. The western sections of the region generally experience fewer significant winter precipitation events on a 4 to 8 day cycle than the eastern sections of the region. Winter precipitation events that occur every 8 to 16 days or longer are least significant along the Atlantic coast states and West Virginia. Central Wisconsin is also characterized by fewer 8- to 16-day precipitation events than in surrounding states. Winter precipitation variability on the longest time scales of 16 to 32 days is most prevalent in Minnesota, Wisconsin, northwestern Iowa, central Missouri, and the upper peninsula of Michigan, while in the Atlantic coastal states, the 16- to 32-day precipitation variability mode is less significant.

In the spring season, defined as the months of April, May, and June, the spatial trends in the significance of 2- to 4-day precipitation events are weaker than in the winter months. Relatively high and low power significance values tend to be randomly scattered throughout the region. However, distinctive spatial patterns exist across the region for the 4- to 8-day, 8- to 16-day, and 16- to 32-day precipitation variability modes.

Springtime precipitation events that occur every 4- to 8-days are most prevalent in the states of Vermont, New Hampshire, eastern New York, New Jersey, and eastern Pennsylvania. They are least prevalent in those states comprising the western half of the region. For the 8- to 16-day springtime precipitation variability mode, Illinois, southern Indiana, southeastern Iowa, and Virginia all tend to have relatively high power significance values. Relatively low power significance values are prevalent over the western (Minnesota, Wisconsin, and most of Iowa) and northeastern (New Hampshire, Vermont, New York, Massachusetts, Connecticut, and Rhode Island) sections of the region. Finally, lower frequency precipitation events that occur every 16 to 32 days are most prevalent in the northwestern sections (western Wisconsin, Minnesota, and western Iowa) of the region as well as Maine during the spring months; they are least prevalent over the rest of the region, especially in Missouri and Ohio.

Fig. 3.11 (color insert) shows the distribution of power significance values across the region during the summer months (July, August, and September) for the 2- to 4-day, 4- to 8-day, 8- to 16-day, and 16- to 32-day precipitation variability modes. Summertime convective precipitation activity leads to relatively large power significance values over most of the region for 2- to 4-day precipitation events (Fig. 3.11a). It is only over the Atlantic coastal region from Massachusetts to Virginia that 2- to 4-day precipitation events are less significant. This is in contrast to the significance of 2- to 4-day precipitation events over the region during the winter months, when precipitation events occurring every 2 to 4 days are more likely to occur along the Atlantic coast and less likely over most other sections of the region (especially in Minnesota and much of the Ohio River Valley). The 4- to 8-day variability mode pattern in the summer is quite variable (Fig. 3.11b); only the area from eastern Ohio eastward through Pennsylvania, southern New York, Massachusetts, and Connecticut tends to be characterized by more precipitation events occurring at intervals of 4 to 8 days than for other areas of the region. Fig. 3.11c suggests that the southern-tier states in the region are more likely to experience precipitation events occurring every 8 to 16 days than the northeastern and northwestern states in the region. At summertime precipitation periods of 16 to 32 days, the Atlantic coastal states from Virginia to Massachusetts along with most of Iowa and northern Minnesota tend to experience a higher proportion of this class of precipitation events than do the Ohio River Valley and northern New England states (Fig. 3.11d). This pattern also contrasts sharply with the 16- to 32-day wintertime variability mode pattern that suggests the Atlantic coastal states experience a *lower* proportion of these precipitation events than most other areas of the region.

In the fall months (October, November, and December), the eastern sections of the region tend to be characterized by a larger proportion of

higher frequency precipitation events (2- to 4-day and 4- to 8-day periods) than the western sections of the region. Conversely, more lower frequency (8- to 16-day and 16- to 32-day periods) precipitation events characterize the western sections of the region than the eastern sections during the fall season. During the fall months, the western portions of the region experience more cool and dry air masses moving southward from Canada, thereby decreasing the frequency of precipitation events in the area in comparison with the higher frequency convective precipitation events that occur in the area during the summer months.

Extreme Weather Events

Extreme weather events, such as tornadoes, destructive straight-line winds, and hurricanes, along with fire-weather episodes that produce atmospheric environments conducive for severe wildland fires can all act as direct or indirect agents of landscape change in some or all areas of the northeast and north central United States. Extreme winds associated with thunderstorms, tornadoes, and hurricanes can damage and uproot trees, destroy agricultural crops, damage or destroy property, and can have a lasting impact on local microclimates and basic ecosystem functions and processes (e.g., species regeneration, wildlife habitat, forest sensitivity to insects and diseases, frost occurrence within ecosystems, heat and moisture exchange between the surface and atmosphere). If surface fuel conditions are appropriate, fire-weather episodes can lead to severe wildland fires that also disturb ecosystems and impact basic ecosystem functions and processes in the region. The following sections provide a brief overview of tornado, straight-line wind, hurricane, and fire-weather occurrences in the region.

Tornado and Straight-Line Wind Events

There are three general types of extreme wind events: tornadoes, hurricanes, and straight-line winds. The last category includes winds of varying duration and areal coverage, ranging from microbursts (lasting less than 10 minutes and covering only a few square kilometers) to mesoscale convective complex and squall-line winds (lasting less than an hour or two and covering a few hundred to 1000 square kilometers) up to frontal winds (lasting several hours and covering areas on the order of 10,000 square kilometers). Local topography can weaken or intensify any of these types of extreme winds.

The most common location for tornadoes to form in North America is the region east of the Rocky Mountains and west of the Appalachian Mountains (NOAA Severe Storms Laboratory, 1999). Tornadoes occur most frequently during the late afternoon or early evening periods in the

spring and summer months. The typical tornado damage path is about 2 to 3 km long and about 50 m wide. The erratic behavior of tornadoes can result in path lengths that vary from basically a single point to more than 150 km and path widths that vary from less than 10 m to more than 1.5 km. The forward speed of tornadoes can range from nearly stationary to more than 25 m s^{-1}, with the typical speed being in the 5 to 10 m s^{-1} range (NOAA Severe Storms Laboratory, 1999). Tornadoes are categorized according to the Fujita Scale, a 6-category "wind-speed" scale based on the amount of observed damage from a tornado:

F_0: 64–115 km h^{-1}	Light damage
F_1: 116–179 km h^{-1}	Moderate damage
F_2: 180–251 km h^{-1}	Considerable damage
F_3: 252–329 km h^{-1}	Severe damage
F_4: 330–417 km h^{-1}	Devastating damage
F_5: 418–508 km h^{-1}	Incredible damage

Since 1950, only 20 tornadoes have been classified as F_5 tornadoes in the region, and they occurred in the states of Wisconsin, Minnesota, Illinois, Ohio, Indiana, Missouri, and Michigan (NOAA Storm Prediction Center, 1999).

Table 3.1 shows the distribution of reported tornadoes over the period 1950 to 1994 along with the Consumer Price Index–adjusted costs of all tornado damages in each state within the region plus the states of Kentucky and Virginia. Approximately 200 tornadoes are reported each year in the region, mostly between March and July. Most of the reported tornadoes have occurred in the western sections of the region. The states of Iowa, Missouri, and Illinois ranked 6th, 7th, and 9th in the United States, respectively, for the number of reported tornadoes during the period 1950 to 1994. Although the states of Indiana, Minnesota, and Ohio ranked 15th, 18th, and 21st, respectively, for reported tornado occurrence during the same period, the states ranked 2nd, 6th, and 7th, respectively, for the cost of tornado damages incurred. The tornadoes that occurred during the 1950 to 1994 period caused 1545 fatalities and 28,280 injuries in the region plus the states of Kentucky and Virginia. The state of Michigan ranked first in the region and 5th nationally in the number of reported fatalities (237) attributed to tornadoes during the 1950 to 1994 period, while Ohio ranked first in the region and 4th nationally in the number of tornado-related injuries (237) (NOAA Storm Prediction Center, 1999).

The effect of intense winds, be they tornadic, hurricane-based, or straight-line, on trees and forests is usually negative. Any strong wind can break numerous branches, uproot poorly anchored trees, or snap off the crowns of trees. Due to their seasonality, tornadoes have a tendency to cause greater damage to trees that flush earlier, as the leaves increase the drag the tree creates in the wind. Direction can also be a factor of

Table 3.1. Number of Tornadoes, State Rank for Tornado Occurrence, Consumer Price Index (CPI) Adjusted Cost of Tornado Damages, and State Rank for Tornado Costs for Each State in the Region Plus the States of Kentucky and Virginia, Based on 1950 to 1994 Reported Tornado Occurrences (From NOAA Storm Prediction Center, 1999)

State	Number of Tornadoes	State Rank	CPI Adjusted Cost	State Rank
Iowa	1374	6	$7,092,119	10
Missouri	1166	7	$7,393,827	9
Illinois	1137	9	$8,238,192	8
Indiana	886	15	$16,486,543	2
Wisconsin	844	17	$4,107,568	19
Minnesota	832	18	$10,153,546	6
Michigan	712	20	$3,450,385	22
Ohio	648	21	$9,654,648	7
Pennsylvania	451	24	$6,150,330	13
Kentucky	373	28	$2,825,786	23
Virginia	279	29	$1,247,380	28
New York	249	30	$1,840,968	26
Maryland	135	34	$387,377	35
Massachusetts	134	35	$6,177,932	12
New Jersey	112	37	$530,843	33
West Virginia	83	38	$216,385	39
Maine	82	39	$71,046	41
New Hampshire	72	41	$90,713	40
Connecticut	61	42	$3,853,888	20
Delaware	52	44	$56,285	42
Vermont	32	47	$35,124	45
Rhode Island	8	49	$19,796	47

importance when considering wind damage to trees. Moderate, ambient winds that flow from a particular direction tend to cause trees to thicken their trunks along a line parallel to the wind direction, thereby enabling trees to effectively brace themselves against the ambient winds. If a sudden strong gust strikes in the same direction from which the ambient wind usually blows, it may cause less damage than if it comes from a perpendicular heading and strikes the tree broadside.

Hurricanes in the Northeastern United States

Hurricanes originating in the Atlantic Ocean or Gulf of Mexico have the potential for causing significant flooding, storm surges, and wind damage in the northeastern United States. Between 1900 and 1996, a total of 835 hurricanes or tropical storms developed in the Atlantic Ocean or Gulf of Mexico (Unisys Corporation, 1999). The distribution by year of Atlantic or Gulf hurricane or tropical storm occurrence is shown in Fig. 3.12.

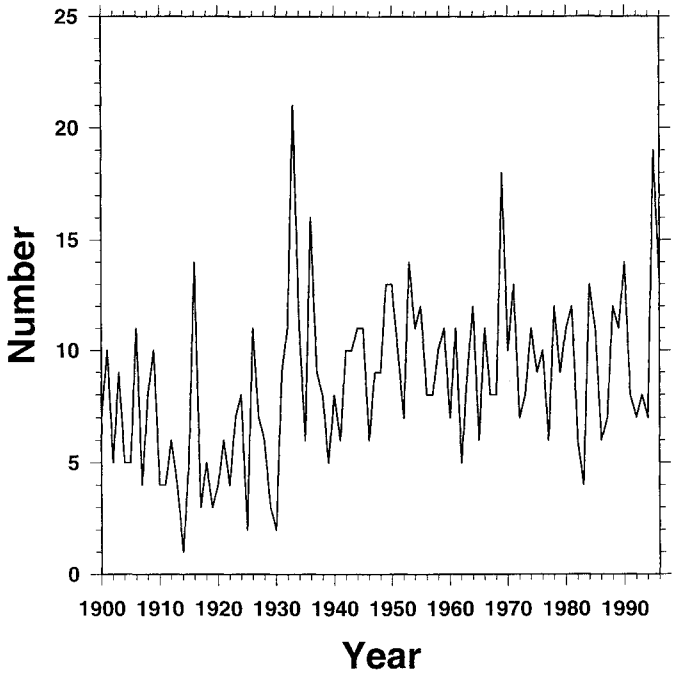

Figure 3.12. Total number of hurricanes or tropical storms that developed in the Atlantic Ocean or Gulf of Mexico each year from 1990 to 1996. (Data from Unisys Corporation, 1999.)

According to Landsea et al. (1996), there has been no significant change in the frequency of tropical storms or hurricanes between 1944 and 1995, but there has been a decrease in the number of intense hurricanes. Between 1991 and 1994, fewer hurricanes occurred in the Atlantic basin than in any other 4-year period since 1994. Peak numbers of hurricanes or tropical storms occurred in 1916, 1933, 1936, 1969, and 1995.

Of the total number of hurricanes or tropical storms that developed in the Atlantic Ocean or Gulf of Mexico between 1900 and 1996, 158 made landfall over the continental United States, with 41 making landfall in Atlantic coastal states within the region. Table 3.2 shows the distribution of hurricane landfall occurrences by state in the region between 1900 and 1996. More hurricanes and tropical storms have made landfall in New York (9) and Connecticut (8) in this period than in any other states within the region. Although hurricanes that make landfall typically produce most damage along coastal areas, extreme flooding and wind damage is possible in further inland areas, especially if convective storms and tornadoes develop in association with inland-moving hurricanes. For example, in 1955, Hurricane Diane made landfall over North Carolina and produced serious flooding in Pennsylvania as well as the coastal states

Table 3.2. Number of Hurricane Direct Hits on States in the Region Between 1900 and 1996 by Saffir/Simpson Categories (Category 1: 119 to 153 km h^{-1}, Category 2: 154 to 177 km h^{-1}, Category 3: 178 to 209 km h^{-1}, Category 4: 210 to 249 km h^{-1}, Category 5: >249 km h^{-1}) (From NOAA National Hurricane Center, 1999)

State	Category 1	Category 2	Category 3	Category 4	Category 5
Virginia	2	1	1	0	0
Maryland	0	1	0	0	0
Delaware	0	0	0	0	0
New Jersey	1	0	0	0	0
New York	3	1	5	0	0
Connecticut	2	3	3	0	0
Rhode Island	0	2	3	0	0
Massachusetts	2	2	2	0	0
New Hampshire	1	1	0	0	0
Maine	5	0	0	0	0

of New Jersey, New York, Delaware, Connecticut, Rhode Island, and Massachusetts.

Flooding can be a major problem, regardless of the strength of the hurricane as measured by its wind speed. Flooding and high winds associated with hurricanes that move up the Atlantic coast or move inland over the northeastern United States can cause severe damage to the region's natural resources, both in the short term and long term. Blowdowns from intense hurricane winds immediately impact forest stands, while trees damaged from high waters and intense winds are susceptible to diseases and insect infestations over time.

Fire-Weather Patterns

Wildland fires typically burn between 150,000 and 600,000 acres each year in the region (USDA Forest Service, 1992). On average, more than 98% of the wildland fires that occur in the region are human-caused. This is in contrast to the western regions of the United States where human-caused fires only account for about 40 to 50% of the total number of reported fires in a typical year. Lightning plays a more significant role in fire occurrence in the western states. Regardless of the cause of wildland fires, the severity of wildland fires in different regions of the United States depends to a large degree on the atmospheric conditions prior to and during fire episodes. There are specific atmospheric circulation, temperature, and moisture patterns that tend to be associated with severe wildland fires in each region of the United States. While these circulation, temperature, and moisture patterns typically do not generate weather that is considered "extreme," they do create conditions that are conducive to wildland fires that can be very destructive and "extreme" in nature.

Heilman (1995) performed empirical-orthogonal-function analyses of the 500-mb heights over the United States at the onset of past severe wildland fires (fires that burned 404.69 ha or more) in six different regions of the United States between 1971 and 1991 in order to determine which large-scale atmospheric circulation patterns and associated temperature and moisture patterns are most conducive to fire occurrence in these regions.

Three middle tropospheric circulation patterns were found most prevalent at the onset of severe wildland fires in the north central United States, including the states of Minnesota and Iowa. Examples of these circulation patterns are shown in Fig. 3.13 when severe wildland fires occurred in the north central United States (see color insert). Fig. 3.13a shows the first pattern consisting of a strong 500-mb ridge centered over the central Great Plains and extending northward into Canada, with the eastern and western regions of the United States dominated by 500-mb troughs. Wind vectors overlaying the 500-mb geopotential height field show southerly and southwesterly flow to the west of the ridge and northerly flow to the east of the ridge. Analyses of the lower tropospheric temperatures during circulation episodes of this type when severe wildland fires occurred in the north central states show positive average departures from monthly means over the entire Great Plains, with maximum departures reaching 6°C over western Minnesota. Lower tropospheric relative humidity departures from monthly mean values under this type of circulation pattern were found to be about 8 to 12% below normal over the western Great Lakes region. The warmer- and drier-than-normal atmospheric conditions over the north central United States under this type of circulation pattern during the spring and fall fire seasons in the north central U.S. can lead to higher probabilities of severe fires occurring in this region.

Fig. 3.13b shows an example of the second middle tropospheric circulation pattern most conducive to severe fire occurrence in the north central United States. This pattern consists of a 500-mb ridge centered over the eastern half of the United States, with the western states dominated by a 500-mb trough. This results in a southwesterly flow over the northern Great Plains, including the states of Minnesota and Iowa. Lower tropospheric temperatures averaged from 6 to 9°C above normal over the western Great Lakes region (Minnesota, Iowa, Wisconsin, and Michigan) when this circulation pattern developed and severe fires occurred in the north central U.S. This pattern also produces relatively dry lower atmospheric conditions over much of the region. Analyses indicate relative humidity departures on the order of 8 to 14% below normal from Wisconsin eastward and southeastward to the Atlantic coast.

The final middle tropospheric circulation pattern associated with severe fires in the north central United States is depicted in Fig. 3.13c. This pattern results in a strong northwesterly flow over the northern Great Plains in response to a strong ridge and trough over the western and eastern

United States, respectively. Unlike the previous circulation patterns, this pattern produces cooler-than-normal lower atmospheric conditions over most of the region. In the western Great Lakes region, lower atmospheric temperatures are typically on the order of 1 to 2°C below the monthly mean. Even though cooler-than-normal conditions prevail over the region under this type of circulation pattern, the lower atmosphere can become very dry. Relative humidity values approached 14 to 16% below normal over the western sections of the region when this circulation pattern appeared during 1971 to 1991 severe wildland fire episodes in the north central states. The extremely dry lower atmosphere is very conducive to fire occurrence in the region if surface fuel conditions are adequate.

When severe wildland fires occur in states east of Minnesota, Iowa, and Missouri, there are typically two types of atmospheric circulation patterns most conducive to their occurrence. The first pattern is characterized by a 500-mb ridge over the western half of the United States and a prominent trough over the eastern half of the United States and southeastern Canada. Refer to the color insert for an example of this pattern as shown in Fig. 3.14a. This circulation pattern transports cool dry air into the northeastern United States. An analysis of average lower atmospheric temperatures when severe wildland fires occurred during circulation patterns of this type between 1971 and 1991 indicates anomalies between −1°C and −5°C over the states northeast of Ohio and West Virginia. The lower atmosphere is typically very dry under this type of circulation pattern. Corresponding relative humidity values are typically 4 to 16% below normal over most of the region in these cases.

An example of the second circulation pattern associated with severe wildland fires in the northeastern United States is shown in Fig. 3.14b. This type of circulation pattern is associated with the westward shift of the Bermuda high pressure system off the southeastern U.S. coast, which results in a blocking of the northward transport of Gulf moisture into the region. Very hot and dry conditions can occur over the eastern U.S. under this circulation pattern, and the probabilities for severe wildland fire occurrence in the eastern half of the United States increase in such cases. The bulk of the moisture from the Gulf region is transported northward in a band to the west of the Mississippi River, where precipitation can be significant. The lower atmospheric temperature and relative humidity patterns associated with this circulation pattern reflect the conduciveness to fire occurrence in the region. Significant positive temperature anomalies occur over most of the eastern half of the United States with this circulation pattern, and negative relative humidity anomalies are prevalent over the eastern half of the region. Average temperature anomalies were generally greater than 5°C over the Great Lakes states during circulation episodes of this type between 1971 and 1991 when severe fires occurred, and average relative humidity anomalies reached as high as −24% over West Virginia and Pennsylvania during the same episodes.

In addition to the middle tropospheric circulation patterns that have been shown to be related to severe wildfire occurrence in the region by Heilman (1995), there are specific surface atmospheric pressure patterns and associated surface circulation patterns that characterize severe fire occurrence in the northeastern United States. Takle et al. (1994) studied surface pressure patterns corresponding to reduced precipitation, high evaporation potential, and enhanced forest-fire danger in the states of West Virginia, Ohio, Pennsylvania, and New York. Their analyses indicate most severe fires in this region occur when (1) an extended surface high pressure system covers most of the eastern United States, (2) a high pressure system is situated just off the Atlantic coast, or (3) a high pressure system is centered in the western Great Lakes region. The near-surface circulations associated with these high-pressure patterns are consistent with the middle tropospheric circulation patterns identified by Heilman (1995) as being conducive to severe fire occurrence in the northeastern United States. Takle et al. (1994) also examined the surface pressure fields generated by the Canadian Climate Centre global circulation model of the present ($1 \times CO_2$) climate and $2 \times CO_2$ climate to determine whether wildfire potential in the eastern U.S. may change under increased atmospheric CO_2 concentrations. The model simulations suggested an increase in frequency of surface circulation patterns in which evaporation generally exceeds precipitation, which is generally conducive to higher wildfire probabilities if surface fuel conditions are adequate.

El Niño–Southern Oscillation Effects

Atmospheric processes span a wide range of temporal and spatial scales. The climate and weather patterns that influence the northeast and north central United States region are the result of these many atmospheric processes at work from the global scale down to the microscale. One particular large-scale atmospheric process that periodically impacts weather and climate across many regions of the Earth, including the region, is the El Niño–Southern Oscillation phenomenon. This phenomenon can have a significant impact on global-scale atmospheric circulation patterns that produce regional temperature and precipitation anomalies across certain areas of the Earth. If the regional temperature and precipitation anomalies associated with an El Niño–Southern Oscillation episode are strong enough in the region, ecosystems in this region can be affected via altered heat and moisture flux regimes, changes in winter snowpack, changes in soil-moisture conditions, fewer or more frequent wildland fire occurrences, altered frequencies of damaging insect infestations and vegetation disease, and other mechanisms. A description of the El Niño–Southern Oscillation phenomenon and its typical seasonal impacts on temperature and precipitation patterns in the region are provided in this section.

What Is El Niño–Southern Oscillation?

Within 30° of latitude from the equator, winds near the surface of the Pacific Ocean generally blow from east to west. These winds are known as the trade winds. The trade winds push surface water away from South America and toward Asia and as they do so, the intense tropical sunlight warms the water. This gradual warming results in a typical sea-surface temperature difference of about 8°C between the western Pacific Ocean and the eastern equatorial Pacific coast (NOAA Pacific Marine Environmental Laboratory, 1997a). The lower sea-surface temperatures off the Pacific coast of South America are due to the upwelling of cold water from deeper levels. Under normal conditions, the upwelling brings nutrient-rich water to the surface and is important for supporting diverse marine ecosystems and major fisheries. Rainfall is normally more abundant over the warmer western Pacific Ocean region.

Sometimes, however, the east-to-west trade winds decrease in intensity, resulting in less upwelling of colder water from lower levels in the ocean and warmer-than-normal sea-surface temperatures off the Pacific coast of South America. The change in the trade winds is part of what is called the Southern Oscillation; the sea-surface temperature anomaly is El Niño. The overall pattern of weakened easterlies and higher sea-surface temperatures is commonly referred to as El Niño–Southern Oscillation (ENSO). Precipitation also tends to increase over the warmer waters of the eastern Pacific Ocean during ENSO episodes, often resulting in flooding in Peru. Drought conditions, on the other hand, often prevail in Indonesia and Australia during ENSO episodes. On average, ENSO episodes tend to occur every 2 to 7 years and last from 12 to 18 months (NOAA Pacific Marine Environmental Laboratory, 1997b).

El Niño–Southern Oscillation Impacts on Temperature and Precipitation

Although the changes in the equatorial sea-surface temperatures in the eastern Pacific Ocean that characterize ENSO episodes occur far away from the continental United States, they can have a profound effect on weather and climate in the United States. The weather and climate we experience in the north central and northeastern United States is controlled to a large extent by the large-scale atmospheric circulations that transport heat and moisture over the entire Earth. The rise in sea-surface temperatures off the equatorial Pacific coast of South America during ENSO and the associated change in the trade winds that characterize ENSO episodes can alter the normal atmospheric circulations over other parts of the Earth, including North America. Analyses of past ENSO episodes indicate that the typical paths of low-pressure and high-pressure systems that control daily weather fluctuations in the midlatitudes are altered during

the ENSO events (NOAA Climate Prediction Center, 1999). These changes can cause certain regions of the United States, including the north central and northeastern United States, to experience relatively large temperature and precipitation deviations from normal, and the deviations are seasonally dependent (Green et al., 1997).

Fig. 3.15 (color insert) shows the climate divisions in the continental United States where there has been a greater likelihood of a warmer or colder season than one would expect by chance during an ENSO event based on 100 years of past monthly climate division temperature data and monthly standardized Southern Oscillation Index values (NOAA-CIRES Climate Diagnostics Center, 1997). It has been during the winter and early spring months that ENSO episodes usually have had the most broad-scale impact on temperatures in the region (Fig. 3.15a). During the January to March period of ENSO episodes, the western Great Lakes region and the state of Maine have usually experienced warmer-than-normal conditions, while most of the southern and northeastern portions of the region experienced colder-than-normal conditions. During the midspring to late spring months of past ENSO episodes, there have been fewer climate divisions within the region that typically experienced higher-than-normal temperatures compared with the number of climate divisions during the winter months (Fig. 3.15b). Temperatures during this period have tended to be higher than normal in an area extending from Missouri eastward and northward into Illinois, Indiana, Kentucky, and Michigan. The overall pattern of significant monthly temperature anomalies in the region during the summer months of ENSO episodes has generally been confined to the states of Iowa, western Illinois, and northern Maine (Fig. 3.15c). Evidence from past ENSO episodes suggests that climate divisions in these areas of the region tend to experience colder-than-normal conditions during the summer. Finally, temperature observations during past ENSO episodes suggest the likelihood of higher-than-normal temperatures over the region in the fall months of an ENSO year is greatest over the Ohio River Valley and the western Great Lakes states (Fig. 3.15d).

Fig. 3.16 (color insert) shows the climate divisions in the continental U.S. where there has been a greater likelihood of a wetter or drier season than one would expect by chance during an ENSO event based on 100 years of past monthly climate division precipitation data and monthly standardized Southern Oscillation Index values (NOAA-CIRES Climate Diagnostics Center, 1997). Wintertime monthly precipitation observations during past ENSO episodes suggest that a large area within the region could experience relatively low precipitation totals during an ENSO event (Fig. 3.16a). The precipitation observations indicate that climate divisions in northern and eastern Wisconsin, northern and eastern Michigan, eastern Illinois, Indiana, Ohio, Kentucky, West Virginia, Pennsylvania, and New York have usually experienced anomalously low monthly precipitation amounts during the winter months. Only portions of Iowa, Minnesota, and

some climate divisions along the eastern U.S. coast typically have relatively high precipitation amounts during ENSO winters. Data presented in Fig. 3.16b–d suggest that during the spring, summer, and fall seasons, only a few climate divisions scattered across the region typically experience relatively low monthly precipitation amounts. During the months of April, May, and June of past ENSO events, the northern Great Plains plus the northern sections of Wisconsin and Michigan have typically been relatively wet (Fig. 3.16b). The summer months of July, August, and September during past ENSO events have been a period of relatively wet conditions for the entire state of Missouri, much of Iowa, and portions of Minnesota, Illinois, Indiana, Wisconsin, and Michigan (Fig. 3.16c). Finally, precipitation observations during past autumn ENSO episodes indicate the likelihood of relatively wet conditions over much of the western sections of the region, including most climate divisions in the states of Minnesota, Iowa, Missouri, and Wisconsin, and some climate divisions in the states of Michigan, Illinois, Indiana, and Kentucky (Fig. 3.16d).

Overview of General Circulation Model Climate Scenario Simulations

Coupled atmosphere–ocean general circulation models (GCMs) have been and continue to be used to provide scenarios of future climate conditions at the global scale under different assumptions of atmospheric greenhouse gas concentrations and emission scenarios. These models include 3-dimensional representations and interactions of the atmosphere, oceans, and land surface on a global time-dependent basis, along with specifications of the chemical composition of the atmosphere and the vegetation on Earth's surface (Gates et al., 1996). Although GCMs are limited in their ability to simulate cloud and radiative effects, the hydrologic balance over land surfaces, and the heat flux at the ocean surface, these models are the most powerful tools currently available for assessing what future climatic conditions may be like (Gates et al., 1996). There have been numerous scenarios of future climate conditions under increased atmospheric greenhouse gas concentrations that have been generated from the current class of GCMs, as outlined by Kattenberg et al. (1996). This section highlight some of the results of the simulations that are particularly important for ecosystem processes and functions in the region: scenarios of annual and seasonal temperature changes, seasonal precipitation changes, soil-moisture changes, and changes in extreme event occurrences.

Patterns of Annual and Seasonal Mean Temperature Changes

At the global scale, GCM simulation results suggest that global mean temperatures could increase between 1 and 4.5°C relative to the present

global mean temperature by the year 2100 due to increased CO_2 concentrations in the atmosphere (Kattenberg et al., 1996). All GCM simulations suggest that the greatest warming will occur over land instead of the oceans because of the diminished impact of evaporative cooling over land in comparison with the oceans. The simulations also suggest that annual mean temperatures will increase most significantly at higher latitudes. For example, simulations performed with the Australian Bureau of Meteorology Research Centre (BMRC) and the Australian Commonwealth Scientific and Industrial Research Organization (CSIRO) GCMs indicate that a 1% increase per year in atmospheric CO_2 concentrations will likely result in an increase in annual mean temperature of 3 to 5°C over the 60 to 90°N latitude range at the time of doubled CO_2 concentrations. These simulations also suggest that the region will experience a corresponding 2 to 3°C increase in annual mean temperature (Kattenberg et al., 1996).

On a seasonal basis, GCM climate scenario simulations indicate that warming on a global scale will be most significant in late autumn and winter, with summertime warming small. Northern hemispheric wintertime (December to February) surface temperature changes from the period 1880 to 1889 to the period 2040 to 2049 have been projected to be on the order of 3 to 5°C over the 60 to 90°N latitude region using the Max-Planck Institute for Meteorology (MPI) GCM (Hasselmann et al., 1995), which takes into account atmospheric aerosol effects that have a cooling impact. Similar temperature changes are projected over the 60 to 90°S latitude region during the southern hemispheric winter (June to August). Average wintertime surface temperatures in years 2040 to 2049 over parts (central and south central) of the region and the north Atlantic have been projected to be 0 to 1°C cooler than the 1880 to 1889 temperatures by the MPI GCM (Kattenberg et al., 1996). Other parts of the region are projected to have surface temperatures about 0 to 1°C higher. During the northern hemispheric summer (June to August), the northwestern sections of the region are projected to be 0 to 2°C cooler on average in years 2040 to 2049 compared with the 1880 to 1889 surface temperatures in the region, while the rest of the region is projected to be 0 to 1°C warmer. The direct forcing by sulfate (SO_4) aerosols is responsible for the net cooling effect projected by the MPI GCM over certain regions of the Earth, although the uncertainty in specifying future S emissions and resulting SO_4 concentrations in the atmosphere must be recognized in the simulation results (Kattenberg et al., 1996).

Patterns of Seasonal Mean Precipitation Changes

An increase in global precipitation has been projected by all GCMs under the various scenarios of increased atmospheric CO_2 concentrations. The GCM simulations suggest that wintertime precipitation will generally

increase over the northern latitudes and midlatitudes as a result of higher atmospheric water vapor content under overall warmer conditions and the transport of more water vapor to the northern high latitudes (Kattenberg et al., 1996; Manabe and Wetherald, 1975). When aerosol effects are included in the GCM simulations, the overall increase in simulated global wintertime precipitation is diminished. Kattenberg et al. (1996) reported on the results of nine different GCM climate scenario simulations. Six of the nine GCMs have projected an increase in wintertime precipitation over central North America when the "current climate" atmospheric CO_2 concentrations are doubled. These increases range from 4 to 18% of the average wintertime "current climate" precipitation over central North America. Colman et al. (1995) reported a projected increase in wintertime precipitation over most of the region using the BMRC GCM, assuming a 1% per year increase in atmospheric CO_2 concentrations over the "current climate" concentration; precipitation increases ranged from 0 to 0.5 mm d^{-1}.

Small changes in summertime precipitation under a doubled atmospheric CO_2 environment have been projected by most GCMs over central North America, although a majority of the nine GCM simulations reported by Kattenberg et al. (1996) indicate a slight decrease (2 to 8%) in average precipitation from "current climate" summertime precipitation amounts. A more significant decrease in precipitation over the eastern United States, including much of the region, has been projected with the BMRC GCM (Colman et al., 1995) under a doubled atmospheric CO_2 environment; precipitation decreases ranged from 0.5 to 1 mm d^{-1}.

Patterns of Seasonal Mean Soil-Moisture Changes

Although patterns of precipitation can provide a useful indication of trends in the Earth's hydrologic cycle, soil-moisture patterns are often more useful indicators because they integrate the combined effects of precipitation, evaporation, and runoff (Kattenberg et al., 1996). The current class of GCMs provide projections of soil-moisture conditions under a "changed climate" due to enhanced atmospheric CO_2 concentrations. However, the current class of GCMs are limited in their ability to simulate land–surface interactions because of the simplicity of their land–surface parameterization schemes. Nevertheless, most GCMs suggest that mean soil moisture will generally increase in the high northern latitudes in winter under a "changed climate." Simulation results from the CSIRO GCM (Gordon and O'Farrell, 1997) suggest an average wintertime soil-moisture increase of 0 to 1 cm along the Atlantic coastal states under a doubled atmospheric CO_2 environment (assuming a 1% per year increase in CO_2 concentrations from the "current climate" conditions). In the western sections of the region, the CSIRO GCM climate simulations

indicate a corresponding 0 to 1 cm decrease in average wintertime soil-moisture contents compared with the average "current climate" conditions.

Summertime soil-moisture conditions are projected to be drier in the northern midlatitudes by most GCMs under a doubled atmospheric CO_2 environment because of the enhanced evaporation in summer under higher global temperatures. Projected soil-moisture decreases tend to be more pronounced over geographical regions where summertime precipitation is reduced. However, within the broad northern midlatitude bands, where overall soil moisture has been projected to decrease under a doubled atmospheric CO_2 environment, some sections are projected to experience an increase in soil moisture. For example, the CSIRO GCM (Gordon and O'Farrell, 1997) simulations suggest that the eastern and north central regions of the U.S. will encounter an average summertime soil-moisture increase of 0 to 2 cm at the time of CO_2 doubling compared with "current climate" soil-moisture conditions.

When atmospheric aerosol effects are included in the GCM simulations, wintertime soil-moisture changes from the current mean conditions are diminished, while summertime soil moisture increases markedly over North America. This summertime effect is a manifestation of reduced warming over certain regions when atmospheric aerosols are present, thereby reducing the amount of evaporation from soil surfaces.

Patterns of Changes in Extreme Events

The occurrences of extreme regional or local weather events are dependent on atmospheric dynamic processes that span a wide range of temporal and spatial scales. Many extreme events, such as heavy rain or snow, frost or freeze episodes, and high wind events, are influenced by small-scale atmospheric processes which, in turn, can depend on regional and local topographic features, vegetation characteristics, and land–water variations. The relatively coarse resolution of the current class of GCMs does not permit these models to resolve the smaller-scale atmospheric dynamic processes that can play a major role in the development of extreme regional and local weather events. For this reason, it is very difficult to draw any conclusions about potential changes in extreme weather events under a doubled CO_2 environment from GCM climate scenario simulations. However, the IPCC has made some tentative assessments of the potential occurrence of various types of extreme weather and climate events under a doubled CO_2 environment based on reasoning from physical principles and down-scaling techniques (Kattenberg et al., 1996). These assessments include:

- Significant changes in the frequency of extreme events can result from changes in the mean climate or climate variability.

- An overall warming of the atmosphere tends to lead to an increase in the number of extremely high temperature events and a decrease in the number of extremely low temperature events during the winter.
- Daily temperature variability under a doubled CO_2 environment may decrease in certain regions, while daily precipitation variability may increase over some areas.
- Simulations from several GCMs suggest precipitation intensity may increase under a doubled CO_2 environment, and more frequent or severe drought periods may occur in a warmer climate.

Although these general assessments of the IPCC are not specific to the region, they do provide a sense of the types of extreme event changes that are possible under a doubled CO_2 environment over some regions of the Earth.

Atmospheric Deposition and Ozone Patterns

Climate change, atmospheric and ozone (O_3) deposition exert strong influences on the forest ecosystems in the northeast and north central United States. The principal components that determine the atmospheric deposition patterns are the air pollution concentration gradients resulting from regional emissions sources, the meteorological conditions that are conducive to the deposition of acidic compounds and O_3, the topography of the region, as well as the prevailing air transport patterns. These factors contribute to the wide gradient of atmospheric deposition found in the region, ranging from low, unpolluted background levels in the northern plains, to the highest national levels in the East. This section focuses on the spatial and temporal trends for deposition of sulfur (S), nitrogen (N), and tropospheric O_3 to the region. These substances have been intensively studied in the region to determine the long-term effects of atmospheric deposition and O_3 on forest ecosystem productivity and health (see Chapter 5).

The air quality of the region is influenced by the high density of population centers, industries, power generation plants, and transportation corridors in this region. The high chronic levels of air pollution in the region come from different sources. Stationary sources include factories, power plants, and smelters. Mobil sources include cars, trucks, planes, and trains, and local area sources include natural processes such as wildfires, geologic venting, and biogenic emissions.

In addition to the local and regional sources of pollutants in the region, acid deposition, O_3, and their contributing precursors are transported from source areas in the Midwest, which has the some of the largest producers of primary pollutants in the United States (USEPA, 1998a). The primary pollutants that are directly emitted from these sources are

transformed in the atmosphere into secondary pollutant forms, such as nitrate (NO_3^-) and sulfate (SO_4) deposition and O_3. Acidic deposition occurs when emissions of sulfur dioxide (SO_2) and nitric oxides (NO_x) in the atmosphere interact with water, oxygen, and oxidants to form acidic compounds, such as nitric acid (HNO_3) and sulfuric acid (H_2SO_4). The emissions sources, atmospheric conditions that create ozone and acidic deposition, regional transport and precipitation patterns, and topography are major factors that determine the pattern and deposition rate of air pollutants to forest systems.

Emissions

The primary anthropogenic cause of acid deposition is the burning of fossil fuels. In the United States, about 70% of the annual SO_2 and 30% of the NO_x emissions are produced by electricity-generating power plants that burn fossil fuels, of which 97% of the SO_2 emissions comes from coal-burning plants (USEPA, 1998b). The Ohio River Valley, with older power plants that burn high-sulfur coal, leads the United States in regional emissions of SO_2 and NO_x. Consequently, areas receiving the most acid rain are the Northeast and Canada, downwind from these emissions sources.

Ground-level O_3 is formed by the reaction of volatile organic compounds (VOCs) and NO_x in the presence of heat and sunlight. The largest source of VOCs are motor vehicles and other mobile sources with the remainder from power plants and other sources of combustion (USEPA, 1998b). The largest source of naturally produced VOCs in the United States are produced by coniferous tree species, making up 60% of the estimated total natural VOC emissions, and deciduous trees, contributing 30%. The annual U.S. production of natural and anthropogenic VOC emissions are estimated to be nearly equal in mass, but VOCs emitted from natural sources have greater reactivity for potential O_3 production (Allen and Gholz, 1996).

Atmospheric Deposition

As these primary pollutants (NO_x, SO_2, VOCs) are transported by weather patterns over the region, they are transformed by a variety of chemical reactions to secondary pollutants, such as sulfuric and nitric acid aerosols, particulate sulfate and nitrate, and ozone. These pollutants can remain in the atmosphere, affecting visibility and air quality, or can be deposited onto terrestrial surfaces and bodies of water.

Atmospheric deposition occurs via three main pathways: wet deposition, in which material is dissolved in droplets and deposited as rain or snow; dry deposition, involving the direct deposition of gases and particles (aerosols) to surfaces; and cloud-water deposition, involving material

dissolved in cloud droplets and intercepted by forest canopies. Atmospheric deposition and air quality data discussed in this section are limited to regional acidic deposition and O_3 patterns.

Acidic deposition is described in this section as the input of wet and dry deposition of inorganic S, N, and H^+ though rain, cloud water, and as aerosols. Sulfur forms include gaseous SO_2 and SO_4 in rain and aerosols. Nitrogen forms are nitrate and ammonium ions in rain and aerosols, nitric acid vapor, and gaseous nitric oxides. Hydrogen ion deposition is through precipitation as rain and snow, and as cloud water.

Monitoring Networks

The National Atmospheric Deposition Program, National Trends Network (NADP/NTN) was initiated in 1978 to monitor the long-term trends in wet acidic deposition. Precipitation is sampled weekly and analyzed for nitrate, ammonium (NH_4^+), sulfate, hydrogen ion (pH), as well as calcium, magnesium, potassium, sodium, chloride, and phosphate (Ca^{2+}, Mg^{2+}, K^+, Na^+, Cl^-, PO_4). The 200 monitoring sites provide national coverage, with stations located mostly in rural locations, away from point sources and large urban centers. The National Oceanic and Atmospheric Administration (NOAA) Atmospheric Integrated Research Monitoring Network (AIRMoN-wet) operates a smaller, more intensive daily sampling network of the NADP.

The Clean Air Status and Trends Network (CASTNet), provides weekly monitoring for dry deposition parameters, including filter-pack measurements of nitric acid and sulfur dioxide, and fine-particle nitrate, ammonium, and sulfate. The network consists of about 50 sites, located primarily on the East and West Coasts. Dry deposition is much more difficult to measure than wet deposition. It is not measured directly, but calculated using measured air concentrations and model estimates of deposition velocity from which dry deposition rates are calculated as the product of deposition velocity and air concentrations. Dry deposition consists of aerosols (gases), small particles, and large particles, and the deposition velocities vary with each component, adding to the difficulty in finding one suitable method. The AIRMoN-dry deposition network operates as a smaller program for developing dry deposition methodologies in CASTNet applications.

Cloud-water deposition was monitored in the Appalachian Mountains from 1986 to 1988 by the Mountain Cloud Chemistry Program (MCCP) at six study sites, and sampling continues at selected sites through the CASTNet Mountain Cloud Deposition Program (MADpro). The purpose of MCCP was to examine the spatial and temporal variation in cloud-water deposition and to determine the importance of cloud-water input to tree canopies relative to wet deposition at high-elevation sites.

The Clean Air Act required each state to establish a network of air monitoring stations called the State and Local Air Monitoring Stations (SLAMS). In order to obtain more timely and in-depth information about air quality at strategic location, The U.S. Environmental Protection Agency (EPA) established the National Air Monitoring Stations (NAMS) as part of the SLAMS network to meet more stringent air monitoring criteria. Approximately a third of these sites are designated rural or remote, but in practice, most are in close proximity to major population centers. The primary focus of this long-term monitoring network is to determine the O_3 concentrations to which large numbers of people are exposed. These monitoring sites are centered in or near urban centers where ambient air concentrations reflect local emissions. In recent years, there has been more interest in the effects of O_3 in rural areas. The CASTNet program also maintains O_3 monitoring at rural sites, where forest and agricultural concerns are the focus.

The EPA manages the Aerometric Information Retrieval System (AIRS) as the primary repository of the nationwide database on the criteria pollutants that must meet the National Ambient Air Quality Standards (NAAQS). Other research groups analyze O_3 production and O_3 transport patterns. The Ozone Transport Assessment Group (OTAG) was established by the Environmental Commissioners of States (ECOS) with the active participation of all 37 states east of the Mississippi (OTAG region). It provides analysis of transport patterns to develop a strategy to deal with long-range transport problems associated with regulating O_3 and its precursors. The Ozone Transport Commission (OTC), consisting of the 12 Northeastern and Mid-Atlantic states, was established by the Clean Air Act Amendment of 1990 to understand and assess the O_3 problems and evaluate control strategies. The North American Research Strategy on Tropospheric Ozone (NARSTO) consists of the Unites States, Canada, and Mexico, and conducts studies on the causes of severe O_3 episodes and the interaction between O_3, NO_x, and VOCs.

Nitrogen and Sulfur Compounds

The N compounds that are of concern for atmospheric deposition and forest interaction are reactive N species in oxidized (NO, NO_2, HNO_3, and NO_3^-) and reduced (NH_3, NH_4^+, and organic nitrogen) forms. About 90% of the nitrogen oxides and about 96% of the sulfur oxides emitted into the atmosphere are anthropogenic by origin (Lovett, 1994; Allen and Gholz, 1996). The primary form of nitrogen oxide emissions is nitric oxide (NO). In the presence of VOCs and sunlight, this gas is rapidly converted to nitrogen dioxide (NO_2), which further reacts to form nitric acid vapor (HNO_3). Nitrogen dioxide is also decomposed by sunlight to produce O_3, therefore both acidic deposition and O_3 formation are intimately tied to NO_x emissions. Nitric acid vapor can be dissolved by rain and cloud-water

to form nitrate (NO_3^-) ions and can be deposited as wet and cloud-water deposition. Dry deposition of nitric acid adsorbs rapidly to the canopy due to a high deposition velocity. Most of the ammonia (NH_3) in the atmosphere is thought to originate from volatilization of animal waste, from fertilized farmlands, and alkaline soils. Atmospheric NH_3 can be deposited as dry deposition or dissolved in rain and cloud water, forming ammonium (NH_4^+), and deposited as wet and cloud-water deposition. Organic N deposition is poorly understood and rarely monitored. It is composed primarily of particulate material from soils, vegetation (pollen, VOCs), animal waste, and reactions of NO_x with organic compounds.

The primary forms of S deposition that are important to forests systems are SO_2 and SO_4. These oxides of sulfur are mainly emitted from coal-burning electricity-generating facilities, predominantly in the form of SO_2 gas. The electricity-generating facilities are often located in rural areas and have a large impact on rural airsheds. Sodium dioxide is oxidized in the gaseous and aqueous phase to ultimately form H_2SO_4 vapor and H_2SO_4 aqueous acid solution. It can react with other aerosols to form particulate SO_4. About 20% of the SO_2 emitted in the United States is converted to SO_4 during its atmospheric lifetime. The main removal pathway for SO_2 is dry deposition to surfaces, and SO_4 can be deposited as wet, cloud-water, and dry deposition.

Acidic Deposition: Regional Trends

The northeastern and north central subregions of the region are distinguished by having the nation's highest levels of acidic, sulfur, and nitrogen deposition (Fig. 3.17, color insert). Maps based on NADP/NTN wet deposition data for the eastern U.S. were produced using surface estimation algorithms for H^+, SO_4^{2-}, NO_3^-, NH_4^+, total inorganic N, and precipitation averaged from 1983 to 1994 to characterize wet-deposition spatial trends (Lynch et al., 1996a). Mean annual H^+ concentration from 1983 to 1994 ranged from pH >5.3 at pristine sites in northwestern Minnesota to acidity levels a full pH unit lower (pH < 4.1) for much of the Ohio River Valley and along the length of the Appalachian Mountains and Appalachian Plateau region (Fig. 3.17a; NADP, 1996, 1998).

The regional pattern of deposition reflects the emissions source areas in the Midwest, the Ohio River Valley, and western Pennsylvania, and the prevailing wind patterns, which transport the elevated levels of acidic deposition to the eastern United States. Sulfate and nitrate deposition patterns over the region were similar to H^+ deposition (pH), with the lowest deposition in the northwestern corner of the region, gradually increasing eastward along a longitudinal gradient. The deposition gradient shifts its axis to the northeast along the Ohio River Valley, reaching the highest values in a region bordered by eastern Ohio, northern West Virginia, western Pennsylvania, and western New York. At the northern

Appalachian Plateau region and the Allegheny Mountains, deposition loads decrease slightly on the eastern side, corresponding to lower precipitation totals in the central Pennsylvania region. Higher deposition loads return with higher precipitation off Lake Ontario, reaching from the Adirondack Mountains to the Catskills, then decreases along a longitudinal gradient, with high values for the Green Mountains and White Mountains, but reaching low deposition levels in northern Maine. Ammonium shows a distinctly different spatial pattern, with higher deposition in the Midwest and eastern Great Plains states (Fig. 3.17e), stemming from greater NH_3 volatilization from fertilizers and animal wastes in the agricultural regions.

Dry deposition contributes a significant portion of the total N and S acid deposition, and can account for the majority of the N deposition in some subregions (Tables 3.3 and 3.4). CASTNet data show that dry deposition could account for up to 52% of total (wet + dry) N deposition in the Northeast and up to 45% of total S deposition (USEPA, 1998c; Allen and Gholz, 1996). Dry deposition is more variable spatially than wet deposition, as it is depleted with greater distance from the source. Dry deposition is a more significant contributor in and near major source regions, and wet deposition is more significant in areas with heavy precipitation, such as mountainous regions. In general, calculated dry

Table 3.3. Regional Averages of Total Nitrogen Deposition by Year and Percentage of Dry Deposition (INS = Insufficient Data)

Region	Total Deposition ($kg\,ha^{-1}$)							
	1989	1990	1991	1992	1993	1994	1995	Average
Northeast	7.6	7.7	6.9	6.7	7.6	7.5	7.1	7.3
Upper NE	3.9	3.1	3.3	3.1	3.3	3.3	3.3	3.3
Midwest	6.3	6.5	5.9	5.8	6.9	6.2	6.5	6.3
Upper MW	4.8	5.0	INS	5.4	4.8	4.4	4.5	4.8
South Central	6.6	5.6	5.3	5.2	5.7	5.6	6.6	5.8
Southern Periferal	4.0	6.1	3.8	3.6	3.8	4.4	4.2	4.3
West	INS	1.7	1.7	1.5	1.4	1.7	1.2	1.5
East	6.1	6.1	5.6	5.5	6.0	5.7	5.9	5.8
Region	Percent Dry Deposition							
	1989	1990	1991	1992	1993	1994	1995	Average
Northeast	43.1	41.1	45.8	42.3	42.4	47.3	51.8	44.8
Upper NE	20.0	20.3	18.8	18.2	21.0	21.6	21.7	20.2
Midwest	41.2	42.2	45.9	42.8	41.3	50.7	51.3	45.1
Upper MW	38.4	34.7	INS	34.6	34.0	37.0	40.9	36.6
South Central	49.9	53.7	49.6	51.1	52.1	51.1	59.5	52.4
Southern Periferal	36.7	41.0	36.6	40.0	41.5	37.9	48.5	40.3
West	INS	49.3	50.3	54.5	47.1	57.4	38.2	49.5
East	42.1	43.9	44.9	43.3	43.3	46.7	50.5	45.0

Table 3.4. Regional Averages of Total Sulfur Deposition by Year and Percentage of Dry Deposition (INS = Insufficient Data)

Region	Total Deposition ($kg\,ha^{-1}$)							
	1989	1990	1991	1992	1993	1994	1995	Average
Northeast	17.1	18.1	15.3	14.9	16.3	15.3	10.9	15.4
Upper NE	6.8	6.3	6.4	6.1	6.0	6.1	5.2	6.1
Midwest	16.3	16.3	13.7	13.3	15.0	13.1	11.3	14.1
Upper MW	6.9	8.7	INS	8.2	7.5	6.4	5.0	7.1
South Central	14.5	11.9	10.7	10.5	11.5	11.3	9.9	11.5
Southern Periferal	7.4	7.3	6.7	6.3	6.4	7.1	5.7	6.7
West	INS	1.8	1.8	1.5	1.7	1.7	1.1	1.6
East	13.4	13.7	12.1	11.4	12.2	11.3	9.1	11.9
Region	Percent Dry Deposition							
	1989	1990	1991	1992	1993	1994	1995	Average
Northeast	41.6	40.4	44.7	41.1	41.2	43.0	45.4	42.5
Upper NE	17.2	17.7	13.1	15.0	16.1	15.9	14.7	15.7
Midwest	39.7	39.1	43.5	38.9	39.0	44.9	42.6	41.1
Upper MW	32.5	26.8	INS	23.0	26.4	28.4	29.0	27.7
South Central	36.1	36.5	33.4	36.3	38.0	35.5	40.8	36.7
Southern Periferal	24.4	26.2	23.0	27.3	27.5	23.4	27.8	25.7
West	INS	34.9	33.6	33.6	37.1	46.8	21.8	34.6
East	37.2	37.2	39.4	36.5	37.4	38.4	39.8	38.0

deposition fluxes for the CASTNet sites (USEPA, 1998c) showed that SO_2 and HNO_3 were the dominant forms of S and N dry deposition, with SO_2 accounting for about 70% of the dry S deposition at eastern sites and HNO_3 accounting for approximately 65% of the dry N deposition. Higher dry deposition percentage occurred along the Ohio River Valley into New York State and also into the Mid-Atlantic sites, as well as drier regions in the south. A low ratio of dry/wet deposition may reflect higher precipitation patterns for those regions.

The ratio of cloud deposition to precipitation deposition varies from 1:1 in the northern sites to 2:1 and 4:1 in the southern sites, providing a substantial fraction of the total chemical deposition to high-elevation forests. Cloud water with a pH of 3.0 was routinely sampled at the MCCP sites. In high-elevation spruce–fir forests, cloud-water pH was approximately 1 pH unit lower than precipitation pH (pH 2.8 to 3.8 vs. pH 3.8 to 4.9) at the same site (NAPAP, 1991). Concentrations of the major ions, H^+, NO_3^-, SO_4^{2-}, and NH_4^+ were substantially higher in cloud water than in precipitation, ranging from a factor of 5× to 20×, depending on location (Mohnen, 1992). Cloud frequency (% hours), in which clouds cover these high-elevation sites may reach 20 to 40% of the time during the growing season, depending on elevation. Total deposition of S and N above cloud base is nearly twice as great as below cloud base.

The MCCP sites experienced the highest concentrations with cloud water originating from trajectories that passed over the Ohio River Valley. The data support the idea that forests exposed to cloud immersion are exposed to higher atmospheric loading despite their distance from major sources. Factors that increase the efficiency of atmosphere-to-surface exchange of pollutants in mountains include cloud immersion, the high surface area of mountain conifers, and generally higher wind speeds.

Total Deposition

Total N and S depositions for forest and rural areas have been calculated for the CASTNet monitoring sites in the region by combining the wet, dry, and cloud-water deposition. Annual average total N deposition from 1989 to 1994 ranged from 2.5 kg ha^{-1} in northern Maine to 8.5 kg ha^{-1} in central Pennsylvania. Annual average total S deposition for the 6-year period ranged from 5.2 kg ha^{-1} for Maine to 18.7 kg ha^{-1} in southern Indiana. Estimates of total N and total S depositions reached as high as 28 kg N ha^{-1} and 36 kg S ha^{-1} in regions of the United States that are subject to cloud-water and high regional loading (Johnson et al., 1991).

The total deposition is most likely underestimated because of limitations in directly measuring dry deposition and cloud-water deposition to forest canopies, and by accounting for only the major inorganic forms of N and S. The contribution that organic N deposition (both wet and dry) adds to the total deposition is poorly understood. At local scales, topography (elevation, slope, aspect) and vegetation canopy cover can cause significant variation in deposition rates, such as at mountainous forest sites. At higher elevations, the orographic uplifting of air masses causes increased precipitation. Wet deposition can increase from direct cloud-water inputs and dry deposition, both of which are thought to increase with elevation.

At larger regional scales, patterns of wet and dry deposition depend of the regional emissions sources, transport patterns, area and local emissions sources, weather and circulation patterns, topography, and land use.

Temporal Trends in Acidic Deposition

An analysis by Lynch et al. (1996a) of the ionic concentration of precipitation at NADP/NTN sites from 1983 to 1994 found that the annual mean SO_2 concentrations decreased east of the Mississippi, with major drops in the Ohio River Valley and the Mid-Atlantic states. Sulfate concentrations at 92% of the selected NADP/NTN monitoring sites in the United States have decreased since 1983. The trends were significant ($p < 0.05$) at 37% of the sites. Hydrogen ion concentration decreased at 82% of the monitoring sites for this period in the Northeast, and these

trends were significant at 35% of the sites. No sites in the Northeast saw a significant increase in SO_4 or H^+ during this period. Nationally, NO_3^- concentrations remained relatively unchanged, with 56% of the sites with decreasing trends, countered by 44% of the sites with increasing trends. However, 14% of the sites had significant increasing trends, while only 1% showed significant decreases. Ammonium concentration increases were larger than those for NO_3^-, with 80% of the sites showing increasing NH_4^+ concentrations since 1983 and 22% of the sites having significantly higher concentrations (Lynch et al., 1996a). The largest increases in NO_3^- and NH_4^+ were in the western states. Unlike the long-term decreasing trend for S concentrations, N concentrations in precipitation have increased in the United States since 1983.

Emissions Reductions and Deposition Rates

In Phase I of Title IV of the 1990 Clean Air Act Amendments (CAAA), Congress set emissions reduction goals for SO_2 beginning on January 1, 1995, at selected high-emitting electricity-generating facilities located primarily in the eastern United States. The first years of compliance in the SO_2 and NO_x emissions programs were 1995 and 1996, respectively. In order to evaluate the effect of the reductions program on acidic deposition, NADP/NTN deposition monitoring data from 1983 to 1994 were analyzed and a seasonal trend model was developed to estimate the expected precipitation chemistry for 1995. The observed 1995 precipitation chemistry was compared with the predicted 1995 estimates based on the pre–Title IV 1983 to 1994 trend model to evaluate the percentage of departure that Title IV compliance for 1995 had on the spatial and temporal patterns for NO_3^-, SO_4, and H^+ concentrations (Lynch et al., 1996a).

In the first year of compliance, SO_2 emissions dropped dramatically and were 39% below the allowable level under Title IV. This resulted in lower SO_4 concentrations in precipitation in the eastern United States, (Fig. 3.18b), particularly along the Ohio River Valley and states downwind in the Mid-Atlantic region. Mean annual SO_4 and H^+ concentrations for the eastern states observed in 1995 were below predicted values at 89 and 79% of the selected monitoring sites, respectively, using the 1983 to 1994 trend model. Measured SO_4 concentrations were about 11% less than estimated for the Northeast, and as much as 25% less in the Mid-Atlantic and Ohio River Valley regions (Fig. 3.18a). Concurrent with these SO_4 reductions have been similar levels of reductions in H^+ concentrations, which decreased 12%. The spatial pattern was identical to the decrease in SO_4 (Figs. 3.18a,b, color insert).

Maximum reductions in SO_4 and H^+ concentrations occurred in the Ohio River basin and the Mid-Atlantic regions immediately downwind of the major stationary sources targeted by Phase I of the CAAA-90, Title IV, as indicated by the plus (+) signs in Fig. 3.18. Precipitation deviations

from the long-term (1983 to 1994) average (Fig. 3.18d) does not explain the observed decreases in SO_4 and H^+ concentrations in 1995 (Fig. 3.18a,b). Lower precipitation volumes are associated with higher concentrations, and most of the eastern states had below-average precipitation volumes in 1995. Precipitation volumes would not selectively reduce only SO_4 and H^+. Nitrate and other ions would be similarly affected, but were not. The lower precipitation volumes resulted in higher 1995 concentrations in virtually all ions except for SO_4 and H^+. The two ions declined independent of precipitation volume. These results clearly support the conclusion that Phase I of the CAAA-90, Title IV, has reduced acid deposition in the eastern United States (Lynch et al., 1996a).

Nitrate concentrations in 1995 were higher than predicted from the reference trend model (Fig. 3.18c, color insert) corresponding to the lower precipitation for that year. Nitrogen oxide reductions for Title IV did not begin until 1996, and had substantially less impact in reducing acid deposition than the 1995 reductions in SO_2 from the targeted stationary sources. In contrast, stationary sources contribute only 30% of the total NO_x emissions for the United States. Because of the wide variety of sources for N emissions, NO_x are more diffcult to regulate and reduce.

Spatial Pattern of Ozone

The northern hemispheric global average O_3 concentration in the lower troposphere is about 40 ppb. This represents the background conditions for O_3 values for the northern United States. The average daily midday O_3 concentration over the entire eastern United States is about 60 ppb. Concentrations over urban industrial areas average 80 ppb, about twice the lower tropospheric background (Fig. 3.19, color insert). Lowest O_3 levels are in northwestern Minnesota and northern Maine, with the highest regional levels occurring in the Washington–New York corridor, where the average daily maximum ozone concentration exceeds 70 ppb. A second area of high O_3 is centered over the Ohio River Valley, including the Kentucky–Indiana–Ohio borders (Fig. 3.20, color insert).

Temporal Patterns of Ozone

Ozone concentrations vary greatly across time and space. The northern U.S. exhibits a strong degree of seasonality for O_3 production. This pattern is predictable as seasonal O_3 tracks air temperature closely. Highest rates develop during the summer months and drop to background levels during the cold winter months. High temperatures can increase the emission rates of natural and anthropogenic VOCs and high temperatures correlate with the meteorological conditions that enhance the photochemical formation of O_3: clear skies, increased solar radiation, low wind speeds, and transport patterns from the south and west.

During the summer months, high ground-level O_3 concentrations are observed within and downwind of many large urban areas in the eastern United States. Ozone patterns for 1991 to 1995 (Husar, 1997; OTAG, 1998) show highest summer (June to August) average daily maximum O_3 levels in the Ohio River Valley and the Mid-Atlantic region, extending up the northeast corridor (Fig. 3.21, color insert). Highest average daily maximum O_3 levels correspond with the large anthropogenic NO_x and VOCs densities near urban centers, such as like the Washington–New York corridor and along the industrial Ohio River Valley.

National trends from 1987 to 1996 show that the ambient average daily maximum 1-hour O_3 concentrations decreased 15%, and the estimated number of 120 ppb 1-hour exceedances declined by 73% over the past decade (USEPA, 1997a). The 1996 mean O_3 concentration dropped 6% lower than in 1995. This large decrease in 1996 was attributed to noticeable changes in the meteorological conditions for the eastern region. The summer of 1995 was hot and dry throughout most of the central and eastern United States, making it ideal for peak O_3 formation, while 1996 was dramatically wetter and cooler, with an unseasonably low number of hot days in the Northeast. Days with temperatures equal or greater than 90°F in the Ohio River Valley for the summer of 1995 reached 20 to 33 days across this region, compared with 5 to 10 days above 90°F in 1996. Along the eastern corridor from Philadelphia to Richmond, the temperature climbed to at least 90°F for 40 to 44 days compared with 3 to 15 days in 1996 (NOAA, 1996). The year 1988 was unusually hot and dry for the eastern United States and produced an anomalous O_3 season, producing the highest national composite mean O_3 level (USEPA, 1997a) and the greatest number of exceedances of the 1-hour 120 ppb standard in the past decade (Baumgardner and Edgerton, 1998).

Ozone production varies daily and seasonally, as the atmospheric chemical reactions depend on sunlight and higher temperatures. As sunlight intensity decreases, O_3 levels drop rapidly, and continue to be depleted during the night. This daily course of O_3 production is less evident in rural and mountainous areas where concentrations can remain elevated into the night, especially at higher elevations under atmospheric inversion conditions (Baumgardner and Edgerton, 1998). Typical daily O_3 peaks for remote forested areas occur from 2 PM to 5 PM with nocturnal predawn lows at 50 to 60% of daytime maximum O_3 levels as for Ashland, ME (Fig. 3.22). Daily cycles for Beltsville, MD show greater amplitude of daily peaks and shorter duration of daily peak O_3, with lower nocturnal minimum from nitric oxide titration in more urban areas (Fig. 3.22). High elevation forested sites show little or no dirunal pattern, with the curve nearly flat for Big Meadows, VA (Fig. 3.22). High-elevation sites in the East could therefore have consistently high O_3 exposure but not high peak concentrations. Topography can explain some of the different patterns between rural sites. Mountaintops are usually above the nocturnal

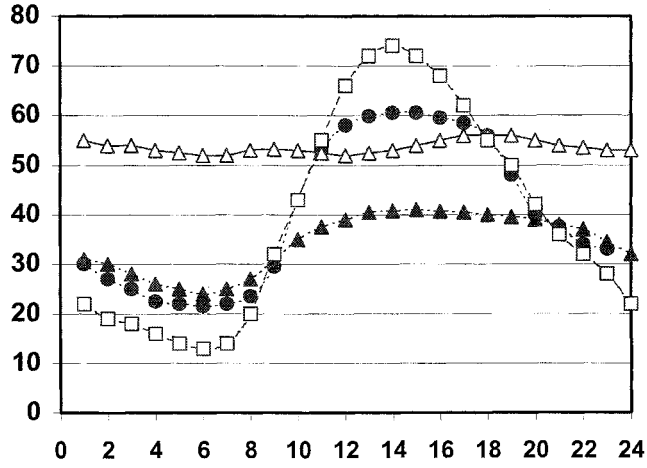

Figure 3.22. Diurnal hourly average ozone concentrations for sites in the Mid-Atlantic region showing the influence of terrain and urbanization in (a) Ashland, ME (▲), (b) Parson, WV (●), (c) Big Meadows, VA (△), and (d) Beltsville, MD (□).

inversion layer, and radiational cooling may circulate O_3-laden air from aloft to the site at night. Lower elevation sites, such as Parson, WV, has complex terrain that is under the nocturnal boundary layer for longer periods, and subject to O_3 loss through surface deposition losses.

New Primary and Secondary Ozone Standards

Recent proposed revisions by EPA on the National Ambient Air Quality Standards, lowering the primary (public health) and secondary (forest and crops) standard from 120 ppb to 80 ppb, and changing the time base average from a 1-hour peak period to an 8-hour average (USEPA, 1997b). Counties that exceeded the current 1-hour primary standard more than once per year (averaged over three consecutive years) were deemed non-attainment areas. Counties must eventually comply with a maximum 8-hour average for each year not to exceed 80 ppb (3-year average of the fourth-highest daily maximum 8-hour average), to be considered in attainment. Therefore, EPA will not designate areas as non-attainment for the new 8-hour O_3 standard until the year 2000.

The spatial pattern of counties in the NGCRP region with 1-hour exceedances is most evident over large urban metropolitan areas along the northeast corridor between Washington and Boston, and between Chicago and St. Louis. On average, the 8-hour daily maximum O_3 is about 85% of 1-hour daily maximum values. However, projections are that more counties will be in non-attainment of the 80 ppb air quality standard than the 120 ppb standard (Fig. 3.23, color insert) as the

industrial states north of the Ohio River, from Illinois to Pennsylvania, will have more exceedances based on the 8-hour standard.

Ozone Transport

Non-attainment states must make reductions to meet the new O_3 standard. However, these states do not have control of pollutants entering their airsheds through regional transport. OTAG has analyzed typical transport patterns of high-O_3 incidents (Husar and Renard, 1997; OTAG, 1998). Regional episodes during the summer can develop when accumulated O_3 covers several states in the eastern region. Ozone concentrations rise as temperature and concentrations of precursors rise in the region. As the winds increase, concentrations in the Midwest decrease, and high regional O_3 can be transported eastward, from one state to another, contributing to exceedance of the O_3 standard.

On high-O_3 days, transport winds are slow with clockwise circulation around the south central and eastern states. On low-O_3 days, faster transport winds originate from outside the domain (Fig. 3.24, color insert). Low-O_3 air comes from outside, while high-O_3 originates from inside this domain. High winds disperse local O_3 but contribute to higher regional O_3 through long-range transport. Stagnation over the multistate areas followed by transport of O_3 downwind results in regional O_3 episodes. There is an increasing O_3 trend from west to east in the midsection of the eastern United States from St. Louis to Baltimore (Husar, 1997).

Significant effort for O_3 reductions at their boundaries will be necessary to reach attainment guidelines locally. New attention has been focused on NO_x as precursor of tropospheric O_3 production. NO_x emissions are highest near cities, and correspond with power generation and fossil fuel usage in the industrial Midwest and Ohio River Valley. Although the role of NO_x in O_3 formation was known, the early focus for controlling O_3 was directed at controlling VOCs. To control O_3 near the ground, it is necessary to link emissions reductions of both NO_x and VOC precursors. The reductions in NO_x were expected to have broad regional O_3 benefits, whereas VOC controls would generate greater O_3 improvements on a local scale.

Ozone Statistics

Ozone is potentially the most damaging of the major air pollutants in terms of negative impacts to forest growth and species composition (Barnard et al., 1990). In the eastern seaboard states, 20% of the forested area and 27% of the croplands are in counties that exceed the NAAQS for O_3 in 1989 (Lefohn et al., 1990). This may be a conservative estimate of area affected, as O_3 damage in plants is known to occur at levels as low as 50 to 60 ppb for sensitive plants (Heck et al., 1982). The use of NAAQS

maximum hourly means correlated well with long-term averages in urban areas, but not for rural forested sites because of different O_3 concentration patterns in sites distant from emissions sources. Ozone and dry HNO_3 deposition at rural forest sites show a positive correlation using a weighted O_3 concentration averaged and dry nitric acid deposition. Therefore, forest that may see high average O_3 concentrations may also have the higher loadings of N and S dry deposition in these forested landscapes (Taylor et al., 1992).

Many O_3 exposure indices have been developed to compare daily, monthly, seasonal, and annual periods to describe the distribution of O_3 to the biological systems across the United States (Allen and Gholz, 1996; Lefohn et al., 1992). In agricultural and forested areas, it has been argued that cumulative O_3 indices are more biologically relevant than the time-based average 1- and 8-hour standards. The cumulative indices, such as SUM06 and W126, weight more strongly the higher values of O_3 measured over the 12-hour periods.

The SUM06 value is calculated as the sum of all O_3 concentrations greater than or equal to 60 ppb for each day (8 AM to 8:00 PM). The daily values are summed over the O_3 season (March through October). The maximum 3-month sum for the site is used an index value for that year. The W126 index (Lefohn et al., 1988) weights high hourly exposures more heavily (>80 ppb) and de-emphasizes lower, less biologically effective levels (< 30 ppb) using a sigmoidally weighted function.

W126 index maps for 1994, 1995, and 1996 were developed by Lefohn for the Forest Health Monitoring Program (Fig. 3.25, color insert) to show the year-to-year variability for the north central and northeastern regions of the United States. Spatial patterns shows higher W126 index values, expressed as parts per million hours (ppm-h), along the Mid-Atlantic region, down the eastern seaboard, and bounded by the Appalachian Mountains to the west. High W126 extend through lower Michigan and through the Ohio River basin. The lowest seasonal W126 values found in the NGCRP region were in the northern extremes of Minnesota and Maine. Ozone production varies greatly year to year, due to meteorological factors. The years 1995 and 1996 represent contrasting very high and very low ozone years based on hot–dry vs. cool–wet summer climate conditions (NOAA, 1996). Conditions that produce local and regional O_3 are much more variable than wet N or S deposition. Although long-term averages of O_3 concentrations may be necessary to identify O_3 trends to the region, the high O_3 years may be more important biologically, due to potential damage from peak O_3 episodes.

Regional Mapping of Atmospheric Deposition

The interpolated maps of long-term wet distribution chemistry and of O_3 concentration have been particularly useful in describing the spatial and

temporal patterns of atmospheric deposition for regional analysis and for providing coverages where data are lacking (Allen and Gholz, 1996; Lefohn et al., 1992; Mohnen, 1992; Smith and Shadwick, 1992; SAMAB, 1996). There is much greater difficulty in modeling and predicting dry deposition and cloud deposition over a landscape or regional basis due to the enormous number of biological, chemical, and physical factors that regulate these deposition processes. The Regional Acid Deposition Model (RADM) (Dennis et al., 1991), a large complex meteorological transport model, has been used to predict wet and dry acidic deposition and oxidants at a 20 to 80 km grid scale. The model considers the emissions of the precursors to acidic deposition, the meteorological processes that transport and mix the atmospheric chemicals over time and space, the physical and chemical reactions that occur, and the meteorological factors and surface properties of the terrain that lead to the deposition of acidic substances. The model is used for episodic runs for areas east of the Great Plains to forecast changes in deposition and air quality resulting from changes in primary emissions, and predicts the amount of acidic deposition received in the assessment area, such as the Chesapeake Bay watershed basin.

Spatial mapping and analysis using climate and atmospheric deposition trends can be used in process models to evaluate the effects of single or multiple stresses on forested systems over an extended geographical area. They require estimates of the deposition of chemicals and acidity of precipitation at much finer geographical scales to resolve important topographic features so the chemical inputs can be accurately matched with site and vegetation conditions. Ollinger et al. (1993) used a regression approach with a digital elevation map (DEM) to produce interpolated maps of deposition for the New England states at 1 km^2 resolution. They found that the gradients for wet and dry deposition rates followed longitude and latitude for the northeastern region, indicating that wet deposition material originates from sources in the Midwest (longitudinal gradient) while dry deposition originates from urban sources along the eastern seaboard (latitudinal gradient).

Lynch et al. (1996b) have produced enhanced regional wet deposition estimates based on modeled precipitation inputs. The model also incorporates topographic features to estimate wet deposition of major ions for the region. The coordinates, elevation, and monthly precipitation from a larger network of NOAA monitoring sites (about 1500) provide an extensive record of precipitation volume, and the wet deposition concentrations from the NADP/NTN network comprise the data set used for the model. The current model is a moving neighborhood, distance-weighted linear least squares regression of precipitation monitoring observations on latitudinal and longitudinal coordinates, elevation, and a set of variates to represent both slope and aspect. The modeled enhancement of wet deposition by this method can be produced at 0.3 to 1 km^2 resolution, but

is limited by the accuracy of the site location for the precipitation station, typically characterized at 1 minute resolution for latitude and longitude.

Human-Induced Climate Cycles with Atmospheric Deposition

Direct human influence on regional climate by air pollution has been hypothesized as the cause of weekly cycles identified in climate and pollution data sets. Urban centers have a prominent weekly pollution cycle, characterized by high late-week pollution levels (Friday) as opposed to low early-week levels (Sunday), as the result of weekly patterns of anthropogenic emissions. Cervaney and Balling (1998) argue that this shows direct anthropogenic forcing of regional climate as the 7-day cycle accumulates higher industrial pollutants levels throughout the workweek, thereby supplying a heavier load of condensation nuclei during the weekend. This fosters the growth of heavier cloud cover, which is estimated to supply 20% more rain during the weekends in the Atlantic seaboard region.

Weekly cycles of O_3 levels corresponding to the workweek have been shown with OTAG daily O_3 data analysis (OTAG, 1998). Highest maximum daily O_3 (90th percentile) shows up to a 15 ppb difference in the Northeast (Fig. 3.26, color insert) from Friday to Sunday, coinciding with human activities of the summer work week.

Conclusions

Overall, the NADP/NTN monitoring network shows acid deposition declining. Sulfate declined at 92% of the study sites between 1983 and 1994, with 38% of the sites showing statistically significant decreases. Hydrogen ion concentration decreased at 82% of the monitoring sites for this period in the Northeast, and this trend was significant at 35% of the sites. Nitrate and ammonium exhibited greater regional variability, showing slight increases since 1983. With the implementation of Title IV of the CAAA of 1990, SO_2 emissions dropped dramatically and were 39% below the allowable level. There was a dramatic 10 to 25 % drop in the 1995 wet deposition SO_4 concentration and acidity pH compared with the 1983 to 1994 reference period (see Fig. 3.18). Regional reductions were at some of the highest acid rain receptor regions in the Midwest, Northeast, and the Mid-Atlantic region. Increases in SO_4 concentrations were found in southern Michigan and the southwest region of the map (see Fig. 3.18b,d) and were attributed to lower rainfall than normal in 1995. Mean annual SO_4 and H^+ concentrations for the eastern states observed in 1995 were below predicted values at 89% and 79% of the selected monitoring sites, respectively, using the 1983 to 1994 trend model. Measured SO_4 concentrations for the Northeast were about 11% less than

estimated and as much as 25% less in the Mid-Atlantic region and the Ohio River Valley (see Fig. 3.18a). Concurrent with these SO_4 reductions, have been similar levels of reductions in acidity. However, NO_3^- deposition has increased nationally, primarily in the West.

Regional transport of pollutants plays an important role in the Northern Region. Acid deposition, O_3, and their contributing precursors are transported from source areas in the Midwest, which has the some of the largest producers of primary pollutants in the United States. Studies estimate that 25 to 35% of the N from atmospheric deposition into Chesapeake Bay is from the surrounding airshed, outside the Chesapeake watershed boundaries.

Ozone and dry nitric acid deposition at rural forest sites show a positive correlation using a weighted O_3 concentration averages, SUM60, and dry nitric acid deposition. Therefore, forest that may see high average O_3 concentrations may also have higher loadings of N and S dry deposition in these forested landscapes, producing conditions of multiple air pollution stress for forested systems over extended geographical areas (Taylor et al., 1992).

In higher elevations, the patterns of acid deposition and O_3 exposure may often differ from rural areas at lower elevations. In the case of acidic deposition, it may underestimate the total loading due to orographically enhanced deposition. Ozone at high-elevation sites may see different exposure patterns, and the maximum O_3 exposure may shift to late evening or early morning in higher elevations than in lower elevations, which can be biologically important.

Acid deposition has produced chronic loading of N, S, and H^+ to the region's forests and forest soils. The amount of wet deposition that falls is highly correlated with local and regional sources and the total amount of precipitation. Ozone deposition properties differ from acidic deposition, as O_3 levels show greater spatial and temporal variations. Ozone does not accumulate and directly affect biogeochemical cycling as does chronic deposition of acidity, N, and S. Plant response time to O_3 deposition has a short timeframe, minutes to hours, and direct plant damage may be more likely to occur from both chronic levels and peak O_3 events, depending on the plant's sensitivity.

Atmospheric deposition maps and indices give us a regional view on which areas may be suspectible to stress from O_3 and acid deposition. However, the uptake response of plants to O_3 is directly influenced by climate and environmental factors (light, temperature, relative humidity, nutrient and plant water status), which control stomatal opening, and genetic factors, which control plant sensitivity. Drought conditions during the active growing season would restrict photosynthesis and growth, but would also limit plant uptake of O_3. During hot, dry summer O_3 episodes, stomatal closure may actually reduce the risk of O_3 to sensitive plants (SAMAB, 1996). This illustrates the complex relationship between

regional atmospheric deposition, climate, plant uptake, and plant ecosystem response, which will be explored in following chapters.

This discussion has centered on the spatial and temporal trends of atmospheric deposition in the Northern Region. The yearly variation in meteorology is a major control on the formation of these air pollutants, on the the total annual N, S, and H^+ loading through wet, dry or cloud deposition, and on the transport and distribution of these deposition compounds throughout the region. Annual precipitation amounts, sunlight and summer temperature conditions, and wind patterns influence the total annual wet deposition to a region, production of ozone, and the transport these compounds to the northern forested regions.

References

Allen ER, Gholz HL (1996) Air quality and atmospheric deposition in Southern U.S. forests. In: Fox S, Mickler RA (eds) *Impact of Air Pollutants on Southern Pine Forests*. Ecological Studies 118. Springer-Verlag, New York, pp 83–170.

Andresen JA, Harman JR (1994) *Springtime Freezes in Western Lower Michigan: Climatology and Trends*. Michigan Agric Exp Sta Res Rep 536. Michigan State Agricultural Experiment Station, East Lansing, MI.

Barnard JE, Lucier AA, Brooks RT et al. (1990) Changes in forest health and productivity in the United States and Canada. In: *National Acid Precipitation Assessment Program. Acidic Deposition State of Science and Technology*. Vol. 3, Report 16. National Acid Precipitation Assessment Program, Washington, DC.

Baumgardner BE, Edgerton ES (1998) Rural ozone across the eastern United States: Analysis of CASTNet data, 1988–1995. J Air Waste Manage Assoc 48:674–688.

Bosart LR, Sanders F (1981) The Johnstown flood of July 1977: a long-lived convective storm. J Atmos Sci 38:1616–1642.

Cerveny RS, Balling RC (1998) Weekly cycles of air pollutants, precipitation and tropical cyclones in the coastal NW Atlantic region. Nature 394:561–563.

Changnon SA (1987) *Detecting Drought Conditions in Illinois*. Illinois State Water Survey Circular 164–87.

Chappell CF (1986) Quasi-stationary convective events. In: Ray PS (ed) *Mesoscale Meteorology and Forecasting*. American Meteorological Society, Boston, Massachusetts, 289–310.

Colman RA, Power SB, McAvaney BJ, Dahni RR (1995) A non-flux-corrected transient CO_2 experiment using the BMRC coupled atmosphere/ocean GCM. Geophys Res Lett 22:3047–3050.

Daly C, Neilson RP, Phillips DL (1994) A statistical-topographic model for mapping climatological precipitation over mountainous terrain. J Appl Meteor 33:140–158.

DeHayes DH (1992) Winter injury and developmental cold tolerance of red spruce. In: Eager C, Adams MB (eds) *The Ecology and Decline of Red Spruce in the Eastern United States*. Springer-Verlag, New York, pp 295–337.

DeHayes DH, Waite CE, Ingle MA, Williams MW (1990) Winter injury susceptibility and cold tolerance of current and year-old needles of red spruce trees from several provenances. Forest Sci 36:982–994.

Dennis RL, Barchet WR, Clark TL, Seilkop SK (1991) Evaluation of regional acidic deposition models. In: *National Acid Precipitation Assessment Program.*

Acidic Deposition State of Science and Technology. Vol. 3, Report 16. National Acid Precipitation Assessment Program, Washington, DC.

Dessens J, Bücher A (1995) Changes in minimum and maximum temperatures at the Pic du Midi in relation with humidity and cloudiness, 1882–1984. Atmos Res 37:147–162.

Diaz HF, Quayle RG (1980) The climate of the United States since 1895: spatial and temporal changes. Mon Wea Rev 108:249–266.

EarthInfo (1995) *Database guide for EarthInfo CD² NCDC Summary of the day*. EarthInfo, Inc., Boulder, Colorado.

Eischeid JK, Baker CB, Karl TR, Diaz HF (1995) The quality control of long-term climatological data using objective data analysis. J Appl Meteor 34:2787–2795.

Friedland AJ, Gregory RA, Karenlamp L, Johnson AH (1984) Winter damage to foliage as a factor in red spruce decline. Can J For Res 14:963–965.

Gates WL et al. (1996) Climate models—evaluation. In: Houghton JT, Meira Filho LG, Callander BA, Harris N, Kattenberg A, Maskell K (eds) IPCC (Intergovernmental Panel on Climate Change) *Climate Change 1995: The Science of Climate Change*. Cambridge University Press, Cambridge, United Kingdom, pp 229–284.

Gordon HB, O'Farrell SP (1997) Transient climate change in the CSIRO coupled model with dynamic sea-ice. Mon Wea Rev 125:875–907.

Green PM, Legler DM, Miranda CJ, O'Brien JJ (1997) *The North American Climate Patterns Associated with the El Niño–Southern Oscillation*. COAPS Project Report Series 97-1. Center for Ocean-Atmospheric Prediction Studies, Florida State University, Tallahassee, FL. <http://www.coaps.fsu.edu/lib/booklet/>

Groisman PY, Easterling DR (1994) Variability and trends of total precipitation and snowfall over the United States and Canada. J Climate 7:184–205.

Hasselmann K et al. (1995) Detection of anthropogenic climate change using a fingerprint method. In: Ditlevsen P (ed) *Proceedings of "Modern Dynamical Meteorology," Symposium in Honor of Aksel Wiin-Nielsen, 1995*. European Centre for Medium-Range Weather Forecasts Press. Reading, England, pp 203–221.

Heck WW, Taylor OC, Adams RM (1982) Assessment of crop loss with ozone. J Air Poll Contr Assoc 32:353–361.

Heilman WE (1995) Synoptic circulation and temperature patterns during severe wildland fires. In: *Proceedings of the Ninth Conference on Applied Climatology*. American Meteorological Society, Dallas, TX, pp 346–351.

Henderson-Sellers A (1992) Continental cloudiness changes this century. GeoJournal 27(3):255–262.

Hirschboeck KK (1991) Climate and floods. In: Paulson RW, Chase EB, Roberts RS, Moody DW (eds) *National Water Summary 1988–1989: Hydrologic Events and Floods and Droughts*. Water Supply Paper 2375. United States Geological Survey (USGS), Denver, CO, pp 67–88.

Holton JR (1979) *An Introduction to Dynamic Meteorology*. Academic Press, New York.

Horton EB (1995) Geographical distribution of changes in maximum and minimum temperatures. Atmos Res 37:102–117.

Houghton JT, Callander BA, Varney SK (eds) IPCC (Intergovernmental Panel on Climate Change) (1992) *Climate Change 1992: The Supplementary Report to the IPCC Scientific Assessment*. Cambridge University Press, Cambridge, United Kingdom.

Houghton JT et al. (eds) IPCC (Intergovernmental Panel on Climate Change) (1994) *Climate Change 1994: Radiative Forcing of Climate Change and an*

Evaluation of the IPCC IS92 Emission Scenarios. Cambridge University Press, Cambridge, United Kingdom.

Houghton JT, Jenkins GJ, Ephraums JJ (eds) IPCC (Intergovernmental Panel on Climate Change) (1990) *Climate Change: The IPCC Scientific Assessment*. Cambridge University Press, Cambridge, United Kingdom.

Houghton JT, Meira Filho LG, Callander BA, Harris N, Kattenberg A, Maskell K (eds) IPCC (Intergovernmental Panel on Climate Change) (1996) *Climate Change 1995: The Science of Climate Change*. Cambridge University Press, Cambridge, United Kingdom.

Hulme M (1991) An intercomparison of model and observed global precipitation climatologies. Geophys Res Lett 18:1715–1718.

Hulme M, Zhao Z-C, Jiang T (1994) Recent and future climate change in East Asia. Int J Climatol 14:637–658.

Husar RB, Renard WP (1997) *Ozone as a Function of Local Wind Speed and Direction: Evidence of Local and Regional Transport*. Center for Air Pollution Impact and Trend Analysis (CAPITA), Washington University, St Louis, MO. <http://capita.wustl.edu/OTAG/reports/otagwind/OTAGWIN4.html>

Husar RB (1997) *Seasonal Pattern of Ozone over the OTAG Region*. Center for Air Pollution Impact and Trend Analysis (CAPITA), Washington University, St. Louis, MO. <http://capita.wustl.edu/otag/reports/otagseas/otagseas.html>

Johnson DW, Van Miegroet H, Lindberg SE, Harrison RB, Todd DE (1991) Nutrient cycling in red spruce forests of the Great Smoky Mountains. Can J For Res 21:769–787.

Jones PD (1994) Hemispheric surface air temperature variations: A reanalysis and an update to 1993. J Climate 7:1794–1802.

Jones PD (1995) Maximum and minimum temperature trends in Ireland, Italy, Thailand, Turkey and Bangladesh. Atmos Res 37:67–78.

Karl TR, Groisman PY, Knight RW, Helm RR Jr. (1993a) Recent variations of snow cover and snowfall in North America and their relation to precipitation and temperature variations. J Climate 6:1327–1344.

Karl TR et al. (1993b) A new perspective on recent global warming: asymmetric trends of daily maximum and minimum temperature. Bull Am Met Soc 74:1007–1023.

Karl TR, Knight RW (1998) Secular trends of precipitation amount, frequency, and intensity in the United States. Bull Am Met Soc 79:231–241.

Kattenberg A et al. (1996) Climate models—projections of future climate. In: Houghton JT, Meira Filho LG, Callander BA, Harris N, Kattenberg A, Maskell K (eds) IPCC (Intergovernmental Panel on Climate Change) *Climate Change 1995: The Science of Climate Change*. Cambridge University Press, Cambridge, United Kingdom, pp 285–357.

Kiehl JT, Trenberth KE (1997) Earth's annual global mean energy budget. Bull Am Met Soc 78:197–208.

Landsea CW, Nicholls N, Gray WM, Avila LA (1996) Downward trends in the frequency of intense Atlantic hurricanes during the past five decades. Geophys Res Lett 23:1697–1700.

Lefohn AS, Benkovitz CM, Tanner M, Shadwick DS, Smith LA (1990) Air Quality Measurements and Characterization for Terrestrial Effects Research. NAPAP State of Science and Technology Report No. 7. National Acid Precipitation Assesment Program, Washington, DC.

Lefohn AS, Laurence JA, Kohut RJ (1988) A comparison of indices that describe the relationship between exposure to ozone and reductions in the yield of agricultural crops. Atmos Environ 22:1229–1240.

Lefohn AS, Knudsen HP, Shadwick DS, Hurmann K (1992) Surface ozone exposures in the eastern United States (1985–1989). In: Flagler RB (ed) *The Response of Southern Commercial Forest to Air Pollution*. TR-21. Air and Waste Management Association, Pittsburgh, PA, pp 81–93.

Lovett, GM (1994) Atmospheric deposition of nutrients and pollutants in North America: an ecological perspective. Ecol Appl 4:629–650.

Lynch JA, Bowersox VC, Grimm JW (1996a) *Trends in Precipitation Chemistry in the United States, 1983–1994: An Analysis of the effects of 1995 of Phase I of the Clean Air Act Amendments of 1990, Title IV*. USGS Open-File Rep 09-0346. US Geological Survey (USGS), Washington, DC.

Lynch JA, Grimm JW, Corbett ES (1996b) Enhancement of regional wet deposition estimates based on modeled precipitation inputs. In: Hom J, Birdsey R, O'Brian K (eds) *Proceedings, 1995 Meeting of the Northern Global Changes Program*. Gen Tech Rep NE-214. USDA Forest Service, NE Forest Experiment Station, Radnor, PA.

Maddox RA (1983) Large-scale meteorological conditions associated with midlatitude, mesoscale convective complexes. Mon Wea Rev 11:1475–1493.

Manabe S, Wetherald RT (1975) The effects of doubling the CO_2 concentration on the climate of a general circulation model. J Atmos Sci 32:3–15.

Mather JR (1974) *Climatology: Fundamentals and Applications*. McGraw-Hill, New York.

McIntosh DH (1972) *Meteorological Glossary*. Chemical Publishing, New York.

McNab AL, Karl TR (1991) Climate and droughts. In: Paulson RW, Chase EB, Roberts RS, Moody DW (eds) *National Water Summary 1988–1989: Hydrologic Events and Floods and Droughts*. Water Supply Paper 2375. United States Geological Survey (USGS), Denver, Colorado, pp 89–98.

Melillo JM, Prentice IC, Farquhar GD, Schulze ED, Sala OE (1996) Terrestrial biotic responses to environmental change and feedbacks to climate. In: Houghton JT, Meira Filho LG, Callander BA, Harris N, Kattenberg A, Maskell K (eds) IPCC (Intergovernmental Panel on Climate Change) *Climate Change 1995: The Science of Climate Change*. Cambridge University Press, Cambridge, United Kingdom, pp 445–481.

Mohnen VA (1992) Atmospheric deposition and pollutant exposure of eastern U.S. forest. In: Eagar C, Adams MB (eds) *Ecology and Decline of Red Spruce in the Eastern United States*. Ecological Studies 96. Springer-Verlag, New York, pp 64–124.

Namias J (1983) Some causes of United States drought. J Climate Appl Meteor 22:30–39.

National Drought Mitigation Center (1997) An Historical look at the Palmer Drought Severity Index. <http://enso.unl.edu/ndmc/climate/palmer/pdsihist.htm>

[NAPAP] National Acid Precipitation Assessment Program (1991) *1990 Integrated Assessment Report*. U.S. National Acid Precipitation Assessment Program, Washington, DC.

[NADP] National Atmospheric Deposition Program (1996) Precipitation chemistry in the United States, 1994. In: *NADP/NTN Annual Data Sumary*. Natural Resource Ecology Laboratory, Colorado State University, Ft Collins, Colorado, pp 25–34.

[NADP] National Atmospheric Deposition Program (1998) *1997 Wet Deposition*. Illinois State Water Survey, Champaign, Illinois.

[NAPAP] National Acid Precipitation Assessment Program (1998) *NAPAP Biennial Report to Congress: An Integrated Assessment*. National Science

and Technology Council, Committee on Environment and Natural Resources. Washington, DC.

Nicholls N, Gruza GV, Jouzel J, Karl TR, Ogallo LA, Parker DE (1996) Observed climate variability and change. In: Houghton JT, Meira Filho LG, Callander BA, Harris N, Kattenberg A, Maskell K (eds) IPCC (Intergovernmental Panel on Climate Change) *Climate Change 1995: The Science of Climate Change*. Cambridge University Press, Cambridge, United Kingdom, pp 133–192.

[NOAA] National Oceanic and Atmospheric Administration (1996) *Special Climate Summary 96/4*. Summer 1996 National Weather Service. National Centers for Environmental Prediction. Climate Prediction Center. Climate Operations Branch and Analysis Branch. <http://nic.fb4.noaa.gov/products/special_summaries/96_4/>

[NOAA-CIRES Climate Diagnostics Center] National Oceanic and Atmospheric Administration (1997) Risk of seasonal climate extremes in the US related to ENSO. <http://www.cdc.noaa.gov/~cas/atlas.html>

[NOAA Climate Prediction Center] National Oceanic and Atmospheric Administration (1999) *Warm Episode Seasonal 250-hPa Wind: Climatological, Actual, and Departure from Normal*. <http://www.cpc.ncep.noaa.gov/products/analysis_monitoring/ensostuff/hist/histcirc.html>

[NOAA National Hurricane Center] National Oceanic and Atmospheric Administration (1999) *U.S. Mainland Hurricane Strikes by State, 1900–1996*. <http://www.nhc.noaa.gov/paststate.html>

[NOAA Pacific Marine Environmental Laboratory] National Oceanic and Atmospheric Administration (1997a) *What is an El Niño?* <http://www.pmel.noaa.gov/toga-tao/el-nino-story.html>

[NOAA Pacific Marine Environmental Laboratory] National Oceanic and Atmospheric Administration (1997b) *Definitions of El Niño, La Niña, and ENSO*. <http://www.pmel.noaa.gov/toga-tao/ensodefs.html>

[NOAA Storm Prediction Center] National Oceanic and Atmospheric Administration (1999) *Historical Tornado Archive*. <http://www.spc.noaa.gov/archive/tornadoes/index.html>

Ollinger SV, Aber JD, Lovett GM, Millham SE, Lathrop RG, Ellis JM (1993) A spatial model of atmospheric deposition for the northeastern US. Ecol Appl 3:459–472.

[OTAG] Ozone Transport Assessment Group (1998) *OTAG Technical Supporting Document: Final Report*. Ozone Transport Assessment Group. Environmental Council of States. <http://www.epa.gov/ttn/otag/finalrpt/>

Palmer WC (1965) *Meteorological Drought*. Research Paper 45. US Weather Bureau, US Department of Commerce, Washington, DC.

Paulson RW, Chase EB, Roberts RS, Moody DW (eds), (1991) *National Water Summary 1988–89: Hydrologic Events and Floods and Droughts*. Water Supply Paper 2375. US Geological Survey, Denver, CO.

Plantico MS, Karl TR, Kukla G, Gavin J (1990) Is recent climate change across the United States related to rising levels of anthropogenic greenhouse gases? J Geophys Res 95:16617–16637.

Press WH, Teukolsky SA, Vetterling WT, Flannery BP (1992) *Numerical Recipes in FORTRAN*: The Art of Scientific Computing. Cambridge University Press, New York.

Schimel D et al. (1996) Radiative forcing of climate change. In: Houghton JT, Meira Filho LG, Callander BA, Harris N, Kattenberg A, Maskell K (eds) IPCC (Intergovernmental Panel on Climate Control) *Climate Change 1995: The Science of Climate Change*. Cambridge University Press, Cambridge, United Kingdom, pp 65–131.

Takle ES, Bramer DG, Heilman WE, Thompson MR (1994) A synoptic climatology for forest fires in the NE US and future implications from GCM simulations. Int J Wildland Fire 4:217–224.

Taylor GE, Ross-Todd BM, Allen E P, Conklin P (1992) *Patterns of tropospheric ozone in forested landscapes of the Integrated Forest Study.* In: Johnson DW, Lindberg SE (eds) Atmospheric Deposition Forest Nutrient Cycling: A Synthesis of the Integrated Forest Study. Ecological Studies 91. Springer-Verlag, New York, pp 50–71.

Trenberth KE, Houghton JT, Meira Filho LG (1996) The climate system: an overview. In: Houghton JT, Meira Filho LG, Callander BA, Harris N, Kattenberg A, Maskell K (eds) IPCC (Intergovernmental Panel on Climate Change) *Climate Change 1995: The Science of Climate Change.* Cambridge University Press, Cambridge, United Kingdom, pp 51–64.

Unisys Corporation (1999) *Atlantic Tropical Storm Tracking by Year.* <http://weather.unisys.com/hurricane/atlantic/index.html>, 1 pp.

[USDA Forest Service] United States Department of Agriculture, Forest Service (1992) *1984–1990 Forest Fire Statistics.* USDA Forest Service, Washington, DC.

[USEPA] United States Environmental Protection Agency (1997a) *National Air Quality and Emissions Trends Report, 1996.* EPA 454/R.97-013. USEPA, Office of Air Quality Planning and Standards, Research Triangle Park, North Carolina.

[USEPA] United States Environmental Protection Agency (1997b) *Final Revisions to the Ozone and Particulate Matter Air Quality Standards.* EPA 456/F-97-004. USEPA, Office of Air and Radiation, Washington, DC.

[USEPA] United States Environmental Protection Agency (1997a) *Acid Rain Program Emissions Scorecard 1996.* EPA 430/R 97-031. USEPA, Office of Air and Radiation, Acid Rain Division, Washington, DC.

[USEPA] United States Environmental Protection Agency (1998b) *National Air Quality and Emissions Trends Report, 1997.* EPA 454/R.98-016. USEPA, Office of Air Quality Planning and Standards, Research Triangle Park, North Carolina.

[USEPA] United States Environmental Protection Agency (1998c) *Clean Air Status and Trends Network (CASTNet) Deposition Summary Report (1987–1995).* EPA 600/R-98-027. USEPA, Office of Research and Development, Washington, DC.

Vining KC, Griffiths JF (1985) Climatic variability at ten stations across the United States. J Climat Appl Meteor 24:363–370.

Vose RS, Schmoyer RL, Steurer PM, Peterson TC, Heim R, Karl TR, Eischeid J (1992) *The Global Historical Climatology Network: Long-Term Monthly Temperature, Precipitation, Sea Level Pressure, and Station Pressure Data.* Report ORNL/CDIAC-53, NDP-041, Oak Ridge National Laboratory, Oak Ridge, TN.

Wallace JM, Hobbs PV (1977) *Atmospheric Science: An Introductory Survey.* Academic Press, New York.

Weisberg JS (1981) *Meteorology: The Earth and Its Weather.* Houghton Mifflin, Boston, MA.

Zasada JC, Teclaw RM, Isebrands JG, Buckley DS, Heilman WE (1994) *Effects of Canopy Cover and Site Preparation on Plant Succession and Microclimate in a Hardwood Forest in Northern Wisconsin. Proceedings of the 1994 Society of American Foresters/Canadian Institute of Forestry Convention, 18–22* September *1994, Anchorage, Alaska,* Society of American Foresters, Bethesda, MD, pp 479–480.

Ecological Studies 139

Robert A. Mickler
Richard A. Birdsey
John Hom Editors

Responses of Northern U.S. Forests to Environmental Change

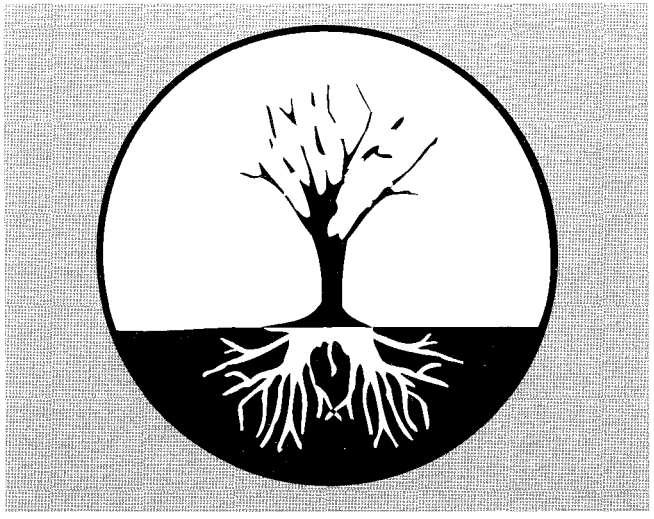

Springer